

Manuscript Number: JQSR-D-16-00135R3

Title: The linking of the upper-middle and lower reaches of the Yellow River as a result of fluvial entrenchment

Article Type: SI:Fluvial Archives Group

Keywords: Yellow River; Sanmen gorge; Fenwei graben; Terrace; Planation surface; Fluvial incision rate

Corresponding Author: Dr. Zhenbo Hu, Ph.D.

Corresponding Author's Institution: Lanzhou University

First Author: Zhenbo Hu, Ph.D.

Order of Authors: Zhenbo Hu, Ph.D.; Baotian Pan, Ph.D.; David R Bridgland, Ph.D.; Jef Vandenberghe, Ph.D.; Lianyong Guo, Master; Yunlong Fan, Ph.D.; Rob Westaway, Ph.D.

Abstract: The upper-middle Yellow River flows through the Fenwei graben, a structure resulting from extensional tectonism that was formed and repeatedly extended during the Cenozoic. The drainage system within this graben was formerly isolated from the lower reaches of the Yellow River system by the Xiaoshan mountains, an actively growing ~NW-SE trending range. The modern course of the Yellow River takes it through this range along the Sanmen gorge, the formation of which was of great significance in that it initiated through-going drainage between the upper-middle and lower reaches of the system. The timing of this event, which was clearly a critical point in the evolution of the Yellow River, can be established by dating the terraces in the gorge. Intermittent deepening of this gorge by the Yellow River from a high-level planation surface capping the mountain range has resulted in the formation of five terraces. Magnetostratigraphic records from aeolian deposits accumulated on these surfaces provide a geochronological sequence for this geomorphic archive, in which the ages of the planation surface and of terraces T5, T4, T3, T2, and T1 have been determined as ~3.63 Ma, ~1.24 Ma, ~0.86 Ma, ~0.62 Ma, ~129 ka, and ~12 ka, respectively.

Under the constraint of this chronological framework, a model for landscape evolution is proposed here. Uplift of the inner Fenwei graben and of the surrounding mountain ranges led to dissection of the 3.63 Ma old planation surface in conjunction with the formation of the Sanmen gorge. Drainage of the lake previously occupying the basin would have promoted incision into the fluvio-lacustrine graben sediments; indeed, gorge formation through the Xiaoshan may have been initiated or intensified by lake overflow. The ages obtained for the planation surface and uppermost terrace suggest that the formation of the Sanmen gorge and the initiation of the through-going eastward drainage of the Yellow River occurred between 3.63 and 1.24 Ma. Before the start of gorge entrenchment, the products of erosion in the modern upper catchment of the Yellow River were unable to reach the sea. The dramatic increase in deposition rates in the Bohai Gulf (at the mouth of the modern Yellow River in the East China Sea), ~1.0 Ma ago, thus resulted from the

initiation of an integral (enlarged) Yellow River catchment drainage through the Sanmen gorge; it does not imply an increase in erosion rates at that time.

Dear Editor,

re: revised manuscript with reference number 'JQSR-D-16-00135R2'.

Title: The linking of the upper-middle and lower reaches of the Yellow River as a result of fluvial entrenchment

Authors: Zhenbo Hu*, Baotian Pan, David Bridgland, Jef Vandenberghe, Lianyong Guo, Yunlong Fan, Rob Westaway

Please, find enclosed our revised manuscript intended for publication in the FLAG special issue of "Quaternary Science Reviews".

It should be pointed out that this work is a thorough improved version of our previous manuscript.

The referee and guest editor stated many valuable comments and constructive suggestions. According to these comments and suggestions, we made a point to point revision to the previous manuscript, with an item-by-item explanation attached.

We like to express our great appreciation for your editorial efforts.

With our best regards,

Zhenbo Hu

Corresponding author of JQSR-D-16-00135R2

1 **The linking of the upper-middle and lower reaches of the Yellow River as a result**
2 **of fluvial entrenchment**

3

4 ZhenBo Hu^{a, *}, BaoTian Pan^{a, *}, David Bridgland^b, Jef Vandenberghe^c, LianYong
5 Guo^a, YunLong Fan^a, Rob Westaway^d

6

7 ^aKey Laboratory of Western China's Environmental Systems (Ministry of Education),
8 College of Earth and Environmental Sciences, Lanzhou University, Lanzhou 730000,
9 People's Republic of China

10

11 ^bDepartment of Geography, Durham University, South Road, Durham DH1 3LE, UK

12

13 ^cDepartment of Earth Sciences, Vrije Universiteit, De Boelelaan 1085, 1081 HV
14 Amsterdam, The Netherlands

15

16 ^dSchool of Engineering, University of Glasgow, James Watt (South) Building,
17 Glasgow G12 8QQ, UK

18

19 *Corresponding author. E-mail: zhbhu@lzu.edu.cn; hu_zhb@126.com (Z. Hu)

20 **Abstract**

21

22 The upper–middle Yellow River flows through the Fenwei graben, a structure
23 resulting from extensional tectonism that was formed and repeatedly extended during
24 the Cenozoic. The drainage system within this graben was formerly isolated from the
25 lower reaches of the Yellow River system by the Xiaoshan mountains, an actively
26 growing ~NW–SE trending range. The modern course of the Yellow River takes it
27 through this range along the Sanmen gorge, the formation of which was of great
28 significance in that it initiated through-going drainage between the upper–middle and
29 lower reaches of the system. The timing of this event, which was clearly a critical
30 point in the evolution of the Yellow River, can be established by dating the terraces in
31 the gorge. Intermittent deepening of this gorge by the Yellow River from a high-level
32 planation surface capping the mountain range has resulted in the formation of five
33 terraces. Magnetostratigraphic records from aeolian deposits accumulated on these
34 surfaces provide a geochronological sequence for this geomorphic archive, in which
35 the ages of the planation surface and of terraces T5, T4, T3, T2, and T1 have been
36 determined as ~3.63 Ma, ~1.24 Ma, ~0.86 Ma, ~0.62 Ma, ~129 ka, and ~12 ka,
37 respectively.

38 Under the constraint of this chronological framework, a model for landscape
39 evolution is proposed here. Uplift of the inner Fenwei graben and of the surrounding
40 mountain ranges led to dissection of the 3.63 Ma old planation surface in conjunction
41 with the formation of the Sanmen gorge. Drainage of the lake previously occupying
42 the basin would have promoted incision into the fluvio-lacustrine graben sediments;
43 indeed, gorge formation through the Xiaoshan may have been initiated or intensified
44 by lake overflow. The ages obtained for the planation surface and uppermost terrace
45 suggest that the formation of the Sanmen gorge and the initiation of the through-going
46 eastward drainage of the Yellow River occurred between 3.63 and 1.24 Ma. Before
47 the start of gorge entrenchment, the products of erosion in the modern upper
48 catchment of the Yellow River were unable to reach the sea. The dramatic increase in
49 deposition rates in the Bohai Gulf (at the mouth of the modern Yellow River in the
50 East China Sea), ~1.0 Ma ago, thus resulted from the initiation of an integral
51 (enlarged) Yellow River catchment drainage through the Sanmen gorge; it does not
52 imply an increase in erosion rates at that time.

53

- 54 *Keywords:* Yellow River; Sanmen gorge; Fenwei graben; Terrace; Planation surface;
- 55 Fluvial incision rate

56 **1. Introduction**

57

58 Many of the world's largest rivers flow along structural lows and major rift
59 systems (Potter, 1978) and, meanwhile, have shaped the landscape over large areas. In
60 those regions that have been entrenched, the interaction between climate, uplift,
61 lithology, and base level have been fundamental controls on the evolution of fluvial
62 systems (Schumm et al., 2000; Veldkamp and van Dijke, 2000; Pan et al., 2003;
63 Bridgland and Westaway, 2008; Vandenberghe et al., 2011). Moreover, information
64 about tectonic activity and climatic change can be imprinted into sedimentary and
65 morphological fluvial archives (e.g., Bridgland, 2000; Stokes, 2008; Westaway, 2009;
66 Craddock et al., 2010; Bridgland et al., 2012; Bridgland and Westaway, 2014). The
67 development of large rivers is thus widely employed to determine the history of
68 structural, environmental, and topographical change during the Quaternary.

69 The formation of the Tibetan Plateau is generally thought to have been an
70 amplifier and driver for the environmental evolution of East Asia, strengthening the
71 East Asian monsoon and thus having an influence on precipitation and related erosion
72 rates (Li, 1991; Pan et al., 1995; Liu and Chen, 2000). Constraint on its uplift history
73 provides the basis for understanding the effects of high topography on climate and on
74 various earth surface processes (An et al., 2001).

75 The development of fluvial systems in East Asia has also been closely associated
76 with topographical evolution since the India–Eurasia collision (e.g., Powell and
77 Conaghan, 1973; Lin et al., 2001; Fan and Li, 2008). The eastward flow direction of
78 the largest rivers in China (e.g., the Yellow River and the Yangtze) is generally
79 attributed to the relative eastward decline of the macro-relief, resulting from the uplift
80 of the Tibetan Plateau (Miao et al., 2008; Craddock et al., 2010; Zheng et al., 2013).
81 Marine accumulation of terrigenous sediments derived from these large fluvial
82 systems may be assumed to have started in the Bohai Gulf immediately after the
83 formation of this drainage pattern (Zheng et al., 2004; Jiang et al., 2007). The
84 establishment of these eastward-flowing drainage systems provides a critical link
85 between upland erosion and the marine accumulation of terrigenous sediments (Nie et
86 al., 2015). Despite much attention having been paid to long-term fluvial landscape
87 development in East Asia, which is related to the uplift of the Tibetan Plateau during
88 the Quaternary, the formation age of the eastward drainage pattern in China is still
89 strongly debated (cf. Lin et al., 2001; Clark et al., 2004; Pan et al., 2005b; Clift, 2006;

90 Zheng et al., 2007, 2013). It is the specific objective of this paper to reconstruct the
91 eastward drainage history of the Yellow River by dating its terraces in the critical
92 reach between its middle and lower catchments. The formation ages of terraces T4, T3
93 and T2 at Sanmenxia were determined previously by Pan et al. (2005a) as 0.86 Ma,
94 0.62 Ma, and 0.129 Ma, respectively, but no dating was available for the highest
95 terrace T5 and the planation level in the study region.

96

97 **2. Regional geological and geomorphic setting**

98

99 2.1. General position of the Ordos block, Fenwei graben and Xiaoshan mountains

100

101 The Ordos block is an upland massif located at the northeastern margin of the
102 Tibetan Plateau and bounded by graben systems. During the Mesozoic, this block was
103 a large basin with an area of ~320,000 km² (Zhu et al., 2008) and was filled with
104 terrigenous clastic sediments. Following the Indo-Asian collision (Molnar et al., 1993),
105 deformation progressively propagated from the collision zone to the northeastern
106 margin of the Tibetan Plateau (Tapponnier et al., 2001; Fig. 1, inset). Arc-shaped
107 thrust faults and strike-slip fault systems were thus generated between the Ordos
108 block and the Tibetan Plateau, leading to the formation, by extensional stress, of the
109 crescent-shaped Fenwei graben (Zhang et al., 1998, 2003; Huang et al., 2008; Liu et
110 al., 2013). Meanwhile, the Ordos block and the Qinling, Huashan, Luliang, and
111 Taihang (including the Xiaoshan) mountains were uplifted with respect to this
112 subsiding graben (AFSOM, 1988). In the middle reaches of the Yellow River, the
113 landscape is characterized by a topography of alternating depressions and rolling
114 uplands, consisting of the above-mentioned ranges. Apatite fission track data and
115 geomorphic chronology have indicated that this area was uplifted in the early
116 Miocene and was then planated by the late Neogene (Yuan et al., 2007; Pan et al.,
117 2012).

118

119

<Fig. 1 hereabout>

120

121 The Fenwei graben is a NE–SW trending, crescent-shaped subsided area
122 constrained by numerous normal and strike-slip faults, covering more than 20,000
123 km² (AFSOM, 1988; Fig. 1). Its basement is further intersected by internal

124 ENE-trending normal faults, forming four sub-basins, the Weihe, Fenhe, Yuncheng,
125 and Lingbao basins (Fig. 1). The Fenwei graben is generally considered to have been
126 an extensional area that was continuously subsiding during the Cenozoic, a response
127 to the eastward extrusion of the Tibetan Plateau (Zhang et al., 1998, 2003); it has
128 simultaneously been filled by ~4000 m of fluvio-lacustrine deposits (AFSOM, 1988).
129 Based on previous investigation, these sediments dominate most of the graben,
130 implying the existence of a large lake, from Sanmenxia in the east, Baoji in the west,
131 the Qinling mountains in the south, and Yumenkou in the north (Liu, 2004; Fig. 1).
132 These fluvio-lacustrine sediments are defined as the Sanmen Formation, characterized
133 by undeformed, generally horizontal and parallel lithostratigraphy (AFSOM, 1988),
134 pointing to regular vertical subsidence.

135

136 <Fig. 2 hereabout>

137

138 Subsidence, extensional tectonics and uplift have remained vigorous and active
139 during the Quaternary in the area of the Fenwei graben. Fault scarps and triangular
140 facets that can be traced for hundreds of kilometers are readily observed along the
141 northern front of the Qinling, Huashan, and the southern front (Xiaoshan) of the
142 Taihang Mountains (Dong et al., 2011). Major earthquakes around this graben are
143 known from historical records (Zhang et al., 2003). The middle and lower reaches of
144 the Yellow River are separated by the Xiaoshan mountains. To cross this topographic
145 barrier the Yellow River has incised deeply into these mountains, creating the Sanmen
146 gorge, between Sanmenxia and Xiaolangdi (Fig. 2 and Fig. 3). The Sanmen gorge is
147 constrained by normal and strike-slip faults (Fig. 2), and is transected by numerous
148 inferred inner faults (Fig. 3). Many ground fissures associated with earthquakes are
149 exposed along these inferred faults within the gorge, indicating that uplift of the
150 Xiaoshan with respect to the Lingbao basin, to the northwest, and the North China
151 Plain (to the southeast) has never ceased (AFSOM, 1988).

152

153 <Fig. 3 hereabout>

154

155 The modern landscape in the vicinity of the Sanmen gorge is an uplifted and
156 rolling surface that is well preserved on resistant rocks in the higher parts of the area.
157 It represents a remnant of a planation surface that was cut through most of the

158 pre-existing tectonic structures and the relief right across the Lingbao basin, the
159 Xiaoshan range, and the North China Plain (Fig. 4A). This geomorphic surface was
160 deformed strongly over the Xiaoshan (Fig. 4B), forming a convexity between the
161 Lingbao basin and the North China Plain (Fig. 2). In general, its altitude exhibits a
162 declining trend towards the east, falling below 400 m in the North China Plain.

163

164

<Fig. 4 hereabout>

165

166 2.2. The downstream part of the Yellow River

167

168 The Yellow River (Huanghe) originating from the northeastern margin of the
169 Tibetan Plateau and flowing eastwards across China, crosses numerous tectonic zones
170 and major active faults. The Xiaoshan mountain range represents the final barrier to
171 be crossed by the river before it flows across the North China Plain and finally
172 debouches, attaining a total length of 5464 km (Wang et al., 2001), with its huge
173 sediment load, into the Bohai Gulf (Saito et al., 2001; Fig. 1, inset). The North China
174 Plain, which was formed from the steady supply of sediments from the upper and
175 middle reaches of the Yellow River, has remained close to sea level throughout the
176 Quaternary (Yang and Chen, 1985), experiencing marine inundation during some
177 interglacial periods (Geng, 1981). Sedimentary cores from this plain were analyzed in
178 an attempt to identify the oldest fluvial sediments from the Yellow River, thereby
179 dating the initiation of its eastward flow (Liu et al., 1988). However, the river has a
180 long history of wandering in disparate courses across the North China Plain, resulting
181 in deposition at different times at different sites, which has led to estimates for the
182 date of eastward-drainage initiation that range from Early to Late Pleistocene (Xia et
183 al., 1993; Yu, 1999; Wu et al., 2000; Yang et al., 2001).

184

185 2.3. The evolution of the Fenwei graben and the Sanmen gorge

186

187 The Fenwei graben, situated upstream of the Sanmen gorge, was occupied,
188 before the formation of the Yellow River, by a lake that covered the Weihe, Fenhe,
189 Yuncheng, and Lingbao basins (Liu, 2004). The ages of the uppermost
190 fluvio-lacustrine sediments within these basins range from 1.85 Ma to 150 ka (He et
191 al., 1984; Yue et al., 1999; Ji et al., 2006), representing an imprecise chronological

192 framework for the formation of the eastward drainage pattern of the Yellow River
193 through the Sanmen gorge. Furthermore, recent work using cosmogenic nuclide
194 dating, combined with provenance analysis of zircon and U–Pb age distributions,
195 suggests that the Sanmen gorge was initially entrenched, during the period from 1.5 to
196 1.3 Ma, by the eastward draining Weihe River, which is now the largest tributary of
197 the Yellow River (Kong et al., 2014). Comparative analysis of ostracod assemblages
198 (*Lishania*) from the fluvio-lacustrine sediments in the Fenwei graben and from the
199 fluvial sediments in the North China Plain suggests a close correlation between the
200 two areas after ~1.0 Ma, implying the existence of eastward drainage by that time
201 (Xue, 1996). Finally, at Mangshan, ~100 km downstream of the Sanmen gorge (Fig.
202 2), a dramatic increase in the accumulation rate of loess since the formation of
203 palaeosol S2 was suggested to result from a proximal contribution of silt blown from
204 the Yellow River floodplain, suggesting that eastward drainage had been formed at the
205 latest by c. 243 ka, which is the formation age of S2 (Jiang et al., 2007; Zheng et al.,
206 2007; Prins et al., 2009).

207 An important objective of this paper is to reconstruct the eastward drainage
208 history of the Yellow River within a geochronological framework. The initiation of
209 this eastward draining river has remained a highly controversial topic. Given that river
210 terraces, as former floodplains (Bull, 1990; Merritt et al., 1994), can provide
211 compelling evidence for determining drainage development (Stokes, 2008; Westaway
212 et al., 2009; Vandenberghe et al., 2011), the dating of such terraces along the Sanmen
213 gorge can provide important evidence (Pan et al., 2005a; Zheng et al., 2007; Kong et
214 al., 2014). Most of the terraces in the gorge are directly overlain by thick aeolian loess
215 covers, which can offer an excellent age control for the underlying terraces sediments
216 (e.g., Liu, 1985; Pan et al., 2009, 2012; Guo et al., 2012). The chronological
217 framework from these loess covers has been based on a combined approach of
218 magnetostratigraphy, pedostratigraphy, electron spin resonance (ESR), and
219 luminescence dating, and cosmogenic radionuclide geochronology (e.g., Cheng et al.,
220 2002; Pan et al., 2009; Craddock et al., 2010; Zhang et al., 2010; Perrineau et al.,
221 2011). From the constraint provided by the loess stratigraphy, the age of the highest
222 Yellow River terrace at the downstream end of the Sanmen gorge was determined at
223 1.2 Ma by Pan et al. (2005b). In contrast, the oldest terrace at the gorge inlet was
224 considered significantly younger, at only 0.8 Ma (Pan et al., 2005a). This temporal
225 mismatch may be attributed to incomplete age control from the loess covers in the

226 gorge.

227 A series of well-preserved terraces was formed by the Yellow River in the
228 Sanmen gorge during its incision into the Xiaoshan. Here, detailed field investigation
229 was performed to establish a complete sequence of geomorphic surfaces. Next, a new
230 geochronology for the geomorphic archive is presented, based on the combined
231 approach of magnetostratigraphy, pedostratigraphy, and optically stimulated
232 luminescence (OSL) dating of the aeolian cover on the geomorphic surfaces. Finally,
233 this geochronology is used to constrain the formation age of the eastward-draining
234 Yellow River.

235

236 <Fig. 5 hereabout>

237

238 **3. Method**

239

240 3.1. Field research

241

242 Intermittent downcutting by the Yellow River, starting from the planation surface
243 and cutting into the bedrock of the Xiaoshan to form the Sanmen gorge, has given rise
244 to a series of terraces along the valley. Field observations suggest that these terrace
245 treads are generally disposed asymmetrically within the valley. To elucidate the
246 formation history of the Yellow River within this gorge, work has focused on five
247 geomorphic cross-sections, from Zhangbian to Kouma (Fig. 3). For each cross-section,
248 terraces below the planation surface were identified and their tread heights (top of
249 fluvial deposits) above river level determined, the characteristics of the fluvial
250 deposits were described, and the thickness of overlying aeolian sediments (loess and
251 Red Clay) was measured.

252

253 <Table 1 hereabout>

254

255 The five transect sites were selected as representative of the supposed relict
256 planation surface and of the suite of lower-level fluvial terraces. The transect at
257 Zhangbian is located within the Lingbao basin. The transects at Sanmenxia, Dongcun,
258 and Xiaolangdi are located, respectively, at the inlet of, within, and at the outlet of the
259 gorge, whereas the Kouma site is ~20 km downstream of the gorge (Fig. 3). Field

260 measurements of terrace elevation and the thickness of overlying aeolian cover were
261 performed using a differential GPS system with an uncertainty of < 5 cm. According
262 to these results, combined with loess stratigraphy and geomorphic surface tracking,
263 terrace sequences at these sites were outlined (Fig. 5) and correlated (Table 1). It
264 appears that the altitude of the planation surface and the vertical separation between
265 high terrace treads and the present-day river level increase considerably at first and
266 then gradually decrease with downstream distance along the gorge (Fig. 6). This
267 topographical pattern corresponds with the convexity, mentioned above, thought to
268 relate to the active uplift of the Xiaoshan range.

269

270 <Fig. 6 hereabout>

271

272 3.2. Aeolian deposits capping the geomorphic surfaces

273

274 The aeolian sediments (Tertiary Red Clay and overlying Quaternary loess)
275 covering the planation surface and terrace treads provide valuable age estimates for
276 the underlying landforms. However, the aeolian covers are rather thin at Dongcun and
277 Xiaolangdi in comparison with those at Zhangbian, Sanmenxia, and Kouma, probably
278 because accumulation was less in the confined Sanmen gorge (Fig. 5). Thus the
279 Sanmenxia transect was selected for the analysis of magnetostratigraphy and
280 pedostratigraphy of the aeolian sequence.

281 With reference to the established timescale of the aeolian sedimentary sequence
282 on the Chinese Loess Plateau, enhanced by astronomical tuning and paleomagnetism,
283 the basal ages of aeolian cover on each terrace along the Sanmen gorge can be
284 determined. Readers are referred to Ding et al. (2002) for a detailed
285 chronostratigraphic framework of the Chinese loess. Thus these aeolian series, in
286 combination with their magnetostratigraphic and pedostratigraphic properties, provide
287 a geochronological framework for the terrace sequences in the five Yellow River
288 transects, as will now be described. The present study concentrates on the, hitherto
289 undated, aeolian deposits above the planation surface and terrace T5.

290

291 3.3. Magnetic susceptibility measurements

292

293 Magnetic susceptibility reflects the layering of loess and palaeosols (Soreghan et

294 al., 1997) and thus can further confirm the identification of pedostratigraphic units
295 and aid correlation. Powder samples were taken at 0.05-m intervals from the aeolian
296 covers of the planation surface and uppermost terrace (T5). A total of 5650 samples
297 were air-dried in the laboratory and then gently ground. Measurements with a
298 Bartington MS2B magnetic susceptibility meter were used to obtain the mass
299 magnetic susceptibility (Fig. 7).

300

301 <Fig. 7 hereabout>

302

303 3.4. Paleomagnetism

304

305 Samples were taken from the 152-m and 130.5-m thick aeolian deposits
306 accumulated respectively on top of the planation surface and the uppermost terrace
307 (T5). A total of 441 oriented block samples were collected at 0.25-m intervals in the
308 Red Clay and at intervals of ~0.5–3.0 m in the loess. In the laboratory these samples
309 were cut into 2-cm³ transects, producing three sets of paleomagnetic logs. All the
310 processed samples were thermally demagnetized in 15–17 steps at 50–30°C intervals
311 (between 50 and 680°C) with an MMTD-80 Thermal Demagnetizer. Remanent
312 magnetization and magnetic orientation were measured on a 2G-755R
313 Superconducting Rock Magnetometer in the magnetically shielded room of the
314 Paleomagnetic Laboratory of the Key Laboratory of western China's Environmental
315 System (MOE), Lanzhou University.

316 Two components are generally distinguished in the palaeomagnetic signal, by
317 contrasting directions and intensities. A low-temperature component (LTC) in roughly
318 the normal polarity direction is removed gradually by thermal treatment in the interval
319 100–150 °C (but sometimes up to 200–350 °C). This LTC is generally interpreted as a
320 secondary remanent magnetization characterized by a viscous superimposed direction.
321 Upon removal of the LTC, a high-temperature component (HTC) shows relatively
322 stable directions and linear decay in intensity toward the origin. This HTC is generally
323 interpreted as the primary magnetization acquired during deposition. The directions of
324 the HTC are calculated using the least-squares fitting technique (Kirschvink, 1980)
325 for selected demagnetization data points (minimum of three, but mostly 5–10).

326

327 4. Results

328

329 4.1. The terrace succession

330

331 A well-preserved sequence of five strath terraces was identified between the
332 present river bed and the planation surface (Fig. 4C and D), within which the
333 uppermost terrace is newly recognized in comparison with the previous study by Pan
334 et al. (2005a). The term strath terrace is used here to describe an erosional terrace with
335 only a relatively thin gravel layer, isolated vertically from the gravels of other terraces.
336 In this terrace sequence, all treads are eroded into the Early Pleistocene lacustrine
337 Sanmen Formation (see Fig. 4E for sedimentary characteristics). The planation
338 surface, cut through pre-existing limestone, basin-fill sediments, and tectonic
339 structures, is overlain by 12.5-m-thick Red Clay and a 139.5 m thick loess sequence,
340 characterized by alternating loess (L) and palaeosol (S) units (Fig. 7). No indications
341 of erosional disconformity between the Red Clay and the loess have been observed.
342 Palaeosol complex S5, consisting of three sub-palaeosols, is the most prominent one
343 within the sequence on the Chinese Loess Plateau, and is distinguished by its great
344 thickness and dark color, being generally regarded as a marker layer (Liu, 1985). It
345 can be discerned by field observations to occur at a depth of 107.6–115.3 m in the
346 aeolian cover of the planation surface at Sanmenxia, which contains 32 palaeosol
347 units (Fig. 7). The loess deposits above the gravels of terraces T5, T4, T3, and T2 are
348 ~130, 114, 64, and 30 m thick respectively (Fig. 7). From detailed field observations,
349 the loess stratigraphy on these four terraces can be divided, respectively, into fifteen,
350 nine, six, and three red palaeosol units, which can be readily correlated with the upper
351 palaeosol units (S14 to S1) on the planation surface. The basal palaeosol units of each
352 terrace can be shown to overlie the fluvial deposits without a significant hiatus. In the
353 case of the planation surface and terrace T5, these pedostratigraphic correlations,
354 based on field observations, have been further corroborated by patterns of magnetic
355 susceptibility variation (see below). The lowermost terrace has been OSL-dated to
356 12.7 ± 1.2 ka (HZB-2; Fig. 5).

357

358 4.2. Magnetic susceptibility

359

360 Magnetic susceptibility reflects the distinction between loess (L) and palaeosols
361 (S), with higher values in palaeosols than in loess (e.g., Kukla et al., 1988; Maher and

362 Thompson, 1991; Soreghan et al., 1997). The variation patterns of magnetic
363 susceptibility in the loess deposits on the planation surface and uppermost terrace (T5)
364 are closely consistent with field observations of pedostratigraphy (Fig. 7). For
365 palaeosol complex S5 in the two studied loess covers, the magnetic susceptibility
366 increases steeply and reaches its highest value in the middle part of this complex,
367 suggesting a prominently developed palaeosol unit. More specifically, large amplitude
368 fluctuations of magnetic susceptibility appear in this palaeosol complex, showing
369 three marked peaks that correspond well with the three subsidiary divisions of this
370 prominent S5 palaeosol. Using S5 as a marker horizon, magnetic susceptibility data
371 were used to divide the loess sequences on the planation surface and terrace T5,
372 respectively, into 32 (from S1 to S32, with the basal loess unit L33) and 15 (Sm–S14)
373 established palaeosol units. The magnetic susceptibility patterns from these two loess
374 covers are in good agreement with comparable records from the Chinese Loess
375 Plateau (e.g., Lu et al., 1999; Pan et al., 2012). Their high magnetic susceptibility
376 values match well with the light red palaeosol units, implying that the
377 pedostratigraphic divisions based on field observations, as described in this paper, are
378 reliable.

379 The Red Clay beneath the Quaternary loess was deposited immediately on top of
380 the planation surface. Its magnetic susceptibility gradually increases upwards,
381 reaching its highest value at the top of the unit. Further upwards, the values decrease
382 markedly in the overlying pedogenic carbonate nodule layer and then recover in the
383 transitional layer (TU) between Red Clay and the overlying Quaternary loess. This
384 pattern of magnetic susceptibility in the Red Clay obtained here concurs with
385 magnetic susceptibility records from late Pliocene Red Clay sections on the Chinese
386 Loess Plateau (Sun et al., 2006; Pan et al., 2011).

387

388 4.3. Paleomagnetism

389

390 Three sets of palaeomagnetic transects, collected from the aeolian covers of the
391 planation surface and terrace T5 at each section, show similar properties. Most
392 samples maintain strong remanent magnetization, with clear separation of
393 characteristic remanent magnetization (ChRM) directions (see Fig. 8 for the typical
394 thermal demagnetization diagrams).

395

<Fig. 8 hereabout>

396

397

398 The pedostratigraphy and magnetic patterns of the aeolian covers on the
399 planation surface and uppermost terrace (T5) are illustrated in Fig. 7. The
400 magnetostratigraphic patterns from the two covers can be correlated with the
401 geomagnetic polarity timescale (GPTS) of Cande and Kent (1995).

402 In the 152.0-m thick aeolian deposits on the planation surface, both the
403 stratigraphic subdivision of the loess and the conformity between the Red Clay and
404 overlying loess deposits provide a reliable indication that the chronology of the
405 aeolian cover extends from the Pliocene to the late Pleistocene (Liu, 1985). Thus the
406 obtained magnetozones correlate typically with the polarity intervals from Brunhes to
407 Gauss in the geomagnetic polarity timescale. The Gauss normal-polarity chron occurs
408 between 0.5 and 11.5 m above the planation surface and includes two
409 reversed-polarity subchrons that pinpoint the basal age of aeolian deposits here to the
410 Kaena and Mammoth subchrons. The Gauss–Matuyama boundary occurs in the lower
411 part of TU, which is also the boundary between the Neogene Red Clay and
412 Quaternary loess (Liu, 1985; Ding et al., 1990). The Olduvai normal subchron,
413 spanning 38–30 m, occurs between S27 and L25. The Jaramillo normal subchron,
414 extending from 74.5 to 82.0 m, is registered between S11 and L10. The
415 Matuyama–Brunhes boundary is found at a depth of 98.0 m in L8. These
416 paleomagnetic polarity events identified in the stratigraphy on the planation surface
417 are in full agreement with the well-established loess and Red Clay
418 magnetostratigraphy on the Chinese Loess Plateau (cf. Kukla and An, 1989; Rutter et
419 al., 1991; Zhu et al., 1994; Ding et al., 1998; Pan et al., 2012). On the Loess Plateau,
420 since the sedimentation rate in the Red Clay (~1.5 cm/ky) was generally lower than
421 that in the Quaternary loess (~10 cm/ky) (e.g., Vandenberghe et al., 2004),
422 extrapolation of the prevailing accumulation rate of the Red Clay (here, ~1.1 cm/ky
423 within the Gauss chron) below the lower boundary of the Gauss normal polarity chron
424 is a more logical approach for dating the basal Red Clay, rather than using an
425 accumulation rate averaged over the entire aeolian sequence (Red Clay and loess).
426 This approach yields an estimated age of ~3.63 Ma for the onset of aeolian deposition
427 on the planation surface.

428 For the ~130 m thick loess cover stacked on the uppermost terrace (T5), the
429 Matuyama–Brunhes boundary occurs at a depth of 49.0 m and coincides with L8. The

430 Jaramillo normal subchron, spanning from 18.0 to 28.5 m, is registered between S11
431 and L10. It is clear that the positions of these paleomagnetic polarity events may
432 readily be correlated with the magnetostratigraphy derived from the aeolian cover of
433 the planation surface. Extrapolation of the prevailing accumulation rate of the loess
434 deposits (~10.5 cm/ky) below the lower boundary of the Jaramillo normal subchron
435 produces an estimated age of ~1.24 Ma for the basal loess deposits lying on this
436 terrace.

437

438 **5. Discussion**

439

440 5.1. Age determination of the fluvial terraces within the Sanmen gorge

441

442 In most cases there is a gradual transition from terrace gravel to overbank
443 sediments and, finally, to primary (in situ) aeolian deposits (Vandenberghe et al.,
444 2012). Therefore, the basal age of the aeolian deposits immediately overlying the
445 planation surface and terrace treads can be roughly equated with the formation times
446 of the geomorphic surfaces (planation and fluvial terrace surfaces). Supplementary to
447 the previous dating of terraces T4, T3, and T2 by Pan et al. (2005a), to 860, 620, and
448 129 ka, respectively, the newly recognized planation surface and uppermost terrace
449 (T5) have now provided age estimates also (Fig. 7). Although the terrace called T5
450 here was previously recognized by Kong et al. (2014), its age was not determined
451 successfully by their cosmogenic radio nuclide (CRN) study, which may be linked to
452 the difficulty of getting reliable burial dates from river terrace deposits (Rixhon et al.,
453 2016). In comparison, the latter authors assigned an age of 1.3 Ma to the lower
454 sediments of terrace T4, which is older than the abandonment age of 860 ka obtained
455 by Pan et al (2005a). According to the magnetostratigraphic analyses of the basal parts
456 of the aeolian covers, the ages of the planation surface and terrace T5 are ~3.63 Ma
457 and ~1.24 Ma, respectively; the latter age is close to the 1.5 – 1.3 Ma suggested by
458 Kong et al. (2014) for the initiation of drainage (by the Weihe River) through the
459 Sanmen gorge.

460 On the basis of field investigation, the tread of the uppermost terrace (T5) at
461 Sanmenxia can be traced over an extensive area upstream and extending downstream
462 into the inner Sanmen gorge, and can be correlated tentatively (based on height above
463 modern river) with the uppermost terraces formed at Zhangbian, Dongcun, and

464 Xiaolangdi (Fig. 6). This distribution pattern indicates that the uppermost terrace
465 below the planation surface is generally continuous, representing the initial fluvial
466 incision by the Yellow River within the gorge. In addition, the magnetostratigraphic
467 record from the uppermost terrace at Kouma, downstream of the Sanmen gorge, has
468 also been dated previously to ~1.2 Ma (Pan et al., 2005b). The temporal coincidence
469 of the uppermost terraces upstream and downstream of this gorge suggests that the
470 first phase of downcutting by the Yellow River from the planation surface to the level
471 of the uppermost terrace was prior to ~1.2 Ma (again in general agreement with the
472 previous conclusions of Kong et al. (2014)).

473

474 5.2. Evolution of the middle to lower Yellow River catchment from basin filling to 475 entrenchment

476

477 The magnetostratigraphic record from the aeolian cover of the planation surface
478 at Sanmenxia suggests that before 3.63 Ma the Fenwei graben (represented by the
479 Lingbao basin) had become progressively filled with the lacustrine sediments (Fig.
480 9AI). Geomorphic investigation along the Sanmen gorge (Fig. 5) indicates that at this
481 time the local relief was progressively lowered to basin-fill level, eventually forming
482 the planation surface (Fig. 9AII) that extends across the Fenwei graben and the
483 surrounding mountain ranges (including the Xiaoshan) as was the case at the northern
484 Tibetan Plateau (Wang et al., 2012).

485

486 <Fig. 9 hereabout>

487

488 Elsewhere, the development of low-relief landscapes ('planation surface') has
489 been claimed as a reliable marker to indicate subsequent landscape rejuvenation,
490 uplift and deformation (e.g., Ollier and Pain, 2000; Clark et al., 2004; Peulvast and
491 Sales, 2004). Before and during the Pliocene, large parts of Europe, Africa, and Asia
492 were planated, all in areas that were unaffected by plate motions, thus leading to the
493 widespread development of low-relief landscapes (e.g., Cui et al., 1996; Danišik et al.,
494 2006; Coltorti et al., 2007; Wagner et al., 2011; Pan et al., 2012; Vandenberghe, 2016).
495 The comparable low-relief landscape or 'planation surface', recognized in and around
496 the Fenwei graben and the Xiaoshan has been significantly uplifted by plate tectonic
497 processes and subsequently dissected. The continuation of tectonic activity after the

498 formation of the planation level during the late Pliocene and Quaternary can be
499 demonstrated. First, as is apparent from the geomorphic section at Sanmenxia (Fig. 5),
500 the downthrow of the hanging-walls along the normal faults bounding the Lingbao
501 basin (within the graben system of the Fenwei; Fig. 9B) disrupted the ‘planation
502 surface’, which itself became uplifted in the Xiaoshan area. Second, seismic data also
503 indicate that the normal faults bounding the Lingbao basin have remained active
504 during the Quaternary (Li et al., 2015). The evolution of this active basin was
505 probably independent of the rest of the southern Shanxi rift. As the Xiaoshan
506 mountains grew higher, the ancestral fluvial system that drained their eastern front
507 began to cut headward, toward the west (Wang et al., 2001).

508 The sedimentary record in the North Pacific indeed shows that dust deposition
509 increased quite rapidly, by an order of magnitude, at 3.6 Ma (Rea, et al., 1998), which
510 may have been associated with the uplift of the Tibetan Plateau and the cooling of the
511 northern hemisphere. Continuous aeolian deposition in the present study region also
512 began by this time, resulting in accumulation on the ‘planation surface’ (our basal
513 age). After this time, this inner sub-basin of the Fenwei graben, which previously
514 drained internally, became filled with fluvio-lacustrine sediments (the Sanmen
515 Formation, illustrated in Fig. 4E) with a paleolake eventually covering much of the
516 graben (Liu, 2004). This lake was then drained and the Sanmen gorge formed,
517 initiating external drainage and linkage to the Yellow River system.

518 We suggest that the remarkable transition of the Fenwei graben, from filling to
519 excavation (incision), was thus associated with the establishment of external drainage
520 and the formation of the Sanmen gorge. The Xiaoshan barrier may have been
521 breached by lake spillover as the ancestral fluvial system at its eastern front cut
522 headward towards the Lingbao basin (Fig. 9C I). Subsequently, following the
523 emptying of the lake, fluvial incision into the sediments of the Sanmen Formation
524 began (Fig. 9CII). The geomorphic evidence indeed suggests that this drainage
525 integration was associated with fluvial downcutting, from the ‘planation surface’
526 down to the level of the uppermost terrace (T5). The approximately synchronous
527 development of this terrace both within the Sanmen gorge and further downstream at
528 Kouma (see above), with dates of ~1.24 Ma and 1.2 Ma (respectively), indicates that
529 the modern Yellow River had been established by this time and subsequently became
530 entrenched (Fig. 9D). The formation of a river terrace staircase within the Fenwei
531 graben is notable, implying that the graben interior is uplifting (a requirement for

532 terrace formation), albeit at a slower rate than the crust outside the faulted interior of
533 the system (cf. Gao et al., 2016).

534 The initial development of the Sanmen gorge was thus an important event, since
535 it marked the initiation of the eastward-flowing drainage of the Yellow River. Once
536 this gorge had begun to form, terrigenous sediments could be transported from the
537 interior of the Tibetan Plateau, in the upper reaches of the Yellow River, to the Bohai
538 Gulf. Although loess began to accumulate in the present study region at significant
539 rates by ~3.6 Ma, terrigenous sedimentation rates on the North China Plain and in the
540 Bohai Gulf did not show dramatic increases until ~1.0 Ma (Xiao et al., 2008; Yao et
541 al., 2010, 2012), in all probability in response to the formation of the Sanmen gorge.
542 As Nie et al. (2015) have suggested, the majority of the sediment liberated by the
543 dissection of the 'planation surface' from the middle and upper Yellow River basins
544 was probably stored on the Chinese Loess Plateau before the through-going Yellow
545 River drainage system was formed.

546 The formation of the Sanmen Gorge, which enabled through drainage from the
547 upper Yellow River to the Bohai Gulf, would appear to have been the last in a series
548 of linkage events joining inland basins. This progressive drainage linkage can now be
549 envisaged to have occurred in sequence from upstream to downstream (contra Molnar,
550 2004), perhaps by means of repeated basin overflow in response to progressive basin
551 filling coupled with increasing precipitation from the strengthening Asian Monsoon.
552 The occurrence of this final eastern completion of the through-flowing Yellow River
553 can also be demonstrated by the change in the type of zircon grains in the thick
554 perched sedimentary sequence at Liujiahou (close to our site at Sanmenxia) reported
555 by Kong et al. (2014), and called T5 by them. Zircon in the lower sediments here were
556 of more local origin, whereas those from a sample high in the sequence (like those
557 from later terrace sediments) were from upstream in the Yellow River, suggesting that
558 basins upstream had been joined to form a through-flowing system by the time these
559 uppermost sediments were deposited, just before incision by the newly-formed river
560 and the development of the lower terrace staircase.

561

562 5.3. Wider comparisons

563

564 Similar sequences of events, whereby ancestral lake basins were disrupted and
565 replaced by fluvial drainage, are also recognized in other continental interior regions

566 worldwide. For example, the history of integration of the upper reaches of the modern
567 River Euphrates (in the eastern Anatolian Plateau) with the rest of its catchment,
568 starting in the Mid-Pleistocene and associated with the disruption of paleolake basins,
569 as investigated by Seyrek et al. (2008), Westaway et al. (2008), and Demir et al.
570 (2009). Regional uplift of the eastern Anatolian Plateau and active faulting both
571 played a part in this sequence of events. Another example, documented by Westaway
572 et al. (2009), was the integration of the modern Rio Grande River in the
573 central-southern USA. In that example the upper reaches of the ancestral river system
574 drained into a paleolake in the Rio Grande Rift, an actively-developing graben;
575 however, faster regional uplift following the Mid-Pleistocene Revolution resulted in
576 disruption of this lake basin and the initiation of fluvial entrenchment, marked by
577 dated river terraces, into its former interior. Numerous other examples of ‘inverted’
578 Late Cenozoic fluvio-lacustrine basins could be documented, including many reported
579 by earlier FLAG research (e.g., Matoshko et al., 2004; Bridgland and Westaway, 2014)
580 and in the present issue (Bridgland et al., 2016; Cunha et al., 2016; Maddy et al.,
581 2016).

582 Attempts have recently been made to integrate onshore datasets indicating rates
583 of erosion and offshore datasets indicating rates of deposition (e.g., Herman et al.,
584 2013; Herman and Champagnac, 2016). It has been argued on the basis of increases in
585 offshore sedimentation rates that accordingly terrestrial erosion rates increased (e.g.,
586 Zhang et al., 2001; Molnar, 2004). However, others have rejected the idea that erosion
587 rates have increased in the Late Cenozoic (e.g., Willenbring and von Blanckenburg,
588 2010; Sadler and Jerolmack, 2015; Willenbring and Jerolmack, 2016). It has been
589 shown here that the Yellow River and other major rivers only became integrated with
590 their present catchment geometries in the relatively recent geological past, such that,
591 beforehand, the products of erosion throughout much of these catchments were
592 trapped in inland depocentres and were thus unable to reach the sea. This has to be
593 considered as an important complicating factor in attempting comparison of global
594 datasets of Late Cenozoic onshore erosion and offshore deposition.

595

596 **6. Conclusions**

597

598 Downcutting by the Yellow River into the Xiaoshan range, below a planation
599 surface dated to ~3.63 Ma, has resulted in the formation of the Sanmen gorge. On the

600 basis of detailed field investigation, a new and uppermost Yellow River terrace, T5,
601 has been recognized along the gorge. As a result, a sedimentary and geomorphic
602 archive of five terraces was formed, in addition to the above-mentioned planation
603 surface. Magnetostratigraphic records from the aeolian deposits accumulated on top of
604 these surfaces provide a geochronological framework for this archive. The ages of the
605 planation surface (P) and terraces T5, T4, T3, T2, and T1 have been determined at
606 ~3.63 Ma, ~1.24 Ma, ~0.86 Ma, ~0.62 Ma, ~129 ka, and ~12 ka, respectively. Thus,
607 the formation ages of the planation surface and uppermost terrace suggest that this
608 gorge was entrenched primarily between 3.63 and 1.24 Ma. At the same time the
609 landscape of the Fenwei region switched from basin filling to excavation ('basin
610 inversion') enabling the formation of a series of terraces within the graben. Before the
611 start of entrenchment of the Sanmen gorge, the products of erosion in the modern
612 upper catchment of the Yellow River were 'trapped' inland and, therefore, unable to
613 reach the sea. The dramatic increase in deposition rates in the Bohai Gulf, at the
614 mouth of the modern Yellow River, at ~1.0 Ma, resulted from the integration of the
615 Yellow River catchment following the initiation of drainage through Sanmen gorge
616 and does not imply an increase in erosion rates at that time.

617 **Acknowledgements**

618

619 We are grateful to Xiaopeng Liu, Jian Zhang, and Prof. Qingyu Guan for
620 assistance with the field sampling and laboratory analyses. The comments by Prof.
621 Frank J. Pazzaglia, an anonymous referee, and the special issue editor, Stéphane
622 Cordier, have led to considerable improvements and are gratefully acknowledged.
623 This research is financially supported by the National Natural Science Foundation of
624 China (Grant no. 41401001, 41571003), the Key Project of the Major Research Plan
625 of the NSFC (Grant no. 91125008), the National Basic Research Program of China
626 (2011CB403301), and the Fundamental Research Funds for the Central Universities.

627 **References**

628

629 AFSOM, 1988. Active fault system around Ordos Massif. Seismological Press,
630 Beijing, pp. 77-136 (in Chinese).

631

632 An, Z., Kutzbach, J.E., Prell, W.L., Porter, S.C., 2001. Evolution of Asian monsoon
633 and phased uplift of the Himalayan-Tibetan Plateau since Late Miocene times. *Nature*
634 411, 62-66.

635

636 Bridgland, D.R., 2000. River terrace systems in north-west Europe: an archive of
637 environmental change, uplift and early human occupation. *Quaternary Science*
638 *Reviews* 19, 1293-1303.

639

640 Bridgland, D.R., Westaway, R., 2008. Climatically controlled river terrace staircases:
641 A worldwide Quaternary phenomenon. *Geomorphology* 98, 285-315.

642

643 Bridgland, D.R., Westaway, R., Abou Romieh, M., Candy, I., Daoud, M., Demir, T.,
644 Galiatsatos, N., Schreve, D., Seyrek, A., Shaw, A., White, T., Whittaker, J., 2012. The
645 River Orontes in Syria and Turkey: Downstream variation of fluvial archives in
646 different crustal blocks. *Geomorphology* 165-166, 25-49.

647

648 Bridgland, D.R., Westaway, R., 2014. Quaternary fluvial archives and landscape
649 evolution: a global synthesis. *Proceedings of the Geologists' Association* 125,
650 600-629.

651

652 Bridgland, D.R., Demir, T., Seyrek, A., Abou Romieh, M., Daoud, M., Westaway, R.,
653 2016. River terrace development in the NE Mediterranean region (Syria and Turkey):
654 patterns in relation to crustal type. *Quaternary Science Reviews*.

655

656 Bull, W.B., 1990. Stream-terrace genesis: implication for soil development.
657 *Geomorphology* 3, 351-367.

658

659 Cande, S.C., Kent, D.V., 1995. Revised calibration of the geomagnetic polarity
660 timescale for the Late Cretaceous and Cenozoic. *Journal of Geophysical Research* 100,

661 6093-6095.
662
663 Cheng, S., Deng, Q., Zhou, S., Yang, G., 2002. Strath terraces of Jinshaan Canyon,
664 Yellow River, and Quaternary tectonic movements of the Ordos Plateau, north China.
665 Terra Nova 14, 215-224.
666
667 Clark, K.M., Schoenbohm, M.L., Royden, H.L., Whipple, X.K., Burchfiel, C.B.,
668 Zhang, X., Tang, W., Wang, E., Chen, L., 2004. Surface uplift, tectonics, and erosion
669 of eastern Tibet from large-scale drainage patterns. Tectonics 23, TC1006,
670 doi:10.1029/2002TC001402.
671
672 Clift, D.P., 2006. Controls on the erosion of Cenozoic Asia and the flux of clastic
673 sediment to the ocean. Earth and Planetary Science Letters 241, 571-580.
674
675 Coltorti, M., Dramis, F., Ollier, D.C., 2007. Planation surfaces in Northern Ethiopia.
676 Geomorphology 89, 287-296.
677
678 Craddock, H.W., Kirby, E., Harkins, W.N., Zhang, H., Shi, X., Liu, J., 2010. Rapid
679 fluvial incision along the Yellow River during headward basin integration. Nature
680 Geoscience 3, 209-213.
681
682 Cui, Z., Gao, Q., Liu, G., Pan, B., Chen, H., 1996. Planation surface, palaeokarst and
683 uplift of Xizang (Tibet) Plateau. Science in China 39, 391-400.
684
685 Cunha, P.P., Martins, A.A., Buylaert, J.P., Murray, A.S., Raposo, L., Mozzi, P., Stokes,
686 M., 2016. New data on the chronology of the Vale do Forno sedimentary sequence
687 (Lower Tejo River terrace staircase) and its relevance as a fluvial archive of the
688 Middle Pleistocene in western Iberia. Quaternary Science Reviews.
689 <http://dx.doi.org/10.1016/j.quascirev.2016.11.001>.
690
691 Danišík, M., Kuhlemann, J., Dunkl, I., Székely, B., Frisch, W., 2006. Significance of
692 high-elevated planation surfaces in interpreting thermotectonic evolution of the
693 mountains. Goldschmidt Conference Abstracts A126.
694

695 Demir, T., Seyrek, A., Guillou, H., Scaillet, S., Westaway, R., Bridgland, D.R., 2009.
696 Preservation by basalt of a staircase of latest Pliocene terraces of the River Murat in
697 eastern Turkey: evidence for rapid uplift of the eastern Anatolian Plateau. *Global and*
698 *Planetary Change* 68, 254-269.
699

700 Ding, Z., Liu, T. S., Liu, X. M., Chen, M. Y., An, Z. S., 1990. Thirty-seven climatic
701 cycles in the last 2.5 Ma. *Chinese Science Bulletin*. 34, 1494-1496.
702

703 Ding, Z., Sun, J.M., Yang, S.L., Liu, T.S., 1998. Preliminary magnetostratigraphy of a
704 thick eolian red clay-loess sequence at Lingtai, the Chinese Loess Plateau.
705 *Geophysical Research Letters*. 25, 1225-1228.
706

707 Ding, Z., Derbyshire, E., Yang, S., Yu, Z., Xiong, S., Liu, T., 2002. Stacked 2.6-Ma
708 grain size record from the Chinese loess based on five sections and correlation with
709 the deep-sea $\delta^{18}\text{O}$ record. *Paleoceanography* 17, 1033-1053.
710

711 Dong, Y., Zhang, G., Neubauer, F., Liu, X., Genser, J., Hauzenberger, C., 2011.
712 Tectonic evolution of the Qinling orogen, China: Review and synthesis. *Journal of*
713 *Asian Earth Sciences* 41, 213-237.
714

715 Fan, D., Li, C., 2008. Timing of the Yangtze initiation during the Tibetan Plateau
716 throughout to the East China Sea: A review. *Front Earth Science China* 2, 302-313.
717

718 Gao, H., Li, Z., Ji, Y., Pan, B., Liu, X., 2016. Climatic and tectonic controls on strath
719 terraces along the upper Weihe River in central China. *Quaternary Research* 86,
720 326-334.
721

722 Geng X., 1981. Marine transgressions and regressions in East China since Late
723 Pleistocene epoch. *Acta Oceanologica Sinica* 3, 114-130 (in Chinese, with English
724 abstract).
725

726 Guo, Y., Zhang, J., Qiu, W., Hu, G., Zhuang, M., Zhou, L., 2012. Luminescence dating
727 of the Yellow River terraces in the Hukou area, China. *Quaternary Geochronology* 10,
728 129-135.

729

730 He, P., Liu, L., Yu, Q., 1984. The age of the Sanmen series and the evolution of its
731 depositional environment discussed in the light of the Dongpogou section in the
732 Sanmen gorge area. *Geological Reviews* 30, 161-169 (in Chinese, with English
733 abstract).

734

735 Herman, F., Champagnac, J.-D., 2016. Plio-Pleistocene increase of erosion rates in
736 mountain belts in response to climate change. *Terra Nova*, 28, 2–10.

737

738 Herman, F., Seward, D., Valla, P.G., Carter, A., Kohn, B., Willett, S.D., Ehlers, T.A.,
739 2013. Worldwide acceleration of mountain erosion under a cooling climate. *Nature*,
740 504, 423–426.

741

742 Huang, Z., Xu, M., Wang, L., Mi, N., Yu, D., Li, H., 2008. Shear wave splitting in the
743 southern margin of the Ordos Block north China. *Geophysical Research Letters* 35,
744 L19301. <http://dx.doi.org/10.1029/2008GL035188>.

745

746 Ji, J., Zheng, H., Li, S., Huang, X., 2006. The terraces of the Huanghe River in Pinglu
747 County, Shanxi Province and their relationship with the disappearance of the Sanmen
748 palaeolake and the formation of the Huanghe River. *Quaternary Sciences* 26, 665-672
749 (in Chinese, with English abstract).

750

751 Jiang, F., Fu, J., Wang, S., Sun, D., Zhao, Z., 2007. Formation of the Yellow River,
752 inferred from loess-palaeosol sequence in Mangshan and lacustrine sediments in
753 Sanmen Gorge, China. *Quaternary International* 175, 62-70.

754

755 Kirschvink, J.L., 1980. The least-squares line and plane and the analysis of
756 palaeomagnetic data. *Geophysical Journal International* 62, 699-718.

757

758 Kong, P., Jia, J., Zheng, Y., 2014. Time constraints for the Yellow River traversing the
759 Sanmen Gorge. *Geochemistry, Geophysics, Geosystems* 15, 395-407.

760

761 Kukla, G., An, Z.S., 1989. Loess stratigraphy in central China. *Palaeogeography,*
762 *Palaeoclimatology, Palaeoecology.* 72, 203-225.

763

764 Kukla, G., Heller, F., Liu, M., Xu, C., Liu, S., An, S., 1988. Pleistocene climates in
765 China dated by magnetic susceptibility. *Geology* 16, 811-814.

766

767 Li, J., 1991. The environmental effects of the uplift of the Qinghai-Xizang Plateau.
768 *Quaternary Science Reviews* 10, 479-483.

769

770 Li, B., Sørensen, M.B., Atakan, K., 2015. Coulomb stress evolution in the Shanxi rift
771 system, North China, since 1303 associated with coseismic, post-seismic and
772 interseismic deformation. *Geophysical Journal International* 203, 1642-1664.

773

774 Lin, A.M., Yang, Z.Y., Sun, Z.M., Yang, T.S., 2001. How and when did the Yellow
775 River develop its square bend? *Geology* 29, 951-954.

776

777 Liu, H., 2004. Formation and evolution of the Weihe River basin and uplift of the
778 eastern Qinling Mountains, Ph.D. thesis, The Northeast University, Xian, China.

779

780 Liu, J., Zhang, P., Lease, R.O., Zheng, D., Wan, J., Wang, W., Zhang, H., 2013.
781 Eocene onset and late Miocene acceleration of Cenozoic intracontinental extension in
782 the North Qinling range-Weihe graben: Insights from apatite fission track
783 thermochronology. *Tectonophysics* 584, 281-296.

784

785 Liu S., Li, G., Li, Y., Jin, J., 1988. The sedimentary characteristics of the North China
786 plain as an indicator for the formation and evolution of the Yellow River. *Henan*
787 *Geology* 6, 20-24 (in Chinese).

788

789 Liu, T., 1985. *Loess and the Environment*. China Ocean Press, Beijing, pp. 31-147.

790

791 Liu, X., Chen, B., 2000. Climatic warming in the Tibetan Plateau during the recent
792 decades. *International Journal of Climatology* 20, 1729-1742.

793

794 Lu, H., Liu, X., Zhang, F., An, Z., Dodson, J., 1999. Astronomical calibration of
795 loess-palaeosol deposits at Luochuan, central Chinese Loess Plateau.

796 Palaeogeography, Palaeoclimatology, Palaeoecology 154, 237-246.
797
798 Maddy, D., Veldkamp, A., Demir, T., van Gorp, W., Wijbrans, J.R., van Hinsbergen,
799 D.J.J., Dekkers, M.J., Schreve, D., Schoorl, J.M., Scaife, R., Stemerink, C., van der
800 Schriek, T., Bridgland, D.R., Ayt a, A.S., 2016. The Gediz River fluvial archive: a
801 benchmark for Quaternary research in Western Anatolia. Quaternary Science Reviews.
802 <http://dx.doi.org/10.1016/j.quascirev.2016.07.031>.
803
804 Maher, B.A., Thompson, R., 1991. Mineral magnetic record of the Chinese loess and
805 palaeosols. *Geology* 19, 3-6.
806
807 Matoshko, A., Gozhik, P., Danukalova, G., 2004. Key Late Cenozoic fluvial archives
808 of eastern Europe: the Dniester, Dnieper, Don and Volga. *Proceedings of the*
809 *Geologists' Association* 115, 141-173.
810
811 Miao, X., Lu, H., Li, Z., Cao, G., 2008. Paleocurrent and fabric analyses of the
812 imbricated fluvial gravel deposits in Huangshui Valley, the northeastern Tibetan
813 Plateau, China. *Geomorphology*. 99, 433-442.
814
815 Molnar, P., 2004. Late Cenozoic increase in accumulation rates of terrestrial sediment:
816 how might climate change have affected erosion rates? *Annu. Rev. Earth Planet. Sci.*
817 32, 67-89.
818
819 Molnar, P., England, P., Martinod, J., 1993. Mantle dynamics, uplift of Tibetan Plateau,
820 and the Indian Monsoon. *Reviews of Geophysics* 31, 357-396.
821
822 Nie, J., Stevens, T., Rittner, M., Stockli, D., Garzanti, E., Limonta, M., Bird, A., Ando,
823 S., Vermeesch, P., Saylor, J., Lu, H., Breecker, D., Hu, X., Liu, S., Resentini, A.,
824 Vezzoli, G., Peng, W., Carter, A., Ji, S., Pan, B., 2015. Loess Plateau storage of
825 Northeastern Tibetan Plateau-derived Yellow River sediment. *Nature*
826 *Communications* 6, 1-8.
827
828 Ollier, C.D., Pain, C.F., 2000. *The Origin of Mountains*. Routledge, London.
829

830 Pan, B., Li, J., Chen, F., 1995. The Qinghai-Tibetan Plateau: Driver and amplifier of
831 the global climate changes. I The characteristics of climate changes in Cenozoic.
832 Journal of Lanzhou University (Natural Science Edition) 31, 120-128 (in Chinese,
833 with English abstract).
834

835 Pan, B.T., Burbank, D., Wang, Y.X., Wu, G.J., Li, J.J., Guan, Q.Y., 2003. A 900 k.y.
836 record of strath terrace formation during glacial-interglacial transitions in northwest
837 China. *Geology* 32, 957-960.
838

839 Pan, B.T., Wang, J.P., Gao, H.S., Chen, Y.Y., Li, J.J., Liu, X.F., 2005a. Terrace dating
840 as an archive of the run-through of the Sanmen Gorge. *Progress in Natural Science*.
841 15, 1096-1103.
842

843 Pan, B.T., Wang, J.P., Gao, H.S., Guan, Q.Y., Wang, Y., Su, H., Li, B.Y., Li, J.J.,
844 2005b. Paleomagnetic dating of the topmost terrace in Kouma, Henan and its
845 indication to the Yellow River's running through Sanmen Gorges. *Chinese Science*
846 *Bulletin*. 50, 657-664.
847

848 Pan, B., Su, H., Hu, Z., Hu, X., Gao, H., Li, J., Kirby, E., 2009. Evaluating the role of
849 climate and tectonics during non-steady incision of the Yellow River: evidence from a
850 1.24 Ma terrace record near Lanzhou, China. *Quaternary Science Reviews* 28,
851 3281-3290.
852

853 Pan, B.T., Hu, Z.B., Wang, J.P., Vandenberghe, J., Hu, X.F., 2011. A
854 magnetostratigraphic record of landscape development in the eastern Ordos Plateau,
855 China: Transition from Late Miocene and Early Pliocene stacked sedimentation to
856 Late Pliocene and Quaternary uplift and incision by the Yellow River.
857 *Geomorphology* 125, 225-238.
858

859 Pan, B.T., Hu, Z.B., Wang, J.P., Vandenberghe, J., Hu, X.F., Wen, Y.H., Li, Q., Cao, B.,
860 2012. The approximate age of the planation surface and the incision of the Yellow
861 River. *Palaeogeography, Palaeoclimatology, Palaeoecology* 356-357, 54-61.
862

863 Perrineau, A., van der Woerd, J., Gaudemer, Y., Jing, Z., Pik, R., Tapponnier, P.,

864 Thuizat, R., Zheng, R., 2011. Incision rate of the Yellow River in Northeastern Tibet
865 constrained by ^{10}Be and ^{26}Al cosmogenic isotope dating of fluvial terraces:
866 implications for catchment evolution and plateau building. In: Gloaguen, R.,
867 Ratschbacher, L. (Eds.), Growth and Collapse of the Tibetan Plateau. Special
868 Publications of the Geological Society, London 353, 189-219.

869

870 Peulvast, J.P., Sales, V., 2004. Stepped surfaces and palaeolandforms in the northern
871 Brazilian <Nordeste>: constraints on models of morphotectonic evolution.
872 *Geomorphology* 62, 89-122.

873

874 Potter, P.E., 1978. Significance and origin of big rivers. *Journal of Geology* 86, 13–33.

875

876 Powell, C., Conaghan, P.J., 1973. Plate tectonics and the Himalayas. *Earth and*
877 *Planetary Science Letters* 20, 1-12.

878

879 Prins, M.A., Zheng, H.B., Beets, K., Troelstra, S., Bacon, P., Kamerling, I., Wester, W.,
880 Konert, M., Huang, X.T., Wang, K.E., Vandenberghe, J., 2009. Dust supply from river
881 floodplains: the case of the lower Huang He (Yellow River) recorded in
882 loess-palaeosol sequence from the Mangshan Plateau. *Journal of Quaternary Science*
883 24, 75-84.

884

885 Rea, D., Snoeckx, H., Joseph, H.L., 1998. Late Cenozoic eolian deposition in the
886 North Pacific: Asian drying, Tibetan uplift, and cooling of the northern hemisphere.
887 *Paleoceanography* 13, 215-224.

888

889 Rixhon, G., Briant, R.M., Cordier, S., Duval, M., Jones, A., Scholz, D., 2016.
890 Revealing the pace of river landscape evolution during the Quaternary: recent
891 developments in numerical dating methods. *Quaternary Science Reviews*.
892 <http://dx.doi.org/10.1016/j.quascirev.2016.08.016>

893

894 Rutter, N.W., Ding, Z.L., Evans, M.E., Liu, T.S., 1991. Baoji-type pedostratigraphic
895 section, Loess Plateau, north-central China. *Quaternary Science Review*. 10, 1-22.

896

897 Sadler, P.M., Jerolmack, D.J., 2015. Scaling laws for aggradation, denudation and

898 progradation rates: the case for time-scale invariance at sediment sources and sinks.
899 Geological Society, London, Special Publications, 404, 69–88.
900

901 Saito, Y., Yang, Z., Hori, K., 2001. The Huanghe (Yellow River) and Changjiang
902 (Yangtze River) deltas: a review on their characteristics, evolution and sediment
903 discharge during the Holocene. *Geomorphology* 41, 219-231.
904

905 Schumm, S.A., Dumont, J.F., Holbrook, J.M., 2000. Active tectonics and alluvial river.
906 Cambridge University Press, Cambridge, UK, pp. 375-376.
907

908 Seyrek, A., Westaway, R., Pringle, M., Yurtmen, S., Demir, T., Rowbotham, G., 2008.
909 Timing of the Quaternary Elazığ volcanism, eastern Turkey, and its significance for
910 constraining landscape evolution and surface uplift. *Turkish Journal of Earth Sciences*
911 17, 497-541.
912

913 Soreghan, G.S., Elmore, R.D., Katz, B., Cogoini, M., Banerjee, S., 1997.
914 Pedogenically enhanced magnetic susceptibility variations preserved in Paleozoic
915 loessite. *Geology* 25, 1003-1006.
916

917 Stokes, M., 2008. Plio-Pleistocene drainage development in an inverted sedimentary
918 basin: Vera basin, Betic Cordillera, SE Spain. *Geomorphology* 100, 193-211.
919

920 Sun, Y., Clemens, C. S., An, Z., Yu, Z., 2006. Astronomical timescale and
921 palaeoclimatic implication of stacked 3.6-Myr monsoon records from the Chinese
922 Loess Plateau. *Quaternary Science Reviews* 25, 33-48.
923

924 Tapponnier, P., Xu, Z., Roger, F., Meyer, B., Arnaud, N., Wittlinger, G., Yang, J., 2001.
925 Oblique stepwise rise and growth of the Tibet Plateau. *Science* 294, 1671-1677.
926

927 Vandenberghe, J., Lu, H. Y., Sun, D. H., Huissteden, J., Konert, M., 2004. The late
928 Miocene and Pliocene climate in East Asia as recorded by grain size and magnetic
929 susceptibility of the Red Clay deposits (Chinese Loess Plateau). *Palaeogeography,*
930 *Palaeoclimatology, Palaeoecology.* 204, 239-255.
931

932 Vandenberghe, J., Wang, X., Lu, H., 2011. Differential impact of small-scaled tectonic
933 movements on fluvial morphology and sedimentology (the Huang Shui catchment,
934 NE Tibet Plateau). *Geomorphology* 134, 171-185.

935

936 Vandenberghe, J., de Moor, J.W. J., Spanjaard, G., 2012. Natural change and human
937 impact in a present-day fluvial catchment: The Geul River, southern Netherlands.
938 *Geomorphology* 159-160, 1-14.

939

940 Vandenberghe, J., 2016. From planation surfaces to river valleys. *BSGLg* 67, 93-106.

941

942 Veldkamp, A., van Dijke, J. J., 2000. Simulating internal and external controls on
943 fluvial terrace stratigraphy: a qualitative comparison with the Mass record.
944 *Geomorphology* 33, 225-236.

945

946 Wagner, T., Fritz, H., Stüwe, K., Nestroy, O., Rodnight, H., Hellstrom, J., Benischke,
947 R., 2011. Correlations of cave levels, stream terraces and planation surfaces along the
948 River Mur-Timing of landscape evolution along the eastern margin of the Alps.
949 *Geomorphology* 134, 62-78.

950

951 Wang, S., Wu, X., Zhang, K., Jiang, F., Xue, B., Tong, G., Tian, G., 2001. Sedimentary
952 records of environmental evolution in the Sanmen Lake Basin and the Yellow River
953 running through the Sanmenxia Gorge eastward into the sea. *Science in China* 31,
954 585-608.

955

956 Wang, X., Lu, H., Vandenberghe, J., Zheng, S., van Balen, R., 2012. Late Miocene
957 uplift of the NE Tibetan Plateau inferred from basin filling, planation and fluvial
958 terraces in the Huang Shui catchment. *Global and Planetary Change* 88-89, 10-19.

959

960 Westaway, R., 2009. Active crustal deformation beyond the SE margin of the Tibetan
961 Plateau: Constraints from the evolution of fluvial systems. *Global and Planetary*
962 *Change* 68, 395-417.

963

964 Westaway, R., Demir, T., Seyrek, A., 2008. Geometry of the Turkey-Arabia and
965 Africa-Arabia plate boundaries in the latest Miocene to Mid-Pliocene: the role of the

966 Malatya-Ovacık Fault Zone in eastern Turkey. *eEarth*, 3, 27-35.
967
968 Westaway, R., Bridgland, D.R., Sinha, R., Demir, T., 2009. Fluvial sequences as
969 evidence for landscape and climatic evolution in the Late Cenozoic: A synthesis of
970 data from IGCP 518. *Global and Planetary Change* 68, 237-253.
971
972 Willenbring, J.K., Jerolmack, D.J., 2016. The null hypothesis: globally steady rates of
973 erosion, weathering fluxes and shelf sediment accumulation during Late Cenozoic
974 mountain uplift and glaciation. *Terra Nova* 28, 11–18.
975
976 Willenbring, J.K., von Blanckenburg, F., 2010. Long-term stability of global erosion
977 rates and weathering during late-Cenozoic cooling. *Nature* 465, 211-214.
978
979 Wu, C., Xu, Q., Yang, X., 2000. Ancient drainage system of the Yellow River on
980 North China Plain. *Journal of Geomechanics* 6, 1-9 (in Chinese, with English
981 abstract).
982
983 Xia, D., Wu, S., Yu, Z., 1993. Changes of the Yellow River since the last glacial age.
984 *Marine Geology & Quaternary Geology* 13, 83-88 (in Chinese, with English abstract).
985
986 Xiao, G., Guo, Z., Chen, Y., Yao, Z., Shao, Y., Wang, X., Hao, Q., Lu, Y., 2008.
987 Magnetostratigraphy of BZ₁ borehole in west coast of Bohai bay, northern China.
988 *Quaternary Sciences* 28, 909-916 (in Chinese, with English abstract).
989
990 Xue, D., 1996. A humble option of the formed age for the eastern section of the
991 Yellow River. *Henan Geology* 14, 110-112 (in Chinese, with English abstract).
992
993 Yang, H., Chen, X., 1985. Quaternary transgressions, eustatic changes and shifting of
994 shoreling in East China. *Marine Geology & Quaternary Geology* 5, 59-80 (in Chinese,
995 with English abstract).
996
997 Yang, S., Cai, J., Li, C., Deng, B., 2001. New discussion about the run-through time
998 of the Yellow River. *Marine Geology & Quaternary Geology* 21, 15-20 (in Chinese,
999 with English abstract).

1000

1001 Yao, Z., Xiao, G., Wu, H., Liu, W., Chen, Y., 2010. Plio-Pleistocene vegetation
1002 changes in the North China Plain: Magnetostratigraphy, oxygen and carbon isotopic
1003 composition of pedogenic carbonates. *Palaeogeography, Palaeoclimatology,*
1004 *Palaeoecology* 297, 502-510.

1005

1006 Yao, Z., Guo, Z., Xiao, G., Wang, Q., Shi, X., Wang, X., 2012. Sedimentary history of
1007 the western Bohai coastal plain since the late Pliocene: Implications on tectonic,
1008 climatic and sea-level changes. *Journal of Asian Earth Sciences* 54-55, 192-202.

1009

1010 Yu, H., 1999. Ages of the Yellow River delta in shelf regions of the Yellow sea and the
1011 Bohai sea. *Journal of Geomechanics* 5, 80-88 (in Chinese, with English abstract).

1012

1013 Yuan, Y., Hu, S., Wang, H., Sun, F., 2007. Meso-Cenozoic tectonothermal evolution
1014 of Ordos Basin, central China: Insight from newly acquired vitrinite reflectance data
1015 and a revision of existing paleothermal indicator data. *Journal of Geodynamics* 44,
1016 33-46.

1017

1018 Yue, L., Zhang, Y., Wang, J., Deng, X., Zhang, L., 1999. Magnetostratigraphic
1019 sequence of continental deposits in Northern China since 5.3 Ma. *Geological Reviews*
1020 45, 444-448 (in Chinese, with English abstract).

1021

1022 Zhang, J., Qiu, W., Wang, X., Hu, G., Li, R., Zhou, L., 2010. Optical dating of a
1023 hyperconcentrated flow deposit on a Yellow River terrace in Hukou, Shaanxi, China.
1024 *Quaternary Geochronology* 5, 194-199.

1025

1026 Zhang, P., Molnar, P., Downs, W.R., 2001. Increased sedimentation rates and grain
1027 sizes 2-4 Myr ago due to the influence of climate change on erosion rates. *Nature* 410,
1028 891-897.

1029

1030 Zhang, Y., Mercier, J.L., Vergély, P., 1998. Extension in the graben systems around the
1031 Ordos (China), and its contribution to the extrusion tectonics of south China with
1032 respect to Gobi-Mongolia. *Tectonophysics* 285, 41-75.

1033

1034 Zhang, Y., Ma, Y., Yang, N., Shi, W., Dong, S., 2003. Cenozoic extensional stress
1035 evolution in North China. *Journal of Geodynamics* 36, 591-613.
1036

1037 Zheng, H., Powell, C., Rea, D., Wang, J., Wang, P., 2004. Late Miocene and
1038 mid-Pliocene enhancement of the East Asian monsoon as viewed from land and sea.
1039 *Global and Planetary Change* 41, 147-155.
1040

1041 Zheng, H., Huang, X., Ji, J., Liu, R., Zeng, Q., Jiang, F., 2007. Ultra-high rates of
1042 loess sedimentation at Zhengzhou since Stage 7: Implication for the Yellow River
1043 erosion of the Sanmen Gorge. *Geomorphology* 85, 131-142.
1044

1045 Zheng, H., Clift, P., Wang, P., Tada, R., Jia, J., He, M., Jourdan, F., 2013. Pre-Miocene
1046 birth of the Yangtze River. *PNAS* 110, 7556-7561.
1047

1048 Zhu, H., Chen, K., Liu, K., He, S., 2008. A sequence stratigraphic model for reservoir
1049 sand-body distribution in the Lower Permian Shanxi Formation in the Ordos Basin,
1050 Northern China. *Marine and Petroleum Geology* 25, 731-743.
1051

1052 Zhu, R. X., Laj, C., Mazaud, A., 1994. The Matuyama-Brunhes and upper Jaramillo
1053 transitions recorded in a loess section at Weinan, north-central China. *Earth and*
1054 *Planetary Science Letters*. 125, 143-158.

1055 **Table Captions**

1056

1057 Table 1. Fluvial terrace correlation between Sanmenxia and Kouma

1058

1059 **Figure Captions**

1060

1061 **Fig. 1.** Map of the Fenwei graben and its surroundings, showing faults (from AFSOM,
1062 1998), rivers, topography, and the locations of the four sub-basins (the Weihe,
1063 Lingbao, Yuncheng, and Fenhe basins). The locations of Figs 2 and 3 are also
1064 indicated. The inset map shows the major fault systems, plate motions, Bohai Gulf,
1065 and location within China.

1066

1067 **Fig. 2.** Maximum, mean, and minimum topography along a 50-km-wide swath along
1068 the Sanmen gorge (see Fig. 1 for location). Active faults and the interpreted long
1069 profile of the planation surface are also depicted (see also Fig. 4).

1070

1071 **Fig. 3.** Map of the study region showing topography (using the same data source as
1072 Fig. 1), active faults, and field localities (see Fig. 1 for location).

1073

1074 **Fig. 4.** Field photos of the Sanmen gorge and its entrance. (A) View of the planation
1075 surface dominating the Xiaoshan along the Sanmen gorge, looking east from
1076 $34^{\circ}51'09.36''$ N, $111^{\circ}19'34.16''$ E. (B) The westward dip of the planation surface
1077 (looking north from $34^{\circ}46'03.27''$ N, $111^{\circ}17'53.48''$ E), the result of deformation close
1078 to the inlet of the Sanmen gorge. (C and D) Fluvial terrace staircase at Sanmenxia,
1079 looking west (C) and south (D). Five terraces have been identified below the planation
1080 surface, of which the uppermost (T5) is newly recognized. (E) Closeup view of the
1081 sedimentary sequence forming terrace T2 at Sanmenxia (see (D) for location). The
1082 fluvio-lacustrine Sanmen Formation, characterized by horizontally bedded mudstone,
1083 siltstone, clay, conglomerate, and sandstone, crops out below the terrace gravel.

1084

1085 **Fig. 5.** Transverse profiles through the fluvial terrace staircases at the field localities
1086 (Zhangbian, Sanmenxia, Dongcun, Xiaolangdi, and Kouma; see Fig. 3 for locations).
1087 Note that the terrace staircases at Zhangbian, Sanmenxia and Dongcun are affected by
1088 normal faulting.

1089

1090 **Fig. 6.** Interpreted longitudinal profile of terrace levels along the Sanmen gorge, using
1091 height data from Table 1. The normal faults that define the ends of the gorge are
1092 depicted in Fig. 2 and 3.

1093

1094 **Fig. 7.** Magnetostratigraphy and pedostratigraphy of the aeolian deposits overlying
1095 the fluvial terraces and planation surface at Sanmenxia. These TL dates for T2 and
1096 interpreted chrons (black for normal geomagnetic polarity, white for reverse) for
1097 terraces T4, T3, and T2 are all from Pan et al. (2005a). For the newly recognized
1098 terrace T5 and the planation surface, paleomagnetic data from the overlying ~130-m-
1099 and 152-m-thick aeolian deposits are used to obtain age interpretations (of ~1.24 Ma
1100 and 3.63 Ma, respectively), using the Cande and Kent (1995) geomagnetic polarity
1101 timescale. However, these data are displayed here without filtering for noise. The
1102 magnetic susceptibility values are higher in the palaeosol units than those in the
1103 neighboring loess layers.

1104

1105 **Fig. 8.** A selection of the data from Fig. 7, illustrating the thermal demagnetization
1106 process used to identify the primary components of rock magnetization that indicate
1107 the polarity of the Earth's magnetic field at the time of deposition. For each figure part,
1108 the left-hand panel shows the horizontal (solid symbols) and vertical (open symbols)
1109 components of rock magnetization, whereas the right-hand panel shows how the
1110 strength of magnetization decreases with increasing temperature. (A) Sample PR-10.0
1111 from the 10.0-m thickness of the aeolian section on the planation surface, a sample of
1112 Carbonate nodules. After a low-temperature overprint is removed, this sample is seen
1113 to be magnetized upward and southward, indicating reverse polarity. (B) Sample
1114 PR-0.5 from 0.5-m thickness of the aeolian section on the planation surface, a sample
1115 of Red Clay. After a low-temperature overprint is removed, this sample is seen to be
1116 magnetized downward and northward, indicating normal polarity. (C) Sample PL-69.0
1117 from 69.0-m thickness of the aeolian section on the planation surface, a sample of
1118 loess. After a substantial overprint is removed, this sample is seen to be magnetized
1119 upward and southward, indicating reverse polarity. (D) Sample PL-109.0 from
1120 109.0-m thickness of the aeolian section on the planation surface, a sample of loess.
1121 This sample is seen to be magnetized downward and northward, indicating normal
1122 polarity. (E) Sample T5-33.0 from 33.0-m thickness of the loess section on terrace T5.

1123 This sample is seen to be magnetized downward and westward, indicating ambiguous
1124 polarity. (F) Sample T5-28.0 from 28.0-m thickness of the loess section on terrace T5.
1125 This sample is seen to be magnetized downward and northward, indicating normal
1126 polarity.

1127

1128 **Fig. 9.** Schematic diagram illustrating landscape evolution within the Fenwei graben.
1129 (A) The initial downfaulting, erosion, and filling of the Fenwei graben. (I)
1130 Development, in the Early Pliocene, of the graben as a result of extensional tectonism.
1131 (II) Planation, circa 3.6 Ma (according to the magnetostratigraphic data), during
1132 infilling of the graben, marked by emplacement of the lower part of the Sanmen
1133 Formation. (B) Uplift and dissection of the planation surface after ~3.6 Ma. At this
1134 time the extension switched from the initial set of normal faults to a newer set in the
1135 hanging-walls of the initial set, resulting in narrowing of the graben. (C) Erosion, fill,
1136 and excavation of this narrower graben. (I) Erosion and fill when the narrower graben
1137 was occupied by an isolated fluvio-lacustrine system, during deposition of the upper
1138 part of the Sanmen Formation in the Early Pleistocene. (II) Initial entrenchment of the
1139 Yellow River into the Sanmen Formation circa 1.2 Ma. At this time the former lake
1140 basin was disrupted and fluvial drainage first developed from west to east across the
1141 Xiaoshan, leading to the formation of the Sanmen gorge and incision into the Sanmen
1142 Formation. (D) Incision and terrace formation by the Yellow River at Sanmenxia since
1143 the late Early Pleistocene, creating the present fluvial terrace staircase.

1 **The linking of the upper-middle and lower reaches of the Yellow River as a result**
2 **of fluvial entrenchment**

3

4 ZhenBo Hu^{a, *}, BaoTian Pan^{a, *}, David Bridgland^b, Jef Vandenberghe^c, LianYong
5 Guo^a, YunLong Fan^a, Rob Westaway^d

6

7 ^aKey Laboratory of Western China's Environmental Systems (Ministry of Education),
8 College of Earth and Environmental Sciences, Lanzhou University, Lanzhou 730000,
9 People's Republic of China

10

11 ^bDepartment of Geography, Durham University, South Road, Durham DH1 3LE, UK

12

13 ^cDepartment of Earth Sciences, Vrije Universiteit, De Boelelaan 1085, 1081 HV
14 Amsterdam, The Netherlands

15

16 ^dSchool of Engineering, University of Glasgow, James Watt (South) Building,
17 Glasgow G12 8QQ, UK

18

19 *Corresponding author. E-mail: zhhhu@lzu.edu.cn; hu_zhb@126.com (Z. Hu)

20 **Abstract**

21

22 The upper-middle Yellow River flows through the Fenwei graben, a structure
23 resulting from extensional tectonism that was formed and repeatedly extended during
24 the Cenozoic. The drainage system within this graben was formerly isolated from the
25 lower reaches of the Yellow River system by the Xiaoshan mountains, an actively
26 growing ~NW-SE trending range. The modern course of the Yellow River takes it
27 through this range along the Sanmen gorge, the formation of which was of great
28 significance in that it initiated through-going drainage between the upper-middle and
29 lower reaches of the system. The timing of this event, which was clearly a critical
30 point in the evolution of the Yellow River, can be established by dating the terraces in
31 the gorge. Intermittent deepening of this gorge by the Yellow River from a high-level
32 planation surface capping the mountain range has resulted in the formation of five
33 terraces. Magnetostratigraphic records from aeolian deposits accumulated on these
34 surfaces provide a geochronological sequence for this geomorphic archive, in which
35 the ages of the planation surface and of terraces T5, T4, T3, T2, and T1 have been
36 determined as ~3.63 Ma, ~1.24 Ma, ~0.86 Ma, ~0.62 Ma, ~129 ka, and ~12 ka,
37 respectively.

38 Under the constraint of this chronological framework, a model for landscape
39 evolution is proposed here. Uplift of the inner Fenwei graben and of the surrounding
40 mountain ranges led to dissection of the 3.63 Ma old planation surface in conjunction
41 with the formation of the Sanmen gorge. Drainage of the lake previously occupying
42 the basin would have promoted incision into the fluvio-lacustrine graben sediments;
43 indeed, gorge formation through the Xiaoshan may have been initiated or intensified
44 by lake overflow. The ages obtained for the planation surface and uppermost terrace
45 suggest that the formation of the Sanmen gorge and the initiation of the through-going
46 eastward drainage of the Yellow River occurred between 3.63 and 1.24 Ma. Before
47 the start of gorge entrenchment, the products of erosion in the modern upper
48 catchment of the Yellow River were unable to reach the sea. The dramatic increase in
49 deposition rates in the Bohai Gulf (at the mouth of the modern Yellow River in the
50 East China Sea), ~1.0 Ma ago, thus resulted from the initiation of an integral
51 (enlarged) Yellow River catchment drainage through the Sanmen gorge; it does not
52 imply an increase in erosion rates at that time.

53

54 *Keywords:* Yellow River; Sanmen gorge; Fenwei graben; Terrace; Planation surface;
55 Fluvial incision rate

56 1. Introduction

57

58 Many of the world's largest rivers flow along structural lows and major rift
59 systems (Potter, 1978) and, meanwhile, have shaped the landscape over large areas. In
60 those regions that have been entrenched, the interaction between climate, uplift,
61 lithology, and base level have been fundamental controls on the evolution of fluvial
62 systems (Schumm et al., 2000; Veldkamp and van Dijke, 2000; Pan et al., 2003;
63 Bridgland and Westaway, 2008; Vandenberghe et al., 2011). Moreover, information
64 about tectonic activity and climatic change can be imprinted into sedimentary and
65 morphological fluvial archives (e.g., Bridgland, 2000; Stokes, 2008; Westaway, 2009;
66 Craddock et al., 2010; Bridgland et al., 2012; [Bridgland and Westaway, 2014](#)). The
67 development of large rivers is thus widely employed to determine the history of
68 structural, environmental, and topographical change during the Quaternary. ~~(An et al.,
69 2001; Westaway et al., 2009; Bridgland and Westaway, 2014; Hu et al., 2016). The
70 specific objective of this paper is to reconstruct the eastward drainage history of the
71 Yellow River by dating its terraces in the critical reach between its middle and lower
72 catchments (the Sanmen gorge).~~

73 ~~The formation of the Tibetan Plateau is generally thought to have been an
74 amplifier and driver for the environmental evolution of East Asia, strengthening the
75 East Asian monsoon and thus having an influence on precipitation and related erosion
76 rates (Li, 1991; Pan et al., 1995; Liu and Chen, 2000). Constraint on its uplift history
77 provides the basis for understanding the effects of high topography on climate and on
78 various earth surface processes (An et al., 2001).~~

79 ~~T1.1. The significance of fluvial archives in reconstructing East Asian landscape
80 evolution~~

81

82 The development of fluvial systems in East Asia has also been closely associated
83 with topographical evolution since the India–Eurasia collision (e.g., Powell and
84 Conaghan, 1973; Lin et al., 2001; Fan and Li, 2008). The eastward flow direction of
85 the largest rivers in China (e.g., the Yellow River and the Yangtze) is generally
86 attributed to the relative eastward decline of the macro-relief, resulting from the uplift
87 of the Tibetan Plateau (Miao et al., 2008; Craddock et al., 2010; Zheng et al., 2013).
88 Marine accumulation of terrigenous sediments derived from these large fluvial
89 systems may be assumed to have started in the Bohai Gulf immediately after the

Formatted: Indent: First line: 2 ch

Formatted: Indent: First line: 0 ch

90 formation of this drainage pattern (Zheng et al., 2004; Jiang et al., 2007). ~~These~~
91 ~~continuous terrigenous sediment stacks within marine basins are generally believed to~~
92 ~~provide an important record of climatically and tectonically controlled mountain~~
93 ~~denudation history and to play a key role in the understanding of Quaternary surface~~
94 ~~uplift and global cooling (Clift, 2006; Willenbring and von Blanckenburg, 2010).~~ The
95 establishment of these eastward-flowing drainage systems ~~thus~~ provides a critical link
96 between upland erosion and the marine accumulation of terrigenous sediments (Nie et
97 al., 2015). Despite much attention having been paid to long-term fluvial landscape
98 development in East Asia, which is related to the uplift of the Tibetan Plateau during
99 the Quaternary ~~(see below)~~, the formation age of the eastward drainage pattern in
100 China is still strongly debated (cf. Lin et al., 2001; Clark et al., 2004; Pan et al., 2005b;
101 Clift, 2006; Zheng et al., 2007, 2013). It is the specific objective of this paper to
102 reconstruct the eastward drainage history of the Yellow River by dating its terraces in
103 the critical reach between its middle and lower catchments. The formation ages of
104 terraces T4, T3 and T2 at Sanmenxia were determined previously by Pan et al. (2005a)
105 as 0.86 Ma, 0.62 Ma, and 0.129 Ma, respectively, but no dating was available for the
106 highest terrace T5 and the planation level in the study region.

109 **1.2. Regional geological and geomorphic setting**

111 2.1. General position of the Ordos block, Fenwei graben and Xiaoshan mountains

113 ~~The motion, during the Cenozoic, of the Indian plate relative to Eurasia led to~~
114 ~~crustal shortening and the formation of the Tibetan Plateau (Molnar et al., 1993;~~
115 ~~Royden et al., 2008; White and Lister, 2012). This major positive topographical~~
116 ~~feature is generally thought to have been an amplifier and driver for the environmental~~
117 ~~evolution of East Asia, strengthening the East Asian monsoon and thus having an~~
118 ~~influence on precipitation and related erosion rates (Li, 1991; Pan et al., 1995; Liu and~~
119 ~~Chen, 2000; Molnar et al., 2010). Constraint on its uplift history provides the basis for~~
120 ~~understanding the effects of high topography on climate and on various Earth surface~~
121 ~~processes (Ruddiman and Kutzbach, 1989; An et al., 2001; G. Pan et al., 2012). Owing~~
122 ~~to an insufficiently reliable chronological framework, however, the relationship~~
123 ~~between paleoenvironmental conditions and landscape evolution is still poorly~~

Formatted: Font: Bold

Formatted: Indent: First line: 0 ch

158 pointing to regular vertical subsidence.

159

160 <Fig. 2 hereabout>

161

162 Subsidence, extensional tectonics and uplift have remained vigorous and active
163 during the Quaternary in the area of the Fenwei graben. Fault scarps and triangular
164 facets that can be traced for hundreds of kilometers are readily observed along the
165 northern front of the Qinling, Huashan, and the southern front (Xiaoshan) of the
166 Taihang Mountains (Dong et al., 2011). Major earthquakes around this graben are
167 known from historical records (Zhang et al., 2003). The middle and lower reaches of
168 the Yellow River are separated by the Xiaoshan mountains. To cross this topographic
169 barrier the Yellow River has incised deeply into these mountains, creating the Sanmen
170 gorge, between Sanmenxia and Xiaolangdi (Fig. 2 and Fig. 3). The Sanmen gorge,
171 ~~through which the Yellow River traverses the Xiaoshan Mountain Range (thus linking~~
172 ~~the graben with river system further downstream),~~ is constrained by normal and
173 strike-slip faults (Fig. 2), and is transected by numerous inferred inner faults (Fig. 3).
174 Many ground fissures associated with earthquakes are exposed along these inferred
175 faults within the gorge, indicating that uplift of the Xiaoshan with respect to the
176 Lingbao basin, to the northwest, and the North China Plain (to the southeast) has
177 never ceased (AFSOM, 1988).

178

179 <Fig. 3 hereabout>

180

181 The modern landscape in the vicinity of the Sanmen gorge is an uplifted and
182 rolling surface that is well preserved on resistant rocks in the higher parts of the area.
183 It represents a remnant of a planation surface that was cut through most of the
184 pre-existing tectonic structures and the relief right across the Lingbao basin, the
185 Xiaoshan range, and the North China Plain (Fig. 4A). This geomorphic surface was
186 deformed strongly over the Xiaoshan (Fig. 4B), forming a convexity between the
187 Lingbao basin and the North China Plain (Fig. 2). In general, its altitude exhibits a
188 declining trend towards the east, ~~falling below~~reaching less than 400 m in the North
189 China Plain.

190

191 <Fig. 4 hereabout>

192

193 | ~~21.23. The downstream part of the Yellow River~~
194 | ~~Yellow River catchment and its~~
195 | ~~relation with the Sanmen gorge~~

196

196 | ~~Here we focus upon T~~ the Yellow River (Huanghe), ~~one of the largest in the~~
197 | ~~world, which~~ originatings from the northeastern margin of the Tibetan Plateau and
198 | flowings eastwards across China, crossing numerous tectonic zones and major
199 | active faults, ~~and finally debouching, with its huge sediment load, into the Bohai Gulf~~
200 | ~~(Saito et al., 2001).~~ ~~The Xiaoshan mountain range represents the final barrier to be~~
201 | ~~crossed by the river before it flows across the North China Plain and finally~~
202 | ~~debouches, attaining a total length of 5464 km (Wang et al., 2001), with its huge~~
203 | ~~sediment load, into the Bohai Gulf (Saito et al., 2001); This large fluvial system~~
204 | ~~represents an exceptional opportunity in that the relationship between terrigenous~~
205 | ~~records within offshore marine basins and inland landscape evolution can be~~
206 | ~~potentially evaluated with reference to Yellow River fluvial archives, which provide~~
207 | ~~an excellent age constraint on the evolution of the eastward flowing drainage pattern.~~

208

208 | ~~In the transition zone between middle and lower reaches of the Yellow River,~~
209 | ~~rapid fluvial incision has been initiated into the Xiaoshan mountains, an actively~~
210 | ~~growing NW-SE trending range, to form the aforementioned Sanmen gorge, an~~
211 | ~~incised valley between Sanmenxia and Xiaolangdi (Fig. 2 and Fig. 3). The Xiaoshan~~
212 | ~~mountain range represents effectively the final barrier to be crossed by the Yellow~~
213 | ~~River in its eastward flow to the Bohai Gulf (Fig. 1, inset).; downstream of the~~
214 | ~~Sanmen gorge, the river flows to the coast across the North China Plain (Fig. 1),~~
215 | ~~attaining a total length of 5464 km (Wang et al., 2001).~~ ~~The North China is P~~plain,
216 | ~~which~~ was formed from the steady supply of sediments from the upper and middle
217 | reaches of the Yellow River. ~~It~~ has remained close to sea level throughout the
218 | Quaternary (Yang and Chen, 1985), experiencing marine inundation during some
219 | interglacial periods (Geng, 1981). Sedimentary cores from this plain were analyzed in
220 | an attempt to identify the oldest fluvial sediments from the Yellow River, thereby
221 | dating the initiation of its eastward flow (Liu et al., 1988). However, the river has a
222 | long history of wandering in disparate courses across the North China Plain, resulting
223 | in deposition at different times at different sites, which has led to estimates for the
224 | date of eastward-drainage initiation that range from Early to Late Pleistocene (Xia et
225 | al., 1993; Yu, 1999; Wu et al., 2000; Yang et al., 2001).

226

227 | 21.34. The evolution of the Yellow River and its relation with the Fenwei graben and
228 | the Sanmen gorge

229

230 | ~~It has been shown previously that the area upstream of the Sanmen gorge, which~~
231 | ~~coincides with the extensional Fenwei graben, situated upstream of the Sanmen~~
232 | ~~gorge structure, was occupied, before the formation of the Yellow River, by a lake that~~
233 | ~~covered the Weihe, Fenhe, Yuncheng, and Lingbao basins (Liu, 2004). According to~~
234 | ~~the distribution of fluvio-lacustrine sediments, the eastward flow of the Yellow River~~
235 | ~~through and downstream from this palaeolake suggests that the river was instrumental~~
236 | ~~in the overflow, drainage and consequent disappearance of the lake (Wang et al., 2001;~~
237 | ~~Zhang et al., 2016).~~The ages of the uppermost fluvio-lacustrine sediments within
238 | these basins range from 1.85 Ma to 150 ka (He et al., 1984; Yue et al., 1999; Ji et al.,
239 | 2006), representing ~~an somewhat~~ imprecise chronological framework for the
240 | formation of the eastward drainage pattern of the Yellow River through the Sanmen
241 | gorge. Furthermore, recent work using cosmogenic nuclide dating, combined with
242 | provenance analysis of zircon and U-Pb age distributions, suggests that the Sanmen
243 | gorge was initially entrenched, during the period from 1.5 to 1.3 Ma, by the eastward
244 | draining Weihe River, which is now the largest tributary of the Yellow River (Kong et
245 | al., 2014). Comparative analysis of ostracod assemblages (Lishania) from the
246 | fluvio-lacustrine sediments in the Fenwei graben and from the fluvial sediments in the
247 | North China Plain suggests a close correlation between the two areas after ~1.0 Ma,
248 | implying the existence of eastward drainage by that time (Xue, 1996). Finally, ~~loess~~
249 | ~~stratigraphy~~ at Mangshan, ~100 km downstream of the Sanmen gorge (Fig. 2), ~~shows~~
250 | a dramatic increase in the ~~loess~~ accumulation rate of loess since the formation of
251 | palaeosol S2 ~~(Prins et al., 2009).~~ This increase is suggested to result from a
252 | proximal contribution of silt blown from the Yellow River floodplain, ~~further~~
253 | suggesting that eastward drainage had been formed at the latest by least c. by 243 ka,
254 | which is the formation age of S2 (Jiang et al., 2007; Zheng et al., 2007; Prins et al.,
255 | 2009), the age of palaeosol S2.

256

257 | 1.5. Dating the formation of the Sanmen gorge

258

259 | An important objective of this paper is to reconstruct the eastward drainage

Formatted: English (United States)

Formatted: English (United States)

Formatted: English (United States)

Formatted: Indent: First line: 0 ch

260 | ~~history of the Yellow River within a geochronological framework.~~ In general, the ~~The~~
261 | initiation of ~~this~~ eastward draining ~~rYellow River~~ has remained a highly
262 | controversial topic. Given that river terraces, as former floodplains (Bull, 1990;
263 | Merritt et al., 1994), can provide compelling evidence for determining drainage
264 | development (Stokes, 2008; Westaway et al., 2009; Vandenberghe et al., 2011), the
265 | dating of such terraces along the Sanmen gorge can provide important evidence (Pan
266 | et al., 2005a; Zheng et al., 2007; Kong et al., 2014). ~~M~~Here, most of the terraces ~~in the~~
267 | gorge are directly overlain by thick aeolian loess covers, which can offer an excellent
268 | age control for the underlying terraces sediments (e.g., Liu, 1985; Pan et al., 2009,
269 | 2012; Guo et al., 2012). The chronological framework from these loess covers has
270 | been based on a combined approach of magnetostratigraphy, pedostratigraphy,
271 | electron spin resonance (ESR), and luminescence dating, and cosmogenic
272 | radionuclide geochronology (e.g., Cheng et al., 2002; Pan et al., 2009; Craddock et al.,
273 | 2010; Zhang et al., 2010; Perrineau et al., 2011). From the constraint provided by the
274 | loess stratigraphy, the age of the highest Yellow River terrace at the downstream end
275 | of the Sanmen gorge was determined at 1.2 Ma by Pan et al. (2005b). In contrast, the
276 | oldest terrace at the gorge inlet was considered significantly younger, at only 0.8 Ma
277 | (Pan et al., 2005a). This temporal mismatch may be attributed to incomplete age
278 | control from the loess covers in the gorge.

279 | ~~The specific objective of this paper is to reconstruct the eastward drainage~~
280 | ~~history of the Yellow River within a geochronological framework.~~ A series of
281 | well-preserved terraces was formed by the Yellow River in the Sanmen gorge during
282 | its incision into the Xiaoshan. Here, detailed field investigation was performed to
283 | establish a complete sequence of geomorphic surfaces. Next, a new geochronology for
284 | the geomorphic archive is presented, based on the combined approach of
285 | magnetostratigraphy, pedostratigraphy, and optically stimulated luminescence (OSL)
286 | dating of the aeolian cover on the geomorphic surfaces. Finally, this geochronology is
287 | used to constrain the formation age of the eastward-draining Yellow River.

288

289 | <Fig. 5 hereabout>

290

291 | **32. Method**

292

293 | **32.1. Field research**

294

295 Intermittent downcutting by the Yellow River, starting from the planation surface
296 and cutting into the bedrock of the Xiaoshan to form the Sanmen gorge, has given rise
297 to a series of terraces along the valley. Field observations suggest that these terrace
298 treads are generally disposed asymmetrically within the valley. To elucidate the
299 formation history of the Yellow River within this gorge, work has focused on five
300 geomorphic cross-sections, from Zhangbian to Kouma (Fig. 3). For each cross-section,
301 terraces below the planation surface were identified and their tread heights (top of
302 fluvial deposits) above river level determined, the characteristics of the fluvial
303 deposits were described, and the thickness of overlying aeolian sediments (loess and
304 Red Clay) was measured.

305

306

<Table 1 hereabout>

307

308 The five transect sites were selected as representative of the supposed relict
309 planation surface and of the suite of lower-level fluvial terraces. The transect at
310 Zhangbian is located within the Lingbao basin. These transects at Sanmenxia,
311 Dongcun, and Xiaolangdi are located, respectively, at the inlet of, within, and at the
312 outlet of the gorge, whereas the Kouma site is ~20 km downstream of the gorge (Fig.
313 3). Field measurements of terrace elevation and the thickness of overlying aeolian
314 cover were performed using a differential GPS system with an uncertainty of < 5 cm.
315 According to these results, combined with loess stratigraphy and geomorphic surface
316 tracking, terrace sequences at these sites were outlined (Fig. 5) and correlated (Table
317 1). It appears that the altitude of the planation surface and the vertical separation
318 between high terrace treads and the present-day river level increases considerably at
319 first and then gradually decreases with downstream distance along the gorge (Fig. 6).
320 This topographical pattern corresponds with the convexity, mentioned above, thought
321 to relate to the active uplift of the Xiaoshan range.

322

323

<Fig. 6 hereabout>

324

325 32.2. Aeolian deposits capping the geomorphic surfaces

326

327 The aeolian sediments (Tertiary Red Clay and overlying Quaternary loess)

328 covering the planation surface and terrace treads provide valuable age estimates for
329 the underlying landforms. However, the aeolian covers are rather thin at Dongcun and
330 Xiaolangdi in comparison with those at Zhangbian, Sanmenxia, and Kouma, probably
331 because accumulation was less in the confined Sanmen gorge (Fig. 5). Thus the
332 Sanmenxia transect was selected for the analysis of magnetostratigraphy and,
333 ~~pedostratigraphy, and OSL geochronology~~ of the aeolian sequence.

334 With reference to the established timescale of the aeolian sedimentary sequence
335 on the Chinese Loess Plateau, enhanced by astronomical tuning and paleomagnetism,
336 the basal ages of aeolian cover on each terrace along the Sanmen gorge can be
337 determined. Readers ~~areean~~ be referred to Ding et al. (2002) for a detailed
338 chronostratigraphic framework of the Chinese loess. ~~Thuse~~ ~~erefore,~~ these aeolian series,
339 in combination with their magnetostratigraphic and pedostratigraphic properties,
340 provide a geochronological framework for the terrace sequences in the five Yellow
341 River transects, as will now be described. The present study concentrates on the,
342 hitherto undated, aeolian deposits above the planation surface and terrace T5. ~~Since the~~
343 ~~formation ages of terraces T4, T3 and T2 at Sanmenxia were determined previously~~
344 ~~by Pan et al. (2005a) as 0.86 Ma, 0.62 Ma, and 129 ka, respectively, the present study~~
345 ~~concentrates on samples of aeolian deposits above the planation surface, terrace (T5),~~
346 ~~and the lowermost (T1) terrace.~~

348 32.3. Magnetic susceptibility measurements

349
350 Magnetic susceptibility reflects the layering of loess and palaeosols (Soreghan et
351 al., 1997) and thus can further confirm the identification of pedostratigraphic units
352 and aid correlation. Powder samples were taken at 0.05-m intervals from the aeolian
353 covers of the planation surface and uppermost terrace (T5). A total of 5650 samples
354 were air-dried in the laboratory and then gently ground. Measurements with a
355 Bartington MS2B magnetic susceptibility meter were used to obtain the mass
356 magnetic susceptibility (Fig. 7).

357
358 <Fig. 7 hereabout>

360 32.4. Paleomagnetism

361

362 Samples were taken from the 152-m and 130.5-m thick aeolian deposits
363 accumulated respectively on top of the planation surface and the uppermost terrace
364 (T5). A total of 441 oriented block samples were collected at 0.25-m intervals in the
365 Red Clay and at intervals of ~0.5–3.0 m in the loess. In the laboratory these samples
366 were cut into 2-cm³ transects, producing three sets of paleomagnetic logs. All the
367 processed samples were thermally demagnetized in 15–17 steps at 50–30°C intervals
368 (between 50 and 680°C) with an MMTD-80 Thermal Demagnetizer. Remanent
369 magnetization and magnetic orientation were measured on a 2G-755R
370 Superconducting Rock Magnetometer in the magnetically shielded room of the
371 Paleomagnetic Laboratory of the Key Laboratory of western China's Environmental
372 System (MOE), Lanzhou University.

373 Two components are generally distinguished in the palaeomagnetic signal, by
374 contrasting directions and intensities. A low-temperature component (LTC) in roughly
375 the normal polarity direction is removed gradually by thermal treatment in the interval
376 100–150 °C (but sometimes up to 200–350 °C). This LTC is generally interpreted as a
377 secondary remanent magnetization characterized by a viscous superimposed direction.
378 Upon removal of the LTC, a high-temperature component (HTC) shows relatively
379 stable directions and linear decay in intensity toward the origin. This HTC is generally
380 interpreted as the primary magnetization acquired during deposition. The directions of
381 the HTC are calculated using the least-squares fitting technique (Kirschvink, 1980)
382 for selected demagnetization data points (minimum of three, but mostly 5–10).

383

384 ~~2.5. OSL dating~~

385

386 ~~In order to evaluate the formation ages of T1, a single OSL sample was collected~~
387 ~~in a metal cylinder, using standard methodology, from the lower part of overbank~~
388 ~~sediments belonging to this terrace (Fig. 5). The sample was pretreated according to~~
389 ~~the method by Zhao and Li (2002) and measurement (in the Luminescence Laboratory~~
390 ~~of the Qinghai Institute of Salt Lakes, Chinese Academy of Sciences) used an~~
391 ~~automated Risø TL/OSL DA 20 reader, applying the double single aliquot~~
392 ~~regeneration dose procedure (Banerjee et al., 2001).~~

393

394 **4.3. Results**

395

396 | 4.3.1. The terrace succession

397

398 A well-preserved sequence of five strath terraces was identified between the
399 present river bed and the planation surface (Fig. 4C and D), within which the
400 uppermost terrace is ~~a newly recognized terrace~~ in comparison with the previous
401 study by Pan et al. (2005a). The term strath terrace is used here to describe an
402 erosional terrace with only a relatively thin gravel layer, isolated vertically from the
403 gravels of other terraces. In this terrace sequence, all terraces are eroded into the Early
404 Pleistocene lacustrine Sanmen Formation (see Fig. 4E for sedimentary characteristics).
405 The planation surface, cut through pre-existing limestone, basin-fill sediments, and
406 tectonic structures, is overlain by 12.5-m-thick Red Clay and a 139.5 m thick loess
407 sequence, characterized by alternating loess (L) and palaeosol (S) units (Fig. 7). No
408 indications of erosional disconformity between the Red Clay and the loess have been
409 observed. Palaeosol complex S5, consisting of three sub-palaeosols, is the most
410 prominent one within the sequence on the Chinese Loess Plateau, and is distinguished
411 by its great thickness and dark color, being generally regarded as a marker layer (Liu,
412 1985). It can be discerned by field observations to occur at a depth of 107.6–115.3 m
413 in the aeolian cover of the planation surface at Sanmenxia, which contains 32
414 palaeosol units (Fig. 7). ~~On the basis of this marker layer, the loess stratigraphy above~~
415 ~~this surface may be divided into 32 palaeosol units (from S32 to S1).~~ The loess
416 deposits above the gravels of terraces T5, T4, T3, and T2 are ~130, 114, 64, and 30 m
417 thick respectively (Fig. 7). From detailed field observations, the loess stratigraphy on
418 these four terraces can be divided, respectively, into fifteen, nine, six, and three red
419 palaeosol units, which can be readily correlated with the upper palaeosol units (S14 to
420 S1) on the planation surface. The basal palaeosol units of each terrace can be shown
421 to overlie the fluvial deposits without a significant hiatus. In the case of the planation
422 surface and terrace T5, these pedostratigraphic correlations, based on field
423 observations, have been further corroborated by patterns of magnetic susceptibility
424 variation ~~and by OSL geochronology~~ (see below). The lowermost terrace has been
425 OSL-dated to 12.7 ± 1.2 ka (HZB-2; Fig. 5).

426

427 | 4.3.2. Magnetic susceptibility and OSL ages

428

429 | ~~As noted above, M~~agnetic susceptibility reflects the distinction between loess

430 (L) and palaeosols (S), with higher values in palaeosols than in loess, ~~proving to be a~~
431 ~~considerable aid in determining the loess soil stratigraphy of the region~~ (e.g., Kukla
432 et al., 1988; Maher and Thompson, 1991; Soreghan et al., 1997). The variation
433 patterns of magnetic susceptibility in the loess deposits on the planation surface and
434 uppermost terrace (T5) are closely consistent with field observations of
435 pedostratigraphy (Fig. 7). For palaeosol complex S5 in the two studied loess covers,
436 the magnetic susceptibility increases steeply and reaches its highest value in the
437 middle part of this complex, suggesting a prominently developed palaeosol unit. More
438 specifically, large amplitude fluctuations of magnetic susceptibility appear in this
439 palaeosol complex, showing three marked peaks that correspond well with the three
440 subsidiary divisions of this prominent S5 palaeosol. Using S5 as a marker horizon,
441 magnetic susceptibility data were used to divide the loess sequences on the planation
442 surface and terrace T5, respectively, into 32 (from S1 to S32, with the basal loess unit
443 L33) and 15 (Sm–S14) established palaeosol units. The magnetic susceptibility
444 patterns from these two loess covers are in good agreement with comparable records
445 from the Chinese Loess Plateau (e.g., Lu et al., 1999; Pan et al., 2012). Their high
446 magnetic susceptibility values match well with the light red palaeosol units, implying
447 that the pedostratigraphic divisions based on field observations, as described in this
448 paper, are reliable.

449 The Red Clay beneath the Quaternary loess ~~was deposited~~
450 immediately on top of the planation surface. Its magnetic susceptibility gradually
451 increases upwards, reaching its highest value at the top of the unit. Further upwards,
452 the values decrease markedly in the overlying pedogenic carbonate nodule layer and
453 then recover in the transitional layer (TU) between Red Clay and the overlying
454 Quaternary loess. This pattern of magnetic susceptibility in the Red Clay obtained
455 here concurs with magnetic susceptibility records from late Pliocene Red Clay
456 sections on the Chinese Loess Plateau (Sun et al., 2006; Pan et al., 2011).

457

458 ~~<Table 2 hereabout>~~

459

460 ~~For the lowest terrace (T1), the analytical data and results from OSL dating are~~
461 ~~tabulated in Table 2. This OSL sample (Laboratory ID: HZB-2) collected from the~~
462 ~~lower part of the overbank sediments on this terrace was dated at 12.7 ± 1.2 ka (Fig.~~
463 ~~5), consistent with emplacement of the overbank sediments of terrace T1 since the last~~

464 ~~glacial maximum of the Late Pleistocene.~~

465
466 4.3.3. Paleomagnetism

467
468 Three sets of palaeomagnetic transects, collected from the aeolian covers of the
469 planation surface and terrace T5 at each section, show similar properties. Most
470 samples maintain strong remanent magnetization, with clear separation of
471 characteristic remanent magnetization (ChRM) directions (see Fig. 8 for the typical
472 thermal demagnetization diagrams).

473
474 <Fig. 8 hereabout>

475
476 The pedostratigraphy and magnetic patterns of the aeolian covers on the
477 planation surface and uppermost terrace (T5) are illustrated in Fig. 7. The
478 magnetostratigraphic patterns from the two covers can be correlated with the
479 geomagnetic polarity timescale (GPTS) of Cande and Kent (1995).

480 In the 152.0-m thick aeolian deposits on the planation surface, both the
481 stratigraphic subdivision of the loess and the conformity between the Red Clay and
482 overlying loess deposits provide a reliable indication that the chronology of the
483 aeolian cover extends from the Pliocene to the late Pleistocene (Liu, 1985). Thus the
484 obtained magnetozones correlate typically with the polarity intervals from Brunhes to
485 Gauss in the geomagnetic polarity timescale. The Gauss normal-polarity chron occurs
486 between 0.5 and 11.5 m above the planation surface and includes two
487 reversed-polarity subchrons that pinpoint the basal age of aeolian deposits here to the
488 Kaena and Mammoth subchrons. The Gauss–Matuyama boundary occurs in the lower
489 part of TU, which is also the boundary between the Neogene Red Clay and
490 Quaternary loess (Liu, 1985; Ding et al., 1990). The Olduvai normal subchron,
491 spanning 38–30 m, occurs between S27 and L25. The Jaramillo normal subchron,
492 extending from 74.5 to 82.0 m, is registered between S11 and L10. The
493 Matuyama-Brunhes boundary is found at a depth of 98.0 m in L8. These
494 paleomagnetic polarity events identified in the stratigraphy on the planation surface
495 are in full agreement with the well-established loess and Red Clay
496 magnetostratigraphy on the Chinese Loess Plateau (cf. Kukla and An, 1989; Rutter et
497 al., 1991; Zhu et al., 1994; Ding et al., 1998; Pan et al., 2012). On the Loess Plateau,

498 since the sedimentation rate in the Red Clay (~1.5 cm/ky) was generally lower than
499 that in the Quaternary loess (~10 cm/ky) (e.g., Vandenberghe et al., 2004),
500 extrapolation of the prevailing accumulation rate of the Red Clay (here, ~1.1 cm/ky
501 within the Gauss chron) below the lower boundary of the Gauss normal polarity chron
502 is a more logical approach for dating the basal Red Clay, rather than using an
503 accumulation rate averaged over the entire aeolian sequence (Red Clay and loess).
504 This approach yields an estimated age of ~3.63 Ma for the onset of aeolian deposition
505 on the planation surface.

506 For the ~130 m thick loess cover stacked on the uppermost terrace (T5), the
507 Matuyama–Brunhes boundary occurs at a depth of 49.0 m and coincides with L8. The
508 Jaramillo normal subchron, spanning from 18.0 to 28.5 m, is registered between S11
509 and L10. It is clear that the positions of these paleomagnetic polarity events may
510 readily be correlated with the magnetostratigraphy derived from the aeolian cover of
511 the planation surface. Extrapolation of the prevailing accumulation rate of the loess
512 deposits (~10.5 cm/ky) below the lower boundary of the Jaramillo normal subchron
513 produces an estimated age of ~1.24 Ma for the basal loess deposits lying on this
514 terrace.

515

516 **54. Discussion**

517

518 **54.1. Age determination of the fluvial terraces within the Sanmen gorge**

519

520 ~~It is well known that the dating of aeolian deposits can provide an indication of~~
521 ~~the age of underlying geomorphic surfaces, particularly river terraces. In the eastern~~
522 ~~part of the Chinese Loess Plateau, it has been shown that dust fall was persistent from~~
523 ~~late Miocene times onwards (Qiang et al., 2001; Zhao et al., 2002) and thus the~~
524 ~~accumulation of aeolian deposits can be assumed to have started immediately after the~~
525 ~~formation of the underlying landforms (e.g., Porter et al., 1992; Pan et al., 2009). In~~
526 ~~addition, In~~ most cases there is a gradual transition from terrace gravel to overbank
527 sediments and, finally, to primary (in situ) aeolian deposits (Vandenberghe et al.,
528 2012). Therefore, the basal age of the aeolian deposits immediately overlying the
529 planation surface and terrace treads can be roughly equated with the formation times
530 of the geomorphic surfaces (planation and fluvial terrace surfaces). Supplementary to
531 the previous dating of~~In the case of the sequence in the research area~~, terraces T4, T3,

532 and T2 ~~were previously dated~~ by Pan et al. (2005a), ~~to~~ ~~to~~ 860, 620, and 129 ka,
533 respectively, ~~t~~. The newly recognized planation surface and uppermost terrace (T5)
534 have now provided age estimates also (Fig. 7). Although the terrace called T5 here
535 was previously recognized by Kong et al. (2014), its age was not determined
536 successfully by their cosmogenic radio nuclide (CRN) study, which may be linked to
537 the difficulty of getting reliable burial dates from river terrace deposits (Rixhon et al.,
538 2016). In comparison, the latter authors assigned an age of 1.3 Ma to the lower
539 sediments of terrace T4, which is older than the abandonment age of 860 ka obtained
540 by Pan et al (2005a). According to the magnetostratigraphic analyses of the basal parts
541 of the aeolian covers, the ages of the planation surface and terrace T5 are ~3.63 Ma
542 and ~1.24 Ma, respectively; the latter age is close to the 1.5 ~~--~~ 1.3 Ma suggested by
543 Kong et al. (2014) for the initiation of drainage (by the Weihe River) through the
544 Sanmen gorge.

545 ~~The OSL age for the lower overbank sediments suggests that the lowest terrace~~
546 ~~(T1) was formed after ~12 ka.~~

547 — On the basis of field investigation, the tread of the uppermost terrace (T5) at
548 Sanmenxia can be traced over an extensive area upstream and extending downstream
549 into the inner Sanmen gorge, and can be correlated tentatively (based on height above
550 modern river) with the uppermost terraces formed at Zhangbian, Dongcun, and
551 Xiaolangdi (Fig. 6). This distributional pattern indicates that the uppermost terrace
552 below the planation surface is generally continuous, representing the initial fluvial
553 incision by the Yellow River within the gorge. In addition, the magnetostratigraphic
554 record from the uppermost terrace at Kouma, downstream of the Sanmen gorge, has
555 also been dated previously to ~1.2 Ma (Pan et al., 2005b). The temporal coincidence
556 of the uppermost terraces upstream and downstream of this gorge suggests that the
557 first phase of downcutting by the Yellow River from the planation surface to the level
558 of the uppermost terrace was prior to ~1.2 Ma (again in general agreement with the
559 previous conclusions of Kong et al. (2014)).

560

561 ~~54.2. Evolution of the middle to lower Yellow River catchment from~~ Fluvial landscape
562 ~~evolution by the Yellow River from~~ basin filling to ~~entrenchment~~ excavation
563

564 The magnetostratigraphic record from the aeolian cover of the planation surface
565 at Sanmenxia suggests that before 3.63 Ma the Fenwei graben (represented by the

Formatted: Indent: First line: 2 ch

566 Lingbao basin) had become progressively filled with the lacustrine sediments (Fig.
567 9AI). Geomorphic investigation along the Sanmen gorge (Fig. 5) indicates that at this
568 time the local relief was progressively lowered to basin-fill level, eventually forming
569 the planation surface (Fig. 9AII) that extends across the Fenwei graben and the
570 surrounding mountain ranges (including the Xiaoshan) as was the case at the northern
571 Tibetan Plateau (Wang et al., 2012).

572

573

<Fig. 9 hereabout>

574

575 Elsewhere, the development of low-relief landscapes ('planation surface') has
576 been claimed as a reliable marker to indicate subsequent landscape rejuvenation,
577 uplift and deformation (e.g., Ollier and Pain, 2000; Clark et al., 2004; Peulvast and
578 Sales, 2004). Before and during the Pliocene, large parts of Europe, Africa, and Asia
579 were planated, all in areas that were unaffected by plate motions, thus leading to the
580 widespread development of low-relief landscapes (e.g., Cui et al., 1996; Danišik et al.,
581 2006; Coltorti et al., 2007; Wagner et al., 2011; Pan et al., 2012; Vandenberghe, 2016).
582 The comparable low-relief landscape or 'planation surface', recognized in and around
583 the Fenwei graben and the Xiaoshan has been significantly uplifted by plate tectonic
584 processes and subsequently and dissected. ~~This is a result, we suggest, of plate~~
585 ~~tectonic processes, with erosion perhaps enhanced by the strengthened of the East~~
586 ~~Asian monsoon (see above).~~ The continuation of tectonic activity after the formation
587 of the planation level during the late Pliocene and Quaternary can be demonstrated.
588 First, as is apparent from the geomorphic section at Sanmenxia (Fig. 5), the
589 downtthrow of the hanging-walls along the ~~indicates that~~ normal faults bounding the
590 Lingbao basin (within the ~~older~~ graben system of the Fenwei; Fig. 9B) ~~were active~~
591 ~~~3.63 Ma; the downthrow in their hanging walls~~ disrupted the ~~older~~ 'planation
592 surface', which itself became uplifted in the Xiaoshan area. Second, seismic data
593 alsoanalysis indicates that the normal faults bounding the Lingbao basin have
594 remained active during the Quaternary (Li et al., 2015). ~~The In this case, the~~
595 ~~subsequent~~ evolution of this active basin was probably independent of the rest of the
596 southern Shanxi rift. As the Xiaoshan mountains grew higher, the ancestral fluvial
597 system that drained theirs eastern front ~~—~~ began to cut headward, toward the west
598 (Wang et al., 2001).

599 The sedimentary record in the North Pacific indeed shows that dust deposition

600 increased quite rapidly, by an order of magnitude, at 3.6 Ma (Rea, et al., 1998), which
601 may have been associated with the uplift of the Tibetan Plateau and the cooling of the
602 northern hemisphere. Continuous aeolian deposition in the present study region also
603 began by this time, resulting in accumulation on the ‘planation surface’ (our basal
604 age). After this time, this inner sub-basin of the Fenwei graben, which previously
605 drained internally, became filled with fluvio-lacustrine sediments (the Sanmen
606 Formation, illustrated in Fig. 4E) with a paleolake eventually covering much of the
607 graben (Liu, 2004). This lake was then drained and the Sanmen gorge formed,
608 initiating external drainage and linkage to the Yellow River system.

609 We suggest that the remarkable transition of the Fenwei graben, from filling to
610 excavation (incision), was thus associated with the establishment of external drainage
611 and the formation of the Sanmen gorge. ~~Our data (Fig. 9CI) imply that gorge incision~~
612 ~~started between 3.63 (the age of the planation surface) and 1.24 Ma (the age of the~~
613 ~~highest terrace, which is below the top of the gorge sides), broadly confirming the~~
614 ~~findings of Kong et al. (2014).~~ The Xiaoshan barrier may have been breached by lake
615 spillover as the ancestral fluvial system at its eastern front cut headward towards the
616 Lingbao basin (Fig. 9C, I). Subsequently, following the emptying of the lake, fluvial
617 incision into the sediments of the Sanmen Formation began (Fig. 9CII). The
618 geomorphic evidence indeed suggests that this drainage integration was associated
619 with fluvial downcutting, from the ‘planation surface’ down to the level of the
620 uppermost terrace (T5). The approximately synchronous development of this terrace
621 both within the Sanmen gorge and further downstream at Kouma (see above), with
622 dates of ~1.24 Ma and 1.2 Ma (respectively), indicates that the modern Yellow River
623 had been established by this time ~~and: s~~Subsequently became entrenched ~~by the~~
624 ~~Yellow River progressively created the present Sanmen gorge~~ (Fig. 9D). ~~The~~
625 ~~formation of a river terrace staircase within the Fenwei graben is notable, implying~~
626 ~~that the graben interior is uplifting (a requirement for terrace formation), albeit at a~~
627 ~~slower rate than the crust outside the faulted interior of the system (cf. Gao et al.,~~
628 ~~2016).~~

629 The initial development of the Sanmen gorge was thus an important event, since
630 it marked the initiation of the eastward-flowing drainage of the Yellow River. Once
631 this gorge had begun to form, terrigenous sediments could be transported from the
632 interior of the Tibetan Plateau, in the upper reaches of the Yellow River, to the Bohai
633 Gulf. ~~Althoughs already noted,~~ loess began to accumulate in the present study region

Formatted: Font: Times New Roman

634 | at significant rates by ~3.6 Ma, (Rea et al., 1998). However, terrigenous sedimentation
635 | rates on the North China Plain and in the Bohai Gulf did not show dramatic increases
636 | until ~1.0 Ma (Xiao et al., 2008; Yao et al., 2010, 2012), in all probability in response
637 | to the formation of the Sanmen gorge. As Nie et al. (2015) have suggested, the
638 | majority of the sediment liberated by the dissection of the 'planation surface' from the
639 | middle and upper Yellow River basins was probably stored on the Chinese Loess
640 | Plateau before the through-going Yellow River drainage system was formed.

641 | ~~Similar sequences of events, whereby ancestral lake basins were disrupted and~~
642 | ~~replaced by fluvial drainage, are also recognized in other continental interior regions~~
643 | ~~worldwide. For example, the history of integration of the upper reaches of the modern~~
644 | ~~River Euphrates (in the eastern Anatolian Plateau) with the rest of its catchment,~~
645 | ~~starting in the Mid-Pleistocene and associated with the disruption of paleolake basins,~~
646 | ~~as investigated by Seyrek et al. (2008), Westaway et al. (2008), and Demir et al.~~
647 | ~~(2009). Regional uplift of the eastern Anatolian Plateau and active faulting both~~
648 | ~~played a part in this sequence of events. Another example, documented by Westaway~~
649 | ~~et al. (2009), was the integration of the modern Rio Grande River in the~~
650 | ~~central southern USA. In that example the upper reaches of the ancestral river system~~
651 | ~~drained into a paleolake in the Rio Grande Rift, an actively developing graben;~~
652 | ~~however, faster regional uplift following the Mid-Pleistocene Revolution resulted in~~
653 | ~~disruption of this lake basin and the initiation of fluvial entrenchment, marked by~~
654 | ~~dated river terraces, into its former interior. Numerous other examples of 'inverted'~~
655 | ~~Late Cenozoic fluvio-lacustrine basins could be documented, including many reported~~
656 | ~~by earlier FLAG research (e.g., Matoshko et al., 2004; Bridgland and Westaway, 2014)~~
657 | ~~and in the present issue (Bridgland et al., 2016; Cunha et al., 2016; Maddy et al.,~~
658 | ~~2016).~~

659 | The formation of the Sanmen Gorge, which enabled through drainage from the
660 | upper Yellow River to the Bohai Gulf, would appear to have been the lastfinal in a
661 | series of linkage events joining inland basins. This progressive drainage linkage can
662 | now be envisaged to have occurred in sequence from upstream to downstream (contra
663 | Molnar, 2004), perhaps by means of repeated basin overflow in response to
664 | progressive basin filling coupled with increasing precipitation from the strengthening
665 | Asian Monsoon. The occurrence of this final eastern completion of the
666 | through-flowing Yellow River can also be demonstrated by the change in the type of
667 | zircons grains in the thick perched sedimentary sequence at Liujiashou (close to our

668 site at Sanmenxia) reported by Kong et al. (2014), and called T5 by them. Zircon in
669 the lower sediments here were of more local origin, whereas those from a sample high
670 in the sequence (like those from later terrace sediments) were from upstream in the
671 Yellow River, suggesting that basins upstream had been joined to form a
672 through-flowing system by the time these uppermost sediments were deposited, just
673 before incision by the newly-formed river and the development of the lower terrace
674 staircase.

675

676 54.3. Wider comparisons

677

678 Similar sequences of events, whereby ancestral lake basins were disrupted and
679 replaced by fluvial drainage, are also recognized in other continental interior regions
680 worldwide. For example, the history of integration of the upper reaches of the modern
681 River Euphrates (in the eastern Anatolian Plateau) with the rest of its catchment,
682 starting in the Mid-Pleistocene and associated with the disruption of paleolake basins,
683 as investigated by Seyrek et al. (2008), Westaway et al. (2008), and Demir et al.
684 (2009). Regional uplift of the eastern Anatolian Plateau and active faulting both
685 played a part in this sequence of events. Another example, documented by Westaway
686 et al. (2009), was the integration of the modern Rio Grande River in the
687 central-southern USA. In that example the upper reaches of the ancestral river system
688 drained into a paleolake in the Rio Grande Rift, an actively-developing graben;
689 however, faster regional uplift following the Mid-Pleistocene Revolution resulted in
690 disruption of this lake basin and the initiation of fluvial entrenchment, marked by
691 dated river terraces, into its former interior. Numerous other examples of ‘inverted’
692 Late Cenozoic fluvio-lacustrine basins could be documented, including many reported
693 by earlier FLAG research (e.g., Matoshko et al., 2004; Bridgland and Westaway, 2014)
694 and in the present issue (Bridgland et al., 2016; Cunha et al., 2016; Maddy et al.,
695 2016).

696 Attempts have recently been made to integrate onshore datasets indicating rates
697 of erosion and offshore datasets indicating rates of deposition (e.g., Herman et al.,
698 2013; Herman and Champagnac, 2016). It has been argued on the basis of increases in
699 offshore sedimentation rates that accordingly terrestrial erosion rates increased (e.g.,
700 Zhang et al., 2001; Molnar, 2004). However, others have rejected the idea that erosion
701 rates have increased in the Late Cenozoic (e.g., Willenbring and von Blanckenburg,

2010; Sadler and Jerolmack, 2015; Willenbring and Jerolmack, 2016). It has been shown here that the Yellow River and other major rivers only became integrated with their present catchment geometries in the relatively recent geological past, such that, beforehand, the products of erosion throughout much of these catchments were trapped in inland depocentres and were thus unable to reach the sea. This has to be considered as an important complicating factor in attempting comparison of global datasets of Late Cenozoic onshore erosion and offshore deposition.

~~An interesting point of comparison with other regions concerns the recognition, within the Fenwei graben, of a river terrace staircase (Fig. 9D), thus implying that the graben interior is uplifting (a requirement for terrace formation), albeit at a slower rate than the crust outside the faulted interior of the system. Absolute uplift has also been recognized within the interiors of onshore grabens flanking the Aegean Sea (e.g., Westaway, 1993a), thus superseding the former paradigm that hanging wall localities are always subsiding (cf. Jackson and McKenzie, 1983). Uplift has also been recognized in graben interiors or normal fault hanging walls in many other regions, including southern Italy (Westaway, 1993; Westaway and Bridgland, 2007), Bulgaria (Westaway, 2006), central southern Turkey (Seyrek et al., 2014), and the aforementioned Rio Grande Rift in the central southern USA (Westaway et al., 2009).~~

65. Conclusions

Downcutting by the Yellow River into the Xiaoshan range, below a planation surface dated to ~3.63 Ma, has resulted in the formation of the Sanmen gorge. On the basis of detailed field investigation, a new and uppermost Yellow River terrace, T5, has been recognized along the gorge. As a result, a sedimentary and geomorphic archive of five terraces was formed, in addition to the above-mentioned planation surface. Magnetostratigraphic records from the aeolian deposits accumulated on top of these surfaces provide a geochronological framework for this archive. The ages of the planation surface (P) and terraces T5, T4, T3, T2, and T1 ~~have been~~ were determined at ~3.63 Ma, ~1.24 Ma, ~0.86 Ma, ~0.62 Ma, ~129 ka, and ~12 ka, respectively. Thus, the formation ages of the planation surface and uppermost terrace suggest that this gorge was entrenched primarily between 3.63 and 1.24 Ma. At the same time the landscape of the Fenwei region switched from basin filling to excavation ('basin inversion') enabling the formation of a series of terraces within the graben, which

Formatted: Indent: First line: 0 cm

736 | ~~could be termed 'basin inversion'~~. Before the start of entrenchment of the Sanmen
737 gorge, the products of erosion in the modern upper catchment of the Yellow River
738 were 'trapped' inland and, therefore, unable to reach the sea. The dramatic increase in
739 deposition rates in the Bohai Gulf, at the mouth of the modern Yellow River, at ~1.0
740 Ma, resulted from the integration of the Yellow River catchment following the
741 initiation of drainage through Sanmen gorge and does not imply an increase in erosion
742 rates at that time.

743 **Acknowledgements**

744

745 We are grateful to Xiaopeng Liu, Jian Zhang, and Prof. Qingyu Guan for
746 assistance with the field sampling and laboratory analyses. The comments by Prof.
747 Frank J. Pazzaglia, [an](#) anonymous referee, and the special issue editor, Stéphane
748 Cordier, have led to considerable improvements and are gratefully acknowledged.
749 This research is financially supported by the National Natural Science Foundation of
750 China (Grant no. 41401001, 41571003), the Key Project of the Major Research Plan
751 of the NSFC (Grant no. 91125008), the National Basic Research Program of China
752 (2011CB403301), and the Fundamental Research Funds for the Central Universities.

753 **References**

754

755 AFSOM, 1988. Active fault system around Ordos Massif. Seismological Press,
756 Beijing, pp. 77-136 (in Chinese).

757

758 An, Z., Kutzbach, J.E., Prell, W.L., Porter, S.C., 2001. Evolution of Asian monsoon
759 and phased uplift of the Himalayan-Tibetan Plateau since Late Miocene times. Nature
760 411, 62-66.

761

762 ~~Banerjee, D., Murray, A.S., Bøtter-Jensen, L., Lang, A., 2001. Equivalent dose~~
763 ~~estimation using a single aliquot of polymineral fine grains. Radiation Measurements~~
764 ~~33, 73-94.~~

765

766 Bridgland, D.R., 2000. River terrace systems in north-west Europe: an archive of
767 environmental change, uplift and early human occupation. Quaternary Science
768 Reviews 19, 1293-1303.

769

770 Bridgland, D.R., Westaway, R., 2008. Climatically controlled river terrace staircases:
771 A worldwide Quaternary phenomenon. Geomorphology 98, 285-315.

772

773 Bridgland, D.R., Westaway, R., Abou Romieh, M., Candy, I., Daoud, M., Demir, T.,
774 Galiatsatos, N., Schreve, D., Seyrek, A., Shaw, A., White, T., Whittaker, J., 2012. The
775 River Orontes in Syria and Turkey: Downstream variation of fluvial archives in
776 different crustal blocks. Geomorphology 165-166, 25-49.

777

778 Bridgland, D.R., Westaway, R., 2014. Quaternary fluvial archives and landscape
779 evolution: a global synthesis. Proceedings of the Geologists' Association 125,
780 600-629.

781

782 Bridgland, D.R., Demir, T., Seyrek, A., Abou Romieh, M., Daoud, M., Westaway, R.,
783 2016. River terrace development in the NE Mediterranean region (Syria and Turkey):
784 patterns in relation to crustal type. Quaternary Science Reviews.

785

786 Bull, W.B., 1990. Stream-terrace genesis: implication for soil development.
787 *Geomorphology* 3, 351-367.
788

789 Cande, S.C., Kent, D.V., 1995. Revised calibration of the geomagnetic polarity
790 timescale for the Late Cretaceous and Cenozoic. *Journal of Geophysical Research* 100,
791 6093-6095.
792

793 Cheng, S., Deng, Q., Zhou, S., Yang, G., 2002. Strath terraces of Jinshaan Canyon,
794 Yellow River, and Quaternary tectonic movements of the Ordos Plateau, north China.
795 *Terra Nova* 14, 215-224.
796

797 Clark, K.M., Schoenbohm, M.L., Royden, H.L., Whipple, X.K., Burchfiel, C.B.,
798 Zhang, X., Tang, W., Wang, E., Chen, L., 2004. Surface uplift, tectonics, and erosion
799 of eastern Tibet from large-scale drainage patterns. *Tectonics* 23, TC1006,
800 doi:10.1029/2002TC001402.
801

802 Clift, D.P., 2006. Controls on the erosion of Cenozoic Asia and the flux of elastic
803 sediment to the ocean. *Earth and Planetary Science Letters* 241, 571-580.
804

805 Coltorti, M., Dramis, F., Ollier, D.C., 2007. Planation surfaces in Northern Ethiopia.
806 *Geomorphology* 89, 287-296.
807

808 Craddock, H.W., Kirby, E., Harkins, W.N., Zhang, H., Shi, X., Liu, J., 2010. Rapid
809 fluvial incision along the Yellow River during headward basin integration. *Nature*
810 *Geoscience* 3, 209-213.
811

812 Cui, Z., Gao, Q., Liu, G., Pan, B., Chen, H., 1996. Planation surface, palaeokarst and
813 uplift of Xizang (Tibet) Plateau. *Science in China* 39, 391-400.
814

815 Cunha, P.P., Martins, A.A., Buylaert, J.P., Murray, A.S., Raposo, L., Mozzi, P., Stokes,
816 M., 2016. New data on the chronology of the Vale do Forno sedimentary sequence
817 (Lower Tejo River terrace staircase) and its relevance as a fluvial archive of the
818 Middle Pleistocene in western Iberia. *Quaternary Science Reviews*.
819 <http://dx.doi.org/10.1016/j.quascirev.2016.11.001>.

820

821 Danišík, M., Kuhlemann, J., Dunkl, I., Székely, B., Frisch, W., 2006. Significance of
822 high-elevated planation surfaces in interpreting thermotectonic evolution of the
823 mountains. Goldschmidt Conference Abstracts A126.

824

825 Demir, T., Seyrek, A., Guillou, H., Scaillet, S., Westaway, R., Bridgland, D.R., 2009.
826 Preservation by basalt of a staircase of latest Pliocene terraces of the River Murat in
827 eastern Turkey: evidence for rapid uplift of the eastern Anatolian Plateau. *Global and*
828 *Planetary Change* 68, 254-269.

829

830 Ding, Z., Liu, T. S., Liu, X. M., Chen, M. Y., An, Z. S., 1990. Thirty-seven climatic
831 cycles in the last 2.5 Ma. *Chinese Science Bulletin*. 34, 1494-1496.

832

833 Ding, Z., Sun, J.M., Yang, S.L., Liu, T.S., 1998. Preliminary magnetostratigraphy of a
834 thick eolian red clay-loess sequence at Lingtai, the Chinese Loess Plateau.
835 *Geophysical Research Letters*. 25, 1225-1228.

836

837 Ding, Z., Derbyshire, E., Yang, S., Yu, Z., Xiong, S., Liu, T., 2002. Stacked 2.6-Ma
838 grain size record from the Chinese loess based on five sections and correlation with
839 the deep-sea $\delta^{18}\text{O}$ record. *Paleoceanography* 17, 1033-1053.

840

841 Dong, Y., Zhang, G., Neubauer, F., Liu, X., Genser, J., Hauzenberger, C., 2011.
842 Tectonic evolution of the Qinling orogen, China: Review and synthesis. *Journal of*
843 *Asian Earth Sciences* 41, 213-237.

844

845 Fan, D., Li, C., 2008. Timing of the Yangtze initiation during the Tibetan Plateau
846 throughout to the East China Sea: A review. *Front Earth Science China* 2, 302-313.

847

848 [Gao, H., Li, Z., Ji, Y., Pan, B., Liu, X., 2016. Climatic and tectonic controls on strath](#)
849 [terraces along the upper Weihe River in central China. *Quaternary Research* 86,](#)
850 [326-334.](#)

851

852 Geng X., 1981. Marine transgressions and regressions in East China since Late
853 Pleistocene epoch. *Acta Oceanologica Sinica* 3, 114-130 (in Chinese, with English

854 abstract).

855

856 Guo, Y., Zhang, J., Qiu, W., Hu, G., Zhuang, M., Zhou, L., 2012. Luminescence dating
857 of the Yellow River terraces in the Hukou area, China. *Quaternary Geochronology* 10,
858 129-135.

859

860 He, P., Liu, L., Yu, Q., 1984. The age of the Sanmen series and the evolution of its
861 depositional environment discussed in the light of the Dongpogou section in the
862 Sanmen gorge area. *Geological Reviews* 30, 161-169 (in Chinese, with English
863 abstract).

864

865 Herman, F., Champagnac, J.-D., 2016. Plio-Pleistocene increase of erosion rates in
866 mountain belts in response to climate change. *Terra Nova*, 28, 2–10.

867

868 Herman, F., Seward, D., Valla, P.G., Carter, A., Kohn, B., Willett, S.D., Ehlers, T.A.,
869 2013. Worldwide acceleration of mountain erosion under a cooling climate. *Nature*,
870 504, 423–426.

871

872 ~~Hu, Z.B., Pan, B.T., Guo, L.Y., Vandenberghe, J., Liu, X., Wang, J., Fan, Y., Mao, J.,~~
873 ~~Gao, H., Hu, X., 2016. Rapid fluvial incision and headward erosion by the Yellow~~
874 ~~River along the Jinshaan gorge during the past 1.2 Ma as a result of tectonic extension.~~
875 ~~*Quaternary Science Reviews* 133, 1–14.~~

876

877 Huang, Z., Xu, M., Wang, L., Mi, N., Yu, D., Li, H., 2008. Shear wave splitting in the
878 southern margin of the Ordos Block north China. *Geophysical Research Letters* 35,
879 L19301. <http://dx.doi.org/10.1029/2008GL035188>.

880

881 ~~Jackson, J., McKenzie, D., 1983. The geometrical evolution of normal fault systems.~~
882 ~~*Journal of Structural Geology* 5, 471–482.~~

883

884 Ji, J., Zheng, H., Li, S., Huang, X., 2006. The terraces of the Huanghe River in Pinglu
885 County, Shanxi Province and their relationship with the disappearance of the Sanmen
886 palaeolake and the formation of the Huanghe River. *Quaternary Sciences* 26, 665-672
887 (in Chinese, with English abstract).

888

889 Jiang, F., Fu, J., Wang, S., Sun, D., Zhao, Z., 2007. Formation of the Yellow River,
890 inferred from loess-palaeosol sequence in Mangshan and lacustrine sediments in
891 Sanmen Gorge, China. *Quaternary International* 175, 62-70.

892

893 Kirschvink, J.L., 1980. The least-squares line and plane and the analysis of
894 palaeomagnetic data. *Geophysical Journal International* 62, 699-718.

895

896 Kong, P., Jia, J., Zheng, Y., 2014. Time constraints for the Yellow River traversing the
897 Sanmen Gorge. *Geochemistry, Geophysics, Geosystems* 15, 395-407.

898

899 Kukla, G., An, Z.S., 1989. Loess stratigraphy in central China. *Palaeogeography,
900 Palaeoclimatology, Palaeoecology*. 72, 203-225.

901

902 Kukla, G., Heller, F., Liu, M., Xu, C., Liu, S., An, S., 1988. Pleistocene climates in
903 China dated by magnetic susceptibility. *Geology* 16, 811-814.

904

905 Li, J., 1991. The environmental effects of the uplift of the Qinghai-Xizang Plateau.
906 *Quaternary Science Reviews* 10, 479-483.

907

908 Li, B., Sørensen, M.B., Atakan, K., 2015. Coulomb stress evolution in the Shanxi rift
909 system, North China, since 1303 associated with coseismic, post-seismic and
910 interseismic deformation. *Geophysical Journal International* 203, 1642-1664.

911

912 Lin, A.M., Yang, Z.Y., Sun, Z.M., Yang, T.S., 2001. How and when did the Yellow
913 River develop its square bend? *Geology* 29, 951-954.

914

915 Liu, H., 2004. Formation and evolution of the Weihe River basin and uplift of the
916 eastern Qinling Mountains, Ph.D. thesis, The Northeast University, Xian, China.

917

918 Liu, J., Zhang, P., Lease, R.O., Zheng, D., Wan, J., Wang, W., Zhang, H., 2013.
919 Eocene onset and late Miocene acceleration of Cenozoic intracontinental extension in
920 the North Qinling range-Weihe graben: Insights from apatite fission track
921 thermochronology. *Tectonophysics* 584, 281-296.

922
923 Liu S., Li, G., Li, Y., Jin, J., 1988. The sedimentary characteristics of the North China
924 plain as an indicator for the formation and evolution of the Yellow River. *Henan*
925 *Geology* 6, 20-24 (in Chinese).
926
927 Liu, T., 1985. *Loess and the Environment*. China Ocean Press, Beijing, pp. 31-147.
928
929 Liu, X., Chen, B., 2000. Climatic warming in the Tibetan Plateau during the recent
930 decades. *International Journal of Climatology* 20, 1729-1742.
931
932 Lu, H., Liu, X., Zhang, F., An, Z., Dodson, J., 1999. Astronomical calibration of
933 loess-palaeosol deposits at Luochuan, central Chinese Loess Plateau.
934 *Palaeogeography, Palaeoclimatology, Palaeoecology* 154, 237-246.
935
936 Maddy, D., Veldkamp, A., Demir, T., van Gorp, W., Wijbrans, J.R., van Hinsbergen,
937 D.J.J., Dekkers, M.J., Schreve, D., Schoorl, J.M., Scaife, R., Stemerink, C., van der
938 Schriek, T., Bridgland, D.R., Aytac, A.S., 2016. The Gediz River fluvial archive: a
939 benchmark for Quaternary research in Western Anatolia. *Quaternary Science Reviews*.
940 <http://dx.doi.org/10.1016/j.quascirev.2016.07.031>.
941
942 Maher, B.A., Thompson, R., 1991. Mineral magnetic record of the Chinese loess and
943 palaeosols. *Geology* 19, 3-6.
944
945 Matoshko, A., Gozhik, P., Danukalova, G., 2004. Key Late Cenozoic fluvial archives
946 of eastern Europe: the Dniester, Dnieper, Don and Volga. *Proceedings of the*
947 *Geologists' Association* 115, 141-173.
948
949 Miao, X., Lu, H., Li, Z., Cao, G., 2008. Paleocurrent and fabric analyses of the
950 imbricated fluvial gravel deposits in Huangshui Valley, the northeastern Tibetan
951 Plateau, China. *Geomorphology*. 99, 433-442.
952
953 Molnar, P., 2004. Late Cenozoic increase in accumulation rates of terrestrial sediment:
954 how might climate change have affected erosion rates? *Annu. Rev. Earth Planet. Sci.*

955 32, 67–89.

956

957 Molnar, P., England, P., Martinod, J., 1993. Mantle dynamics, uplift of Tibetan Plateau,
958 and the Indian Monsoon. *Reviews of Geophysics* 31, 357-396.

959

960 ~~Molnar, P., Boos, R.W., Battisti, S.D., 2010. Orographic controls on climate and~~
961 ~~paleoclimate of Asia: Thermal and mechanical roles for the Tibetan Plateau. *Annu-*~~
962 ~~*Rev. Earth Planet. Sci.* 38, 77-102.~~

963

964 Nie, J., Stevens, T., Rittner, M., Stockli, D., Garzanti, E., Limonta, M., Bird, A., Ando,
965 S., Vermeesch, P., Saylor, J., Lu, H., Breecker, D., Hu, X., Liu, S., Resentini, A.,
966 Vezzoli, G., Peng, W., Carter, A., Ji, S., Pan, B., 2015. Loess Plateau storage of
967 Northeastern Tibetan Plateau-derived Yellow River sediment. *Nature*
968 *Communications* 6, 1-8.

969

970 Ollier, C.D., Pain, C.F., 2000. *The Origin of Mountains*. Routledge, London.

971

972 Pan, B., Li, J., Chen, F., 1995. The Qinghai-Tibetan Plateau: Driver and amplifier of
973 the global climate changes. I The characteristics of climate changes in Cenozoic.
974 *Journal of Lanzhou University (Natural Science Edition)* 31, 120-128 (in Chinese,
975 with English abstract).

976

977 Pan, B.T., Burbank, D., Wang, Y.X., Wu, G.J., Li, J.J., Guan, Q.Y., 2003. A 900 k.y.
978 record of strath terrace formation during glacial-interglacial transitions in northwest
979 China. *Geology* 32, 957-960.

980

981 Pan, B.T., Wang, J.P., Gao, H.S., Chen, Y.Y., Li, J.J., Liu, X.F., 2005a. Terrace dating
982 as an archive of the run-through of the Sanmen Gorge. *Progress in Natural Science*.
983 15, 1096-1103.

984

985 Pan, B.T., Wang, J.P., Gao, H.S., Guan, Q.Y., Wang, Y., Su, H., Li, B.Y., Li, J.J.,
986 2005b. Paleomagnetic dating of the topmost terrace in Kouma, Henan and its
987 indication to the Yellow River's running through Sanmen Gorges. *Chinese Science*
988 *Bulletin*. 50, 657-664.

989
990 Pan, B., Su, H., Hu, Z., Hu, X., Gao, H., Li, J., Kirby, E., 2009. Evaluating the role of
991 climate and tectonics during non-steady incision of the Yellow River: evidence from a
992 1.24 Ma terrace record near Lanzhou, China. *Quaternary Science Reviews* 28,
993 3281-3290.
994
995 Pan, B.T., Hu, Z.B., Wang, J.P., Vandenberghe, J., Hu, X.F., 2011. A
996 magnetostratigraphic record of landscape development in the eastern Ordos Plateau,
997 China: Transition from Late Miocene and Early Pliocene stacked sedimentation to
998 Late Pliocene and Quaternary uplift and incision by the Yellow River.
999 *Geomorphology* 125, 225-238.
1000
1001 Pan, B.T., Hu, Z.B., Wang, J.P., Vandenberghe, J., Hu, X.F., Wen, Y.H., Li, Q., Cao, B.,
1002 2012. The approximate age of the planation surface and the incision of the Yellow
1003 River. *Palaeogeography, Palaeoclimatology, Palaeoecology* 356-357, 54-61.
1004
1005 ~~Pan, G., Wang, L., Li, R., Yuan, S., Ji, W., Yin, F., Zhang, W., Wang, B., 2012.~~
1006 ~~Tectonic evolution of the Qinghai-Tibet Plateau. *Journal of Asian Earth Sciences* 53,~~
1007 ~~3-14.~~
1008
1009 Perrineau, A., van der Woerd, J., Gaudemer, Y., Jing, Z., Pik, R., Tapponnier, P.,
1010 Thuizat, R., Zheng, R., 2011. Incision rate of the Yellow River in Northeastern Tibet
1011 constrained by ¹⁰Be and ²⁶Al cosmogenic isotope dating of fluvial terraces:
1012 implications for catchment evolution and plateau building. In: Gloaguen, R.,
1013 Ratschbacher, L. (Eds.), *Growth and Collapse of the Tibetan Plateau*. Special
1014 Publications of the Geological Society, London 353, 189-219.
1015
1016 Peulvast, J.P., Sales, V., 2004. Stepped surfaces and palaeolandforms in the northern
1017 Brazilian <Nordeste>: constraints on models of morphotectonic evolution.
1018 *Geomorphology* 62, 89-122.
1019
1020 Potter, P.E., 1978. Significance and origin of big rivers. *Journal of Geology* 86, 13-33.
1021
1022 ~~Porter, S.C., An, Z., Zheng, H., 1992. Cyclic Quaternary alleviation and terracing in a~~

1023 ~~nonglaciaded drainage basin on the north flank of the Qinling Shan, central China.~~
1024 ~~Quaternary Research 38, 157-169.~~
1025
1026 Powell, C., Conaghan, P.J., 1973. Plate tectonics and the Himalayas. Earth and
1027 Planetary Science Letters 20, 1-12.
1028
1029 Prins, M.A., Zheng, H.B., Beets, K., Troelstra, S., Bacon, P., Kamerling, I., Wester, W.,
1030 Konert, M., Huang, X.T., Wang, K.E., Vandenberghe, J., 2009. Dust supply from river
1031 floodplains: the case of the lower Huang He (Yellow River) recorded in
1032 loess-palaeosol sequence from the Mangshan Plateau. Journal of Quaternary Science
1033 24, 75-84.
1034
1035 ~~Qiang, X.K., Li, Z.X., Powell, C.McA., Zheng, H.B., 2001. Magnetostratigraphic~~
1036 ~~record of the Late Miocene onset of the East Asian monsoon, and Pliocene uplift of~~
1037 ~~northern Tibet. Earth and Planetary Science Letters 187, 83-93.~~
1038
1039 Rea, D., Snoeckx, H., Joseph, H.L., 1998. Late Cenozoic eolian deposition in the
1040 North Pacific: Asian drying, Tibetan uplift, and cooling of the northern hemisphere.
1041 Paleocanography 13, 215-224.
1042
1043 ~~Rixhon, G., Briant, R.M., Cordier, S., Duval, M., Jones, A., Scholz, D., 2016.~~
1044 ~~Revealing the pace of river landscape evolution during the Quaternary: recent~~
1045 ~~developments in numerical dating methods. Quaternary Science Reviews.~~
1046 ~~<http://dx.doi.org/10.1016/j.quascirev.2016.08.016>~~
1047
1048 ~~Royden, H.L., Burchfiel, C.B., van der Hilst, D.R., 2008. The geological evolution of~~
1049 ~~the Tibetan Plateau. Science 1054-1058.~~
1050
1051 ~~Ruddiman, W.F., Kutzbach, J.E., 1989. Forcing of Late Cenozoic Northern~~
1052 ~~Hemisphere climate by plateau uplift in Southern Asia and the American West.~~
1053 ~~Journal of Geophysical Research 94, 18,409-18,427.~~
1054
1055 Rutter, N.W., Ding, Z.L., Evans, M.E., Liu, T.S., 1991. Baoji-type pedostratigraphic
1056 section, Loess Plateau, north-central China. Quaternary Science Review. 10, 1-22.

Formatted: Justified, Line spacing: 1.5 lines, Adjust space between Latin and Asian text, Adjust space between Asian text and numbers

Formatted: Font: (Default) Times New Roman

Formatted: Font: (Default) Times New Roman

Formatted: Font: (Default) Times New Roman

- 1057
1058 Sadler, P.M., Jerolmack, D.J., 2015. Scaling laws for aggradation, denudation and
1059 progradation rates: the case for time-scale invariance at sediment sources and sinks.
1060 Geological Society, London, Special Publications, 404, 69–88.
1061
1062 Saito, Y., Yang, Z., Hori, K., 2001. The Huanghe (Yellow River) and Changjiang
1063 (Yangtze River) deltas: a review on their characteristics, evolution and sediment
1064 discharge during the Holocene. *Geomorphology* 41, 219-231.
1065
1066 Schumm, S.A., Dumont, J.F., Holbrook, J.M., 2000. Active tectonics and alluvial river.
1067 Cambridge University Press, Cambridge, UK, pp. 375-376.
1068
1069 Seyrek, A., Westaway, R., Pringle, M., Yurtmen, S., Demir, T., Rowbotham, G., 2008.
1070 Timing of the Quaternary Elazığ volcanism, eastern Turkey, and its significance for
1071 constraining landscape evolution and surface uplift. *Turkish Journal of Earth Sciences*
1072 17, 497-541.
1073
1074 ~~Seyrek, A., Demir, T., Westaway, R., Guillou, H., Scaillet, S., White, S.T., Bridgland,~~
1075 ~~D., 2014. The kinematics of central southern Turkey and northwest Syria revisited.~~
1076 ~~*Tectonophysics* 618, 35–66.~~
1077
1078 Soreghan, G.S., Elmore, R.D., Katz, B., Cogoini, M., Banerjee, S., 1997.
1079 Pedogenically enhanced magnetic susceptibility variations preserved in Paleozoic
1080 loessite. *Geology* 25, 1003-1006.
1081
1082 Stokes, M., 2008. Plio-Pleistocene drainage development in an inverted sedimentary
1083 basin: Vera basin, Betic Cordillera, SE Spain. *Geomorphology* 100, 193-211.
1084
1085 Sun, Y., Clemens, C. S., An, Z., Yu, Z., 2006. Astronomical timescale and
1086 palaeoclimatic implication of stacked 3.6-Myr monsoon records from the Chinese
1087 Loess Plateau. *Quaternary Science Reviews* 25, 33-48.
1088
1089 Tapponnier, P., Xu, Z., Roger, F., Meyer, B., Arnaud, N., Wittlinger, G., Yang, J., 2001.
1090 Oblique stepwise rise and growth of the Tibet Plateau. *Science* 294, 1671-1677.

1091

1092 Vandenberghe, J., Lu, H. Y., Sun, D. H., Huissteden, J., Konert, M., 2004. The late
1093 Miocene and Pliocene climate in East Asia as recorded by grain size and magnetic
1094 susceptibility of the Red Clay deposits (Chinese Loess Plateau). *Palaeogeography,*
1095 *Palaeoclimatology, Palaeoecology.* 204, 239-255.

1096

1097 Vandenberghe, J., Wang, X., Lu, H., 2011. Differential impact of small-scaled tectonic
1098 movements on fluvial morphology and sedimentology (the Huang Shui catchment,
1099 NE Tibet Plateau). *Geomorphology* 134, 171-185.

1100

1101 Vandenberghe, J., de Moor, J.W. J., Spanjaard, G., 2012. Natural change and human
1102 impact in a present-day fluvial catchment: The Geul River, southern Netherlands.
1103 *Geomorphology* 159-160, 1-14.

1104

1105 Vandenberghe, J., 2016. From planation surfaces to river valleys. *BSGLg* 67, 93-106.

1106

1107 | Veldkamp, A., van Dijke, J. J., 2000. Simulating internal and external controls on
1108 fluvial terrace stratigraphy: a qualitative comparison with the Mass record.
1109 *Geomorphology* 33, 225-236.

Formatted: Dutch (Netherlands)

1110

1111 Wagner, T., Fritz, H., Stüwe, K., Nestroy, O., Rodnight, H., Hellstrom, J., Benischke,
1112 R., 2011. Correlations of cave levels, stream terraces and planation surfaces along the
1113 River Mur-Timing of landscape evolution along the eastern margin of the Alps.
1114 *Geomorphology* 134, 62-78.

1115

1116 Wang, S., Wu, X., Zhang, K., Jiang, F., Xue, B., Tong, G., Tian, G., 2001. Sedimentary
1117 records of environmental evolution in the Sanmen Lake Basin and the Yellow River
1118 running through the Sanmenxia Gorge eastward into the sea. *Science in China* 31,
1119 585-608.

1120

1121 Wang, X., Lu, H., Vandenberghe, J., Zheng, S., van Balen, R., 2012. Late Miocene
1122 uplift of the NE Tibetan Plateau inferred from basin filling, planation and fluvial
1123 terraces in the Huang Shui catchment. *Global and Planetary Change* 88-89, 10-19.

1124 |

1125 ~~Westaway, R., 1993. Quaternary uplift of southern Italy. Journal of Geophysical~~
1126 ~~Research 98, 21741-21772.~~

1127

1128 ~~Westaway, R., 2006. Late Cenozoic extension in southeast Bulgaria: a synthesis. In:~~
1129 ~~Robertson, A.H.F., Mountrakis, D. (Eds.), Tectonic Development of the Eastern~~
1130 ~~Mediterranean Region. Special Publication, vol. 260. Geological Society, London, pp.~~
1131 ~~557-590.~~

1132

1133 Westaway, R., 2009. Active crustal deformation beyond the SE margin of the Tibetan
1134 Plateau: Constraints from the evolution of fluvial systems. Global and Planetary
1135 Change 68, 395-417.

1136

1137 ~~Westaway, R., Bridgland, D.R., 2007. Late Cenozoic uplift of southern Italy deduced~~
1138 ~~from fluvial and marine sediments: coupling between surface processes and lower~~
1139 ~~crustal flow. Quaternary International 175, 86-124.~~

1140

1141 Westaway, R., Demir, T., Seyrek, A., 2008. Geometry of the Turkey-Arabia and
1142 Africa-Arabia plate boundaries in the latest Miocene to Mid-Pliocene: the role of the
1143 Malatya-Ovacik Fault Zone in eastern Turkey. eEarth, 3, 27-35.

1144

1145 Westaway, R., Bridgland, D.R., Sinha, R., Demir, T., 2009. Fluvial sequences as
1146 evidence for landscape and climatic evolution in the Late Cenozoic: A synthesis of
1147 data from IGCP 518. Global and Planetary Change 68, 237-253.

1148

1149 ~~White, T.L., Lister, S.G., 2012. The collision of India with Asia. Journal of~~
1150 ~~Geodynamics 56-57, 7-17.~~

1151

1152 Willenbring, J.K., Jerolmack, D.J., 2016. The null hypothesis: globally steady rates of
1153 erosion, weathering fluxes and shelf sediment accumulation during Late Cenozoic
1154 mountain uplift and glaciation. Terra Nova 28, 11-18.

1155

1156 Willenbring, J.K., von Blanckenburg, F., 2010. Long-term stability of global erosion
1157 rates and weathering during late-Cenozoic cooling. Nature 465, 211-214.

1158

1159 Wu, C., Xu, Q., Yang, X., 2000. Ancient drainage system of the Yellow River on
1160 North China Plain. *Journal of Geomechanics* 6, 1-9 (in Chinese, with English
1161 abstract).
1162

1163 Xia, D., Wu, S., Yu, Z., 1993. Changes of the Yellow River since the last glacial age.
1164 *Marine Geology & Quaternary Geology* 13, 83-88 (in Chinese, with English abstract).
1165

1166 Xiao, G., Guo, Z., Chen, Y., Yao, Z., Shao, Y., Wang, X., Hao, Q., Lu, Y., 2008.
1167 Magnetostratigraphy of BZ₁ borehole in west coast of Bohai bay, northern China.
1168 *Quaternary Sciences* 28, 909-916 (in Chinese, with English abstract).
1169

1170 Xue, D., 1996. A humble option of the formed age for the eastern section of the
1171 Yellow River. *Henan Geology* 14, 110-112 (in Chinese, with English abstract).
1172

1173 Yang, H., Chen, X., 1985. Quaternary transgressions, eustatic changes and shifting of
1174 shoreling in East China. *Marine Geology & Quaternary Geology* 5, 59-80 (in Chinese,
1175 with English abstract).
1176

1177 Yang, S., Cai, J., Li, C., Deng, B., 2001. New discussion about the run-through time
1178 of the Yellow River. *Marine Geology & Quaternary Geology* 21, 15-20 (in Chinese,
1179 with English abstract).
1180

1181 Yao, Z., Xiao, G., Wu, H., Liu, W., Chen, Y., 2010. Plio-Pleistocene vegetation
1182 changes in the North China Plain: Magnetostratigraphy, oxygen and carbon isotopic
1183 composition of pedogenic carbonates. *Palaeogeography, Palaeoclimatology,*
1184 *Palaeoecology* 297, 502-510.
1185

1186 Yao, Z., Guo, Z., Xiao, G., Wang, Q., Shi, X., Wang, X., 2012. Sedimentary history of
1187 the western Bohai coastal plain since the late Pliocene: Implications on tectonic,
1188 climatic and sea-level changes. *Journal of Asian Earth Sciences* 54-55, 192-202.
1189

1190 Yu, H., 1999. Ages of the Yellow River delta in shelf regions of the Yellow sea and the
1191 Bohai sea. *Journal of Geomechanics* 5, 80-88 (in Chinese, with English abstract).
1192

- 1193 Yuan, Y., Hu, S., Wang, H., Sun, F., 2007. Meso-Cenozoic tectonothermal evolution
1194 of Ordos Basin, central China: Insight from newly acquired vitrinite reflectance data
1195 and a revision of existing paleothermal indicator data. *Journal of Geodynamics* 44,
1196 33-46.
- 1197
- 1198 Yue, L., Zhang, Y., Wang, J., Deng, X., Zhang, L., 1999. Magnetostratigraphic
1199 sequence of continental deposits in Northern China since 5.3 Ma. *Geological Reviews*
1200 45, 444-448 (in Chinese, with English abstract).
- 1201 ▲
- 1202 Zhang, J., Qiu, W., Wang, X., Hu, G., Li, R., Zhou, L., 2010. Optical dating of a
1203 hyperconcentrated flow deposit on a Yellow River terrace in Hukou, Shaanxi, China.
1204 *Quaternary Geochronology* 5, 194-199.
- 1205
- 1206 Zhang, P., Molnar, P., Downs, W.R., 2001. Increased sedimentation rates and grain
1207 sizes 2-4 Myr ago due to the influence of climate change on erosion rates. *Nature* 410,
1208 891-897.
- 1209
- 1210 Zhang, Y., Mercier, J.L., Vergély, P., 1998. Extension in the graben systems around the
1211 Ordos (China), and its contribution to the extrusion tectonics of south China with
1212 respect to Gobi-Mongolia. *Tectonophysics* 285, 41-75.
- 1213
- 1214 Zhang, Y., Ma, Y., Yang, N., Shi, W., Dong, S., 2003. Cenozoic extensional stress
1215 evolution in North China. *Journal of Geodynamics* 36, 591-613.
- 1216
- 1217 ~~Zhang, Z., Tyrrell, S., Li, C., Daly, S.J., Sun, X., Blowick, A., Lin, X., 2016.~~
1218 ~~Provenance of detrital K-feldspar in Jiangnan Basin sheds new light on the~~
1219 ~~Pliocene-Pleistocene evolution of the Yangtze River. *Geological Society of America*~~
1220 ~~*Bulletin* doi: 10.1130/b31445.1~~
1221 ~~<http://gsabulletin.gsapubs.org/content/early/2016/04/27/B31445.1.abstract>~~
- 1222
- 1223 ~~Zhao, H., Li, S.H., 2002. Luminescence isochron dating: A new approach using~~
1224 ~~different grain sizes. *Radiation Protection Dosimetry* 101, 333-338.~~
- 1225
- 1226 ~~Zhao, Z., Wang, S., Jiang, F., Wu, X., Xiao, H., Tian, G., Liu, K., Yin, W., Xue, B.,~~

1227 | ~~Wang, S., 2002. Magnetostratigraphy and environmental records of laterite in~~
1228 | ~~Sanmenxia area. Marine Geology & Quaternary Geology 22, 93-97.~~
1229 |
1230 | Zheng, H., Powell, C., Rea, D., Wang, J., Wang, P., 2004. Late Miocene and
1231 | mid-Pliocene enhancement of the East Asian monsoon as viewed from land and sea.
1232 | Global and Planetary Change 41, 147-155.
1233 |
1234 | Zheng, H., Huang, X., Ji, J., Liu, R., Zeng, Q., Jiang, F., 2007. Ultra-high rates of
1235 | loess sedimentation at Zhengzhou since Stage 7: Implication for the Yellow River
1236 | erosion of the Sanmen Gorge. Geomorphology 85, 131-142.
1237 |
1238 | Zheng, H., Clift, P., Wang, P., Tada, R., Jia, J., He, M., Jourdan, F., 2013. Pre-Miocene
1239 | birth of the Yangtze River. PNAS 110, 7556-7561.
1240 |
1241 | Zhu, H., Chen, K., Liu, K., He, S., 2008. A sequence stratigraphic model for reservoir
1242 | sand-body distribution in the Lower Permian Shanxi Formation in the Ordos Basin,
1243 | Northern China. Marine and Petroleum Geology 25, 731-743.
1244 |
1245 | Zhu, R. X., Laj, C., Mazaud, A., 1994. The Matuyama-Brunhes and upper Jaramillo
1246 | transitions recorded in a loess section at Weinan, north-central China. Earth and
1247 | Planetary Science Letters. 125, 143-158.

1248 **Table Captions**

1249

1250 Table 1. Fluvial terrace correlation between Sanmenxia and Kouma

1251

1252 ~~Table 2. Optically stimulated luminescence dating~~

1253

1254 **Figure Captions**

1255

1256 **Fig. 1.** Map of the Fenwei graben and its surroundings, showing faults (from AFSOM,
1257 1998), rivers, topography, and the locations of the four sub-basins (the Weihe,
1258 Lingbao, Yuncheng, and Fenhe basins). The locations of Figs 2 and 3 are also
1259 indicated. The inset map shows the major fault systems, plate motions, Bohai Gulf,
1260 and location within China.

1261

1262 **Fig. 2.** Maximum, mean, and minimum topography along a 50-km-wide swath along
1263 the Sanmen gorge (see Fig. 1 for location). Active faults and the interpreted long
1264 profile of the planation surface are also depicted (see also Fig. 4).

1265

1266 **Fig. 3.** Map of the study region showing topography (using the same data source as
1267 Fig. 1), active faults, and field localities (see Fig. 1 for location).

1268

1269 **Fig. 4.** Field photos of the Sanmen gorge and its entrance. (A) View of the planation
1270 surface dominating the Xiaoshan along the Sanmen gorge, looking east from
1271 $34^{\circ}51'09.36''$ N, $111^{\circ}19'34.16''$ E. (B) The westward dip of the planation surface
1272 (looking north from $34^{\circ}46'03.27''$ N, $111^{\circ}17'53.48''$ E), the result of deformation close
1273 to the inlet of the Sanmen gorge. (C and D) Fluvial terrace staircase at Sanmenxia,
1274 looking west (C) and south (D). Five terraces have been identified below the planation
1275 surface, of which the uppermost (T5) is newly recognized. (E) Closeup view of the
1276 sedimentary sequence forming terrace T2 at Sanmenxia (see (D) for location). The
1277 fluvio-lacustrine Sanmen Formation, characterized by horizontally bedded mudstone,
1278 siltstone, clay, conglomerate, and sandstone, crops out below the terrace gravel.

1279

1280 **Fig. 5.** Transverse profiles through the fluvial terrace staircases at the field localities
1281 (Zhangbian, Sanmenxia, Dongcun, Xiaolangdi, and Kouma; see Fig. 3 for locations).

1282 Note that the terrace staircases at Zhangbian, Sanmenxia and Dongcun are affected by
1283 normal faulting.

1284

1285 **Fig. 6.** Interpreted longitudinal profile of terrace levels along the Sanmen gorge, using
1286 height data from Table 1. The normal faults that define the ends of the gorge are
1287 depicted in Fig. 2 and 3.

1288

1289 **Fig. 7.** Magnetostratigraphy and pedostratigraphy of the aeolian deposits overlying
1290 the fluvial terraces and planation surface at Sanmenxia. These TL dates for T2 and
1291 interpreted chrons (black for normal geomagnetic polarity, white for reverse) for
1292 terraces T4, T3, and T2 are all from Pan et al. (2005a). For the newly recognized
1293 terrace T5 and the planation surface, paleomagnetic data from the overlying ~130-m-
1294 and 152-m-thick aeolian deposits are used to obtain age interpretations (of ~1.24 Ma
1295 and 3.63 Ma, respectively), using the Cande and Kent (1995) geomagnetic polarity
1296 timescale. However, these data are displayed here without filtering for noise. The
1297 magnetic susceptibility values are higher in the palaeosol units than those in the
1298 neighboring loess layers.

1299

1300 **Fig. 8.** A selection of the data from Fig. 7, illustrating the thermal demagnetization
1301 process used to identify the primary components of rock magnetization that indicate
1302 the polarity of the Earth's magnetic field at the time of deposition. For each figure part,
1303 the left-hand panel shows the horizontal (solid symbols) and vertical (open symbols)
1304 components of rock magnetization, whereas the right-hand panel shows how the
1305 strength of magnetization decreases with increasing temperature. (A) Sample PR-10.0
1306 from the 10.0-m thickness of the aeolian section on the planation surface, a sample of
1307 Carbonate nodules. After a low-temperature overprint is removed, this sample is seen
1308 to be magnetized upward and southward, indicating reverse polarity. (B) Sample
1309 PR-0.5 from 0.5-m thickness of the aeolian section on the planation surface, a sample
1310 of Red Clay. After a low-temperature overprint is removed, this sample is seen to be
1311 magnetized downward and northward, indicating normal polarity. (C) Sample PL-69.0
1312 from 69.0-m thickness of the aeolian section on the planation surface, a sample of
1313 loess. After a substantial overprint is removed, this sample is seen to be magnetized
1314 upward and southward, indicating reverse polarity. (D) Sample PL-109.0 from
1315 109.0-m thickness of the aeolian section on the planation surface, a sample of loess.

1316 This sample is seen to be magnetized downward and northward, indicating normal
1317 polarity. (E) Sample T5-33.0 from 33.0-m thickness of the loess section on terrace T5.
1318 This sample is seen to be magnetized downward and westward, indicating ambiguous
1319 polarity. (F) Sample T5-28.0 from 28.0-m thickness of the loess section on terrace T5.
1320 This sample is seen to be magnetized downward and northward, indicating normal
1321 polarity.

1322

1323 **Fig. 9.** Schematic diagram illustrating landscape evolution within the Fenwei graben.

1324 (A) The initial downfaulting, erosion, and filling of the Fenwei graben. (I)
1325 Development, in the Early Pliocene, of the graben as a result of extensional tectonism.
1326 (II) Planation, circa 3.6 Ma (according to the magnetostratigraphic data), during
1327 infilling of the graben, marked by emplacement of the lower part of the Sanmen
1328 Formation. (B) Uplift and dissection of the planation surface after ~3.6 Ma. At this
1329 time the extension switched from the initial set of normal faults to a newer set in the
1330 hanging-walls of the initial set, resulting in narrowing of the graben. (C) Erosion, fill,
1331 and excavation of this narrower graben. (I) Erosion and fill when the narrower graben
1332 was occupied by an isolated fluvio-lacustrine system, during deposition of the upper
1333 part of the Sanmen Formation in the Early Pleistocene. (II) Initial entrenchment of the
1334 Yellow River into the Sanmen Formation circa 1.2 Ma. At this time the former lake
1335 basin was disrupted and fluvial drainage first developed from west to east across the
1336 Xiaoshan, leading to the formation of the Sanmen gorge and incision into the Sanmen
1337 Formation. (D) Incision and terrace formation by the Yellow River at Sanmenxia since
1338 the late Early Pleistocene, creating the present fluvial terrace staircase.

Table 1

Table 1: Fluvial terrace correlation between Sanmenxia and Kouma

Site			Terrace 1			Terrace 2		Terrace 3		Terrace 4		Terrace 5		Planation surface
Name	Co-ordinates	H _o (m)	H (m)	h (m)	H (m)	h (m)	H (m)	h (m)	H (m)	h (m)	H (m)	h (m)	H (m)	
Zhangbian	34°42'51"N, 111°01'13"E	307.0	317.0	1.0	NO	NO	338.0	3.0	381.7	1.0	395.4	0	520.0	
Sanmenxia	34°48'06"N, 111°14'25"E	306.6	317.2	0	325.5	2.0	338.0	4.0	382.1	2.0	394.1	2.0	557.8	
Dongcun	34°50'46"N, 111°34'07"E	249.5	261.9	0	270.3	3.9	300.5	2.3	325.0	0.6	427.0	0.4	647.0	
Xiaolangdi	34°55'15"N, 112°23'58"E	133.8	142.3	3.1	NO	NO	193.5	3.9	229.9	3.6	291.7	5.8	381.4	
Kouma	34°49'20"N, 112°46'18"E	89.8	99.8	0	NO	NO	115.0	0	NO	NO	145.0	0	200.0	

For each site, H_o denotes the height of the Yellow River above sea level. For each river terrace and for the planation surface, H denotes height above sea level and h denotes the thickness of fluvial sediments (h=0 denoting sites where the terrace surface is cut into bedrock). NO denotes river terraces that are not observed at particular sites.

Figure 1
[Click here to download high resolution image](#)

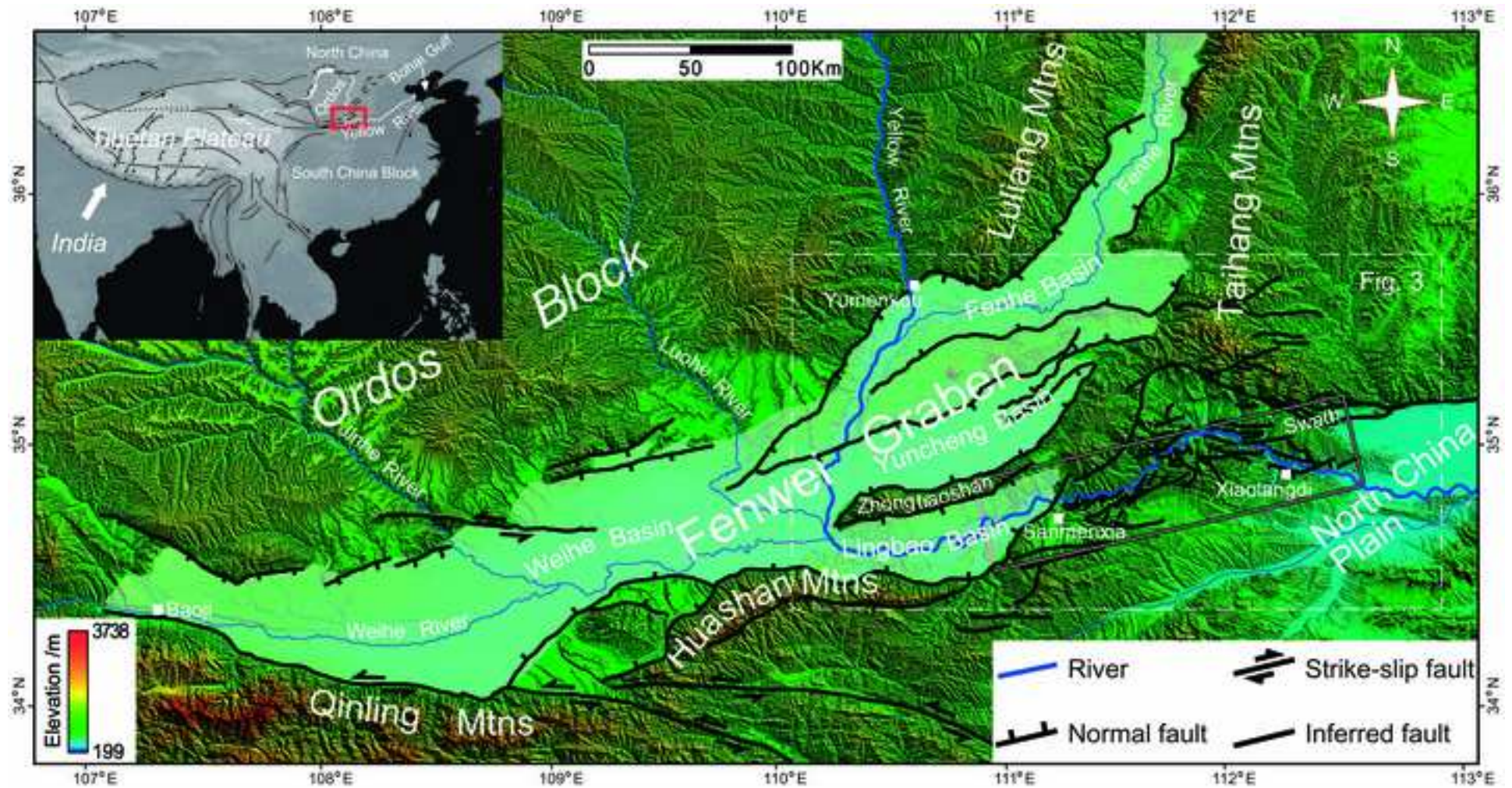


Figure 2
[Click here to download high resolution image](#)

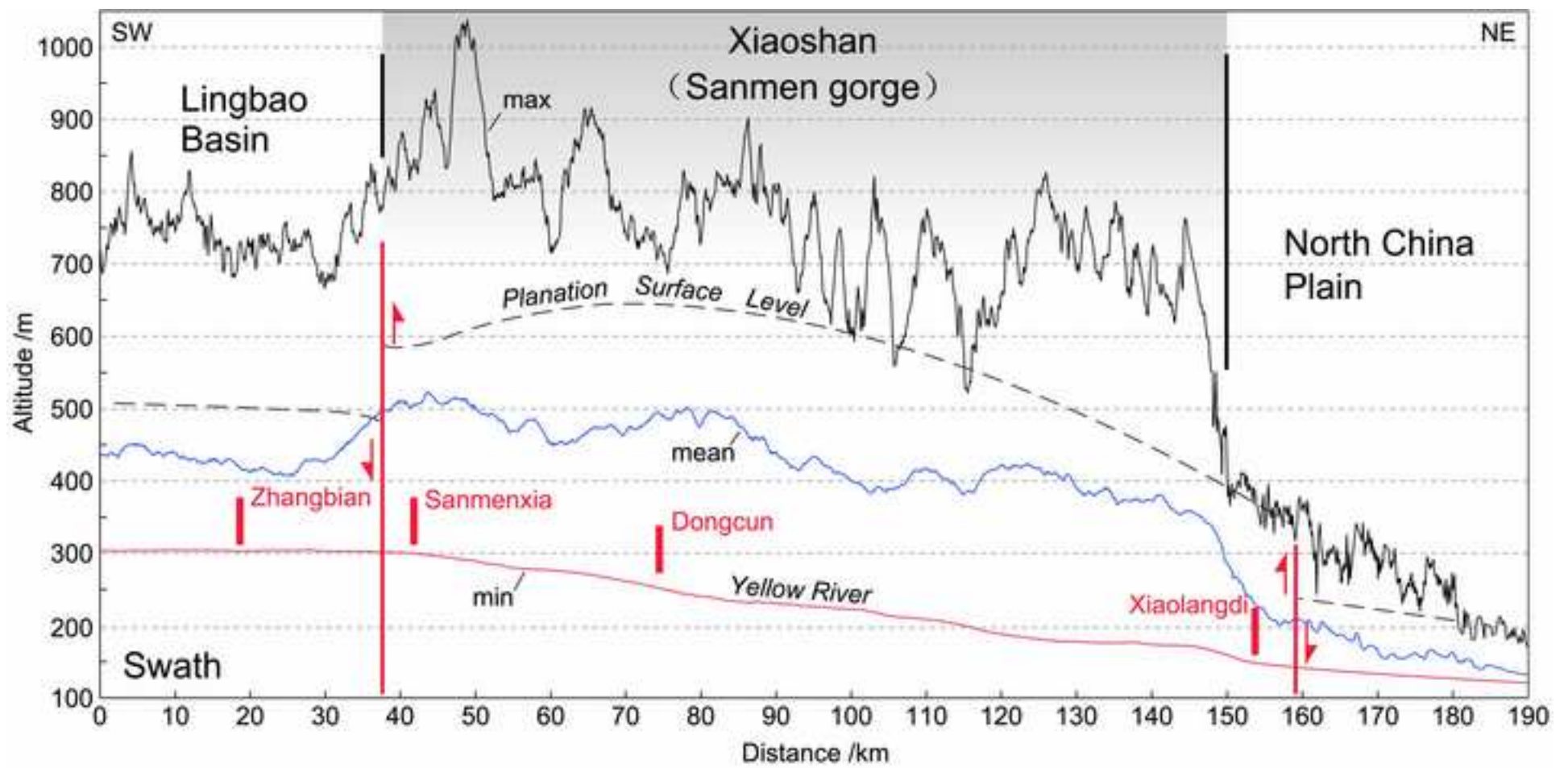


Figure 3
[Click here to download high resolution image](#)

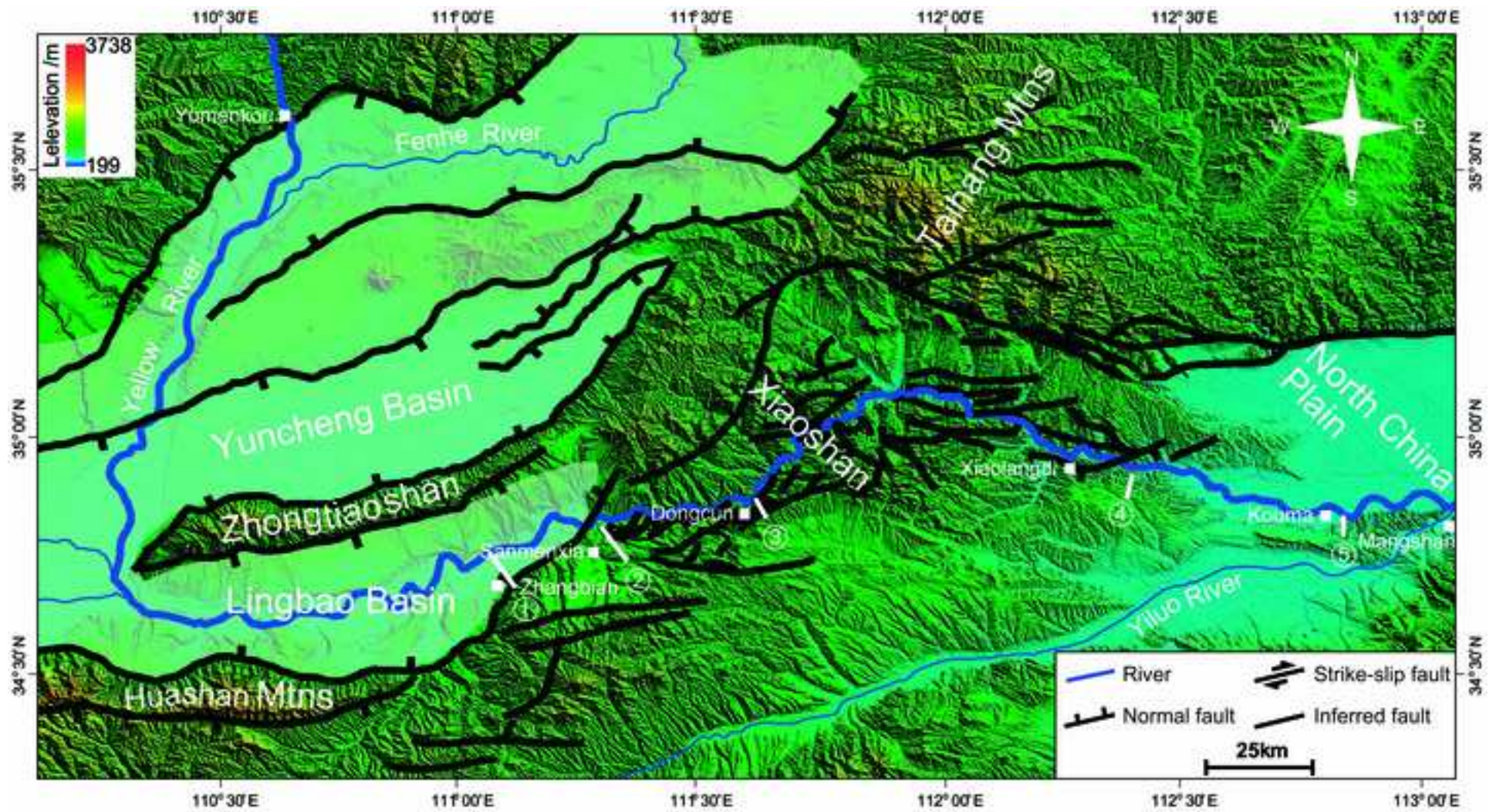


Figure 4
[Click here to download high resolution image](#)

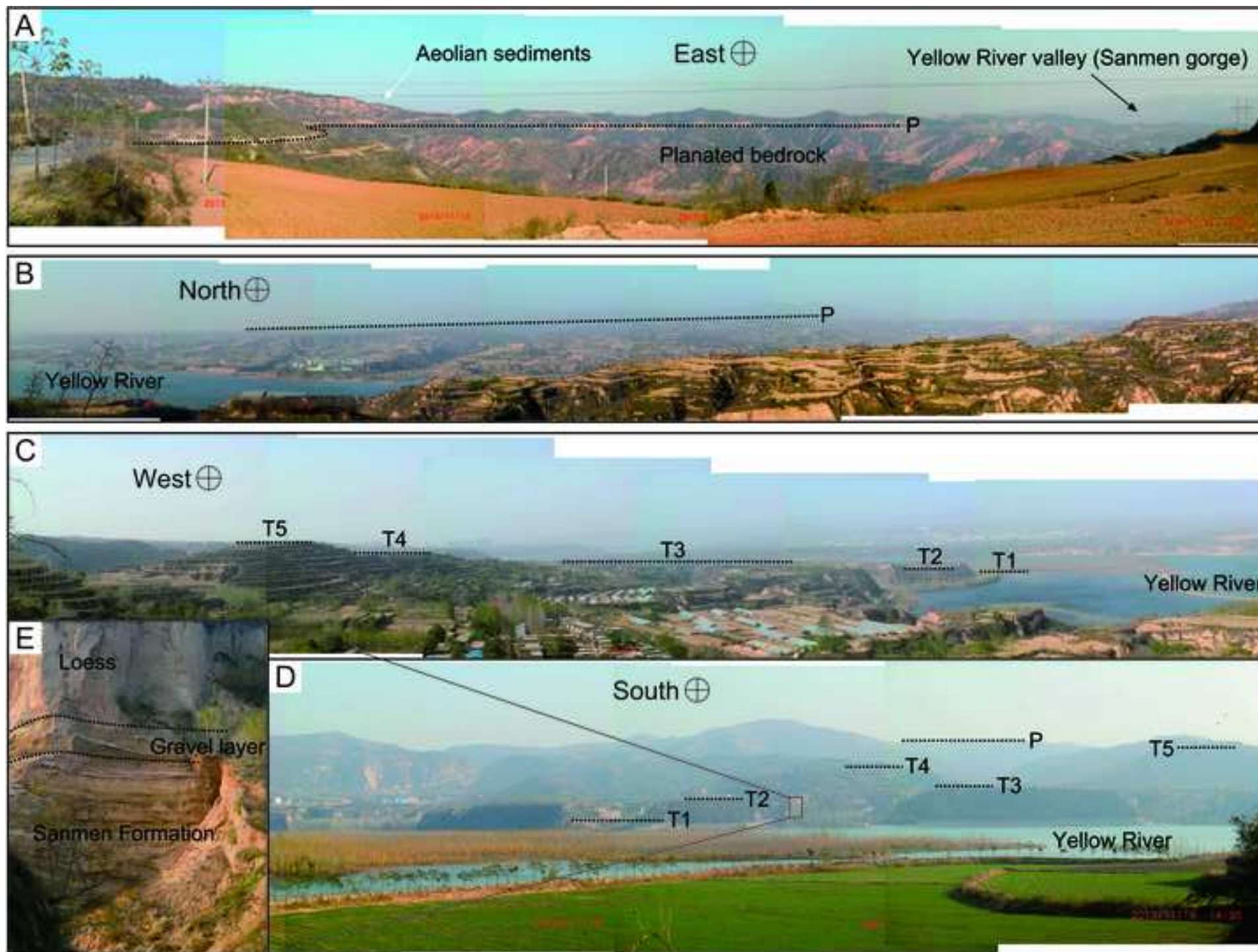


Figure 5
[Click here to download high resolution image](#)

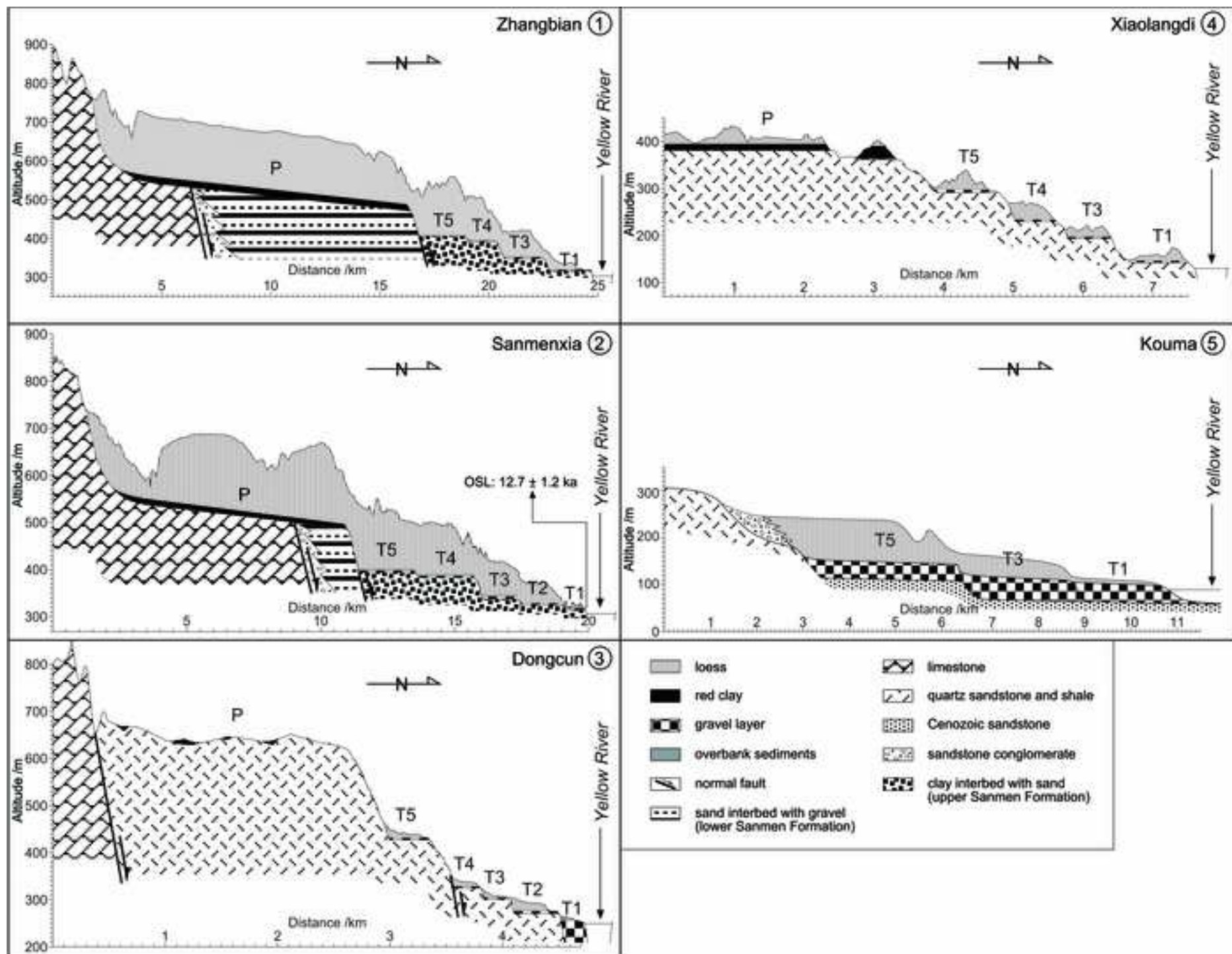


Figure 6
[Click here to download high resolution image](#)

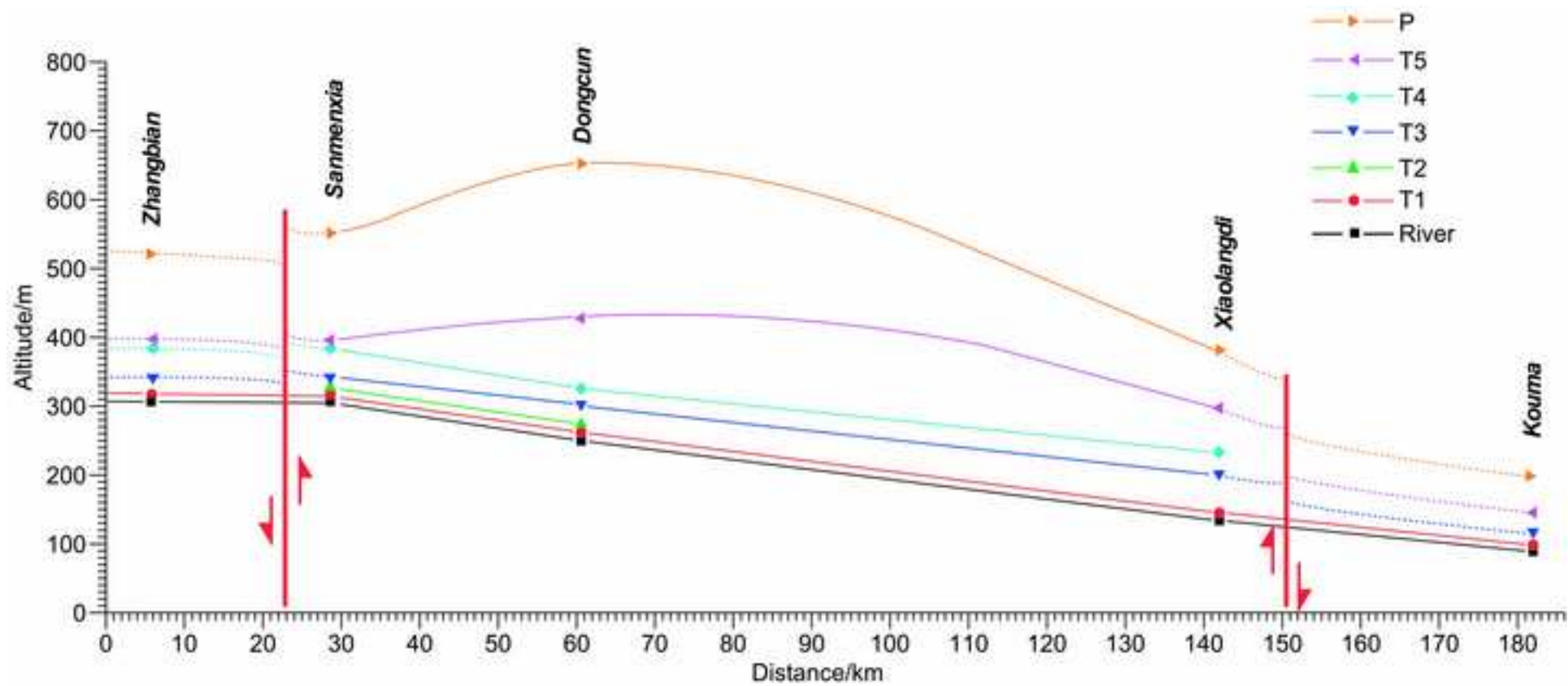


Figure 7
[Click here to download high resolution image](#)

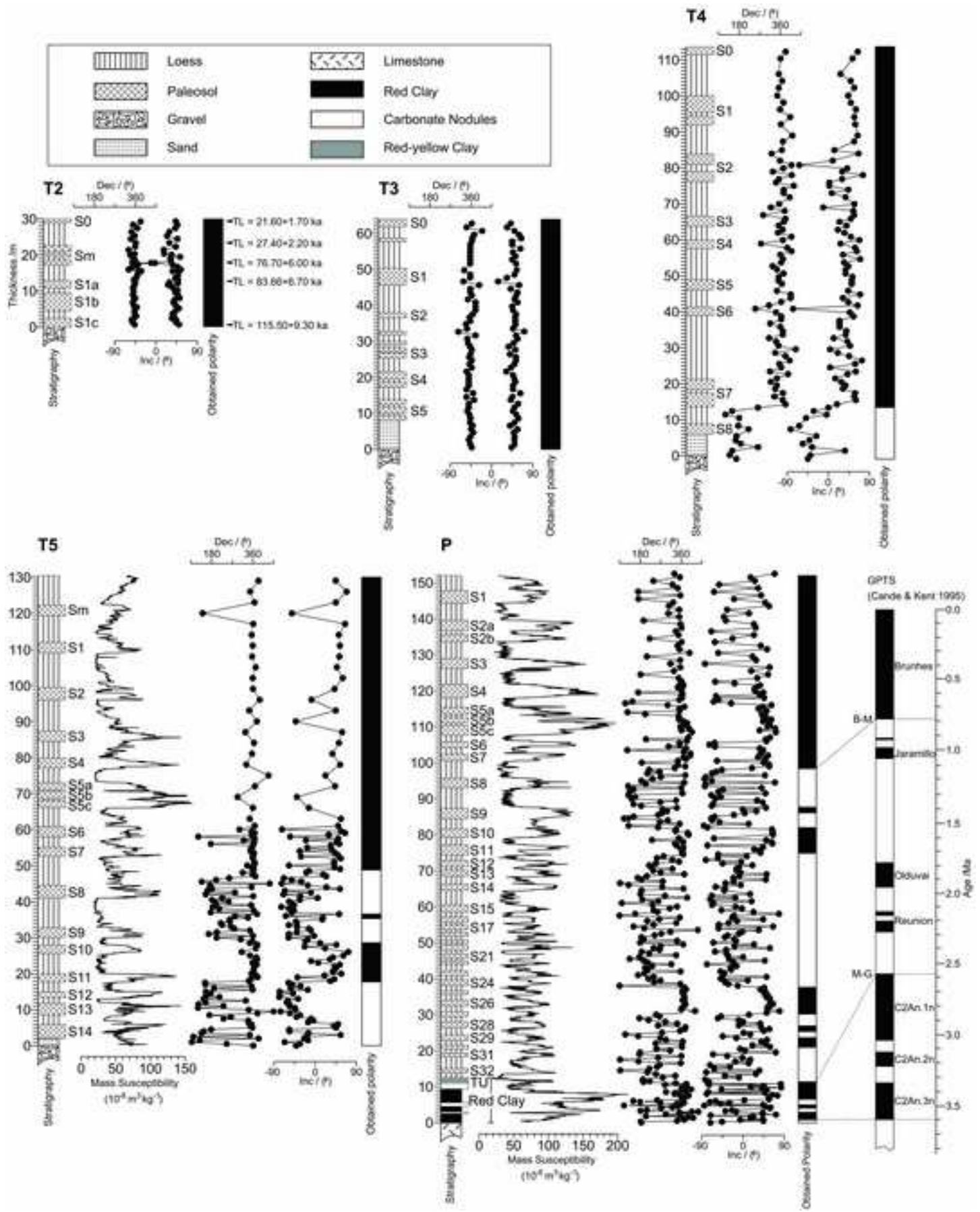


Figure 8
[Click here to download high resolution image](#)

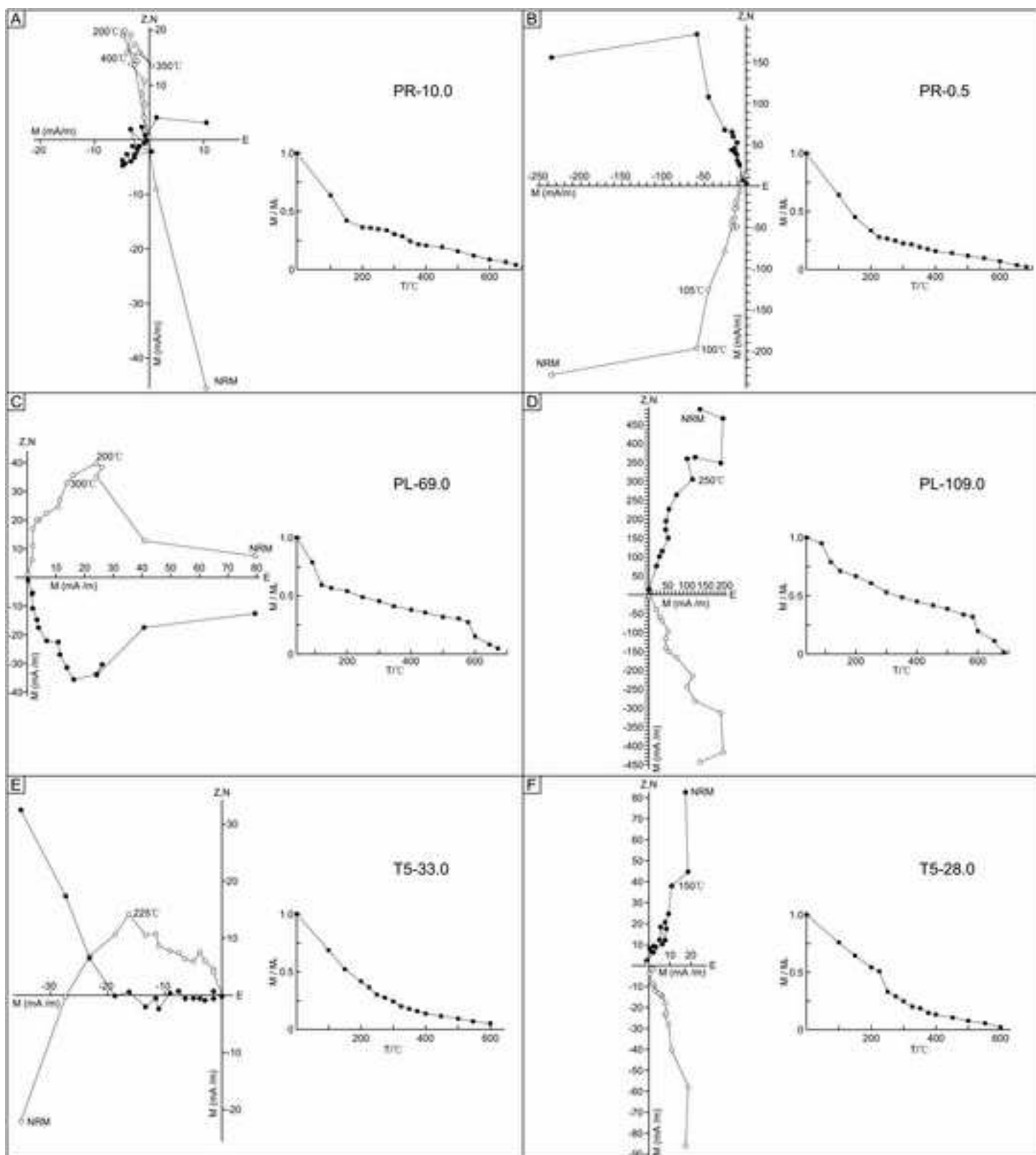
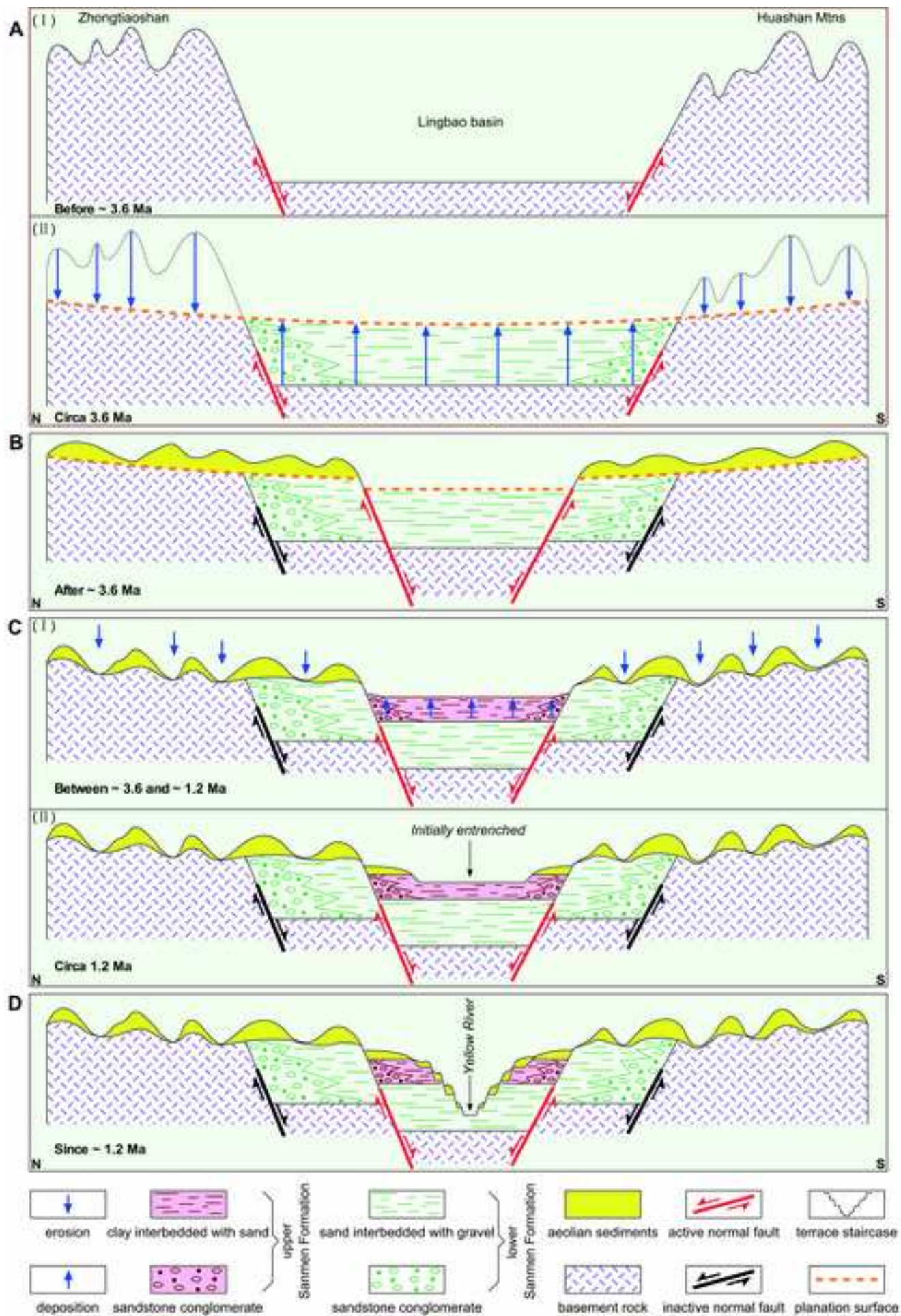


Figure 9
[Click here to download high resolution image](#)



Research Highlights

- We reconstructed a 3.6 Ma sequence based on the planation surface and terraces along the Sanmen gorge.
- The landscape evolution from basin filling to excavation was outlined under the constraint of this chronology.
- The present-day Sanmen gorge was formed by westward capturing the paleolake within the Fenwei graben.
- Gorge formation may have been initiated by lake overflow during the period 3.63–1.24 Ma.
- The dramatic increase in deposition rates in the Bohai Gulf resulted from the establishment of an integral Yellow River catchment.

Dear authors,

I reviewed the re-revised version of your manuscript submitted as part of the FLAG special issue in QSR. Despite some improvements, the key issues raised in my last review remain :

-concerning the structure : the « methods » section still include data, especially in section 2.2. Similarly some essential information which should appear early in the manuscript is only exposed in the discussion. This especially concerns the existing age control (lines)

-actually, the state of the art related to the previous geochronological interpretation (your section 1.4, which should also include section 1.5 since both deal with the same topic) must be improved, especially 1) by including all the chronological evidences, 2) by underlining the inconsistencies, and 3) by explaining that your aim is to try to provide a more consistent reconstruction. Otherwise we are left with the feeling that this paper does not bring new information !! So I strongly advice you to rewrite carefully this section, which is according to me one of the most important of the manuscript.

- We are grateful to the referee for valuable comments and constructive suggestions. The structure of this manuscript has been revised completely following the comments by the reviewer. The section mentioned by the referee has been rewrite to make a good expression.

-the text is at several places redundant (this is underlined by your use of « see below », or « abovementioned »), and this makes it more confusing. Please check the ms to remove all useless repetitions. I also advice you not to develop too much some parts that does not directly relate to the aim of your study, for example the OSL dating of the youngest terraces does not appears to be really significant...

- Reply: Yes according to the comment by the reviewer, our manuscript has been reconstructed and these useless repetitions has also been removed. Now it seems to be compendious and clear.

- despite not being native speaker I think a check of the language is really necessary ! this could be easily done by some of the co-authors

- Reply: As co-authors of our manuscript, Prof. David Bridgland and Jef Vandenberghe have done this work.

Some more specific comments (but to be considered as well) :

-sections 1.1 and 1.2 to be merged : actually it is difficult to deal with the significance of fluvial archives without having provided a general overview of the morphostructural context.

-the hiatus between the ≥ 1.24 Ma age for the gorge formation and the 1 Ma age for the deposition must be explained in a less allusive way than done in the cover letter and lines

Actually 250 ka is quite a long time...And if you want to explain this by dating uncertainty, please provide all uncertainties throughout the manuscript (I strongly advice you to do so)

- Reply: The paleomagnetic dating does not provide a exact uncertainty, despite a statistical error within this method. This inaccuracy can reach 240 ka in comparison with a long time

scale of 1 Ma. In addition, we have no data to discuss the chronological discrepancy. Therefore, we have added a symbol of ‘circa’ at the front of the age to express an approximate relationship.

-1.120 vs 1.131 : crescent of S shaped ?

- Reply: This has been revised into ‘crescent-shape’.

-1.177 : please rephrase beginning of section.

- Reply: Yes, it has been revised.

-1.181-185 : sentence not clear

- Reply: It has been removed.

-1.192 : length of the Yellow river to be provided earlier

- Reply: The construct of this manuscript has been revised. here is suitable to provide the information of the Yellow River.

-1.210 : distribution of sediments : too allusive

-sections 1.4 and 1.5 to be merged (see above)

- Reply: It has been removed. The sections 1.4 and 1.5 have been modified according to the referee’s comment.

-1.250 : incomplete age control : too allusive

- Reply: Yes, this should be attributed to incomplete age control, because previous work by Pan et al. (2005a) did not find the uppermost terrace.

-1.283 : these -> the

-section 2.2 to be placed elsewhere, it is not methods

- Reply: They has been revised based on the suggestion of this referee.

-1.315-316 : please be consistent to use either ka or Ma...

- Reply: It has been revised.

-1.323 : aid correlation : how ?

- Reply: Based on the pattern of magnetic susceptibility.

-1.357 : formation age

- Reply: It was removed.

-1.381 : it would be helpful to have the Loess plateau located on a map...

- Reply: The object of this paper is not concerned with the distribution of the loess within China. Anyone who want to know about the information of the Chinese loess plateau can go to the reference of Liu (1985). This literature has been listed in the reference of our paper. In addition, so much information was superposed on the map, providing the extent of the loess plateau will make a confused expression.

-1.414-413 : not clear

- Reply: This is a clear expression. The loess stratigraphy can be correlated on the basis of the magnetic susceptibility pattern.

-1.419-426 : better focus on the Red clau before the loess as they are older ?

- Reply: This is just a description of magnetic susceptibility pattern in the result section.

-1.433-434 too allusive, remove or explain.

- Reply: It has been removed.

-section 3.3 : please to not mix depths and elevation above reference levels (eg 1.456/463)

- Reply: We never mix, this is thickness.

-1.482 : cm/ky

- Reply: It has revised.

-1.502/504 : T5 is not new if it has been recognized earlier...

- Reply: In comparison with the work by Pan et al. (2005a), the terrace T5 is newly recognized. Although, this terrace may be identified by Kong et al. (2014), the age determination is not successful. Therefore, our paper still define T5 as a newly recognized terrace.

-1.517 : height above river : is it reliable ? please discuss this to justify your choice.

- Reply: Fluvial terrace is the remnant of previous river bed. If the terrace is not affected by tectonic activity, the same terrace maybe have a approximate height above river. Therefore

the height of one terrace above river bed is a important evidence for terrace correlation. Taking account of the height error, we have to say 'tentative correlation'.

-1.566-567 please provide evidences

- Reply: The evidence for the continuous aeolian deposition in the present study region has been provided early in this manuscript.

-1.622 : reference to Molnar too allusive.

- Reply: No, we have described our result early, and then made a comparison with Molnar (2004).

-1.639-644 too allusive

- Reply: No, we have made a clear expression.

1.650 and after : this does not look a very original conclusion, better remove this section...

- Reply: Removed.

-1.672 : some of the ages you indicate do not derive from your research !

- Reply: Providing a complete chronological framework for the terrace sequence is helpful for readers.

I hope you'll be able to take this comments into consideration (and especially the main ones exposed at the beginning of this review), to prepare the definitive version of the manuscript. best wishes, Stéphane Cordier

Dear Cordier, many thanks for your help. We have got much suggestion and help for David and Jef. Based on their revision and suggestion, I have made a thorough modification to the construct of this manuscript.